Chemical Science

ROYAL SOCIETY OF CHEMISTRY

REVIEW

View Article Online
View Journal | View Issue

Cite this: *Chem. Sci.*, 2025, **16**, 20181

The rise of rubber-like synthetic polymers in next-gen transistor technologies

Livy Laysandra, †[a] Dinda Bazliah, †[a] Daniel Muara Sentosa, †[a] Ayu Cahyarani Heksa, [a] Hai-Khue Bui, [a] Yu-Cheng Li [b] and Yu-Cheng Chiu *[ac]

Integrating rubber-like synthetic polymers into next-generation transistor technologies offers a transformative approach to advancing wearable electronics, positioning these elastomers as ideal substrates and essential companions to conjugated polymers and other active materials. From six distinct types of rubber-like synthetic polymers, this review spotlights polydimethylsiloxane (PDMS) and styrene–ethylene–butylene–styrene (SEBS) as the leading elastomeric polymers propelling wearable transistor innovations. PDMS is highly favored for its exceptional mechanical flexibility, high electrical resistivity, optical transparency, biocompatibility, and compatibility with soft lithography techniques, making it an ideal substrate for skin-like electronics. SEBS stands out as an elastomeric substrate for soft sensor integration due to its unique ability to form nanoconfined and phase-separated layers with semiconducting polymers that maintain high charge mobility under mechanical strain, while its tissue-like softness and mechanical compliance ensure comfort, durability, and suitability for advanced large-area flexible electronics. A comprehensive overview of recent progress in incorporating these elastomers is discussed, ranging from individual layers to fully integrated components into transistor devices. By bridging polymer chemistry with device engineering, it outlines a strategic research roadmap for developing tunable multifunctional rubber-like synthetic polymers to meet the complex performance requirements of emerging wearable transistor technologies. Finally, key technical challenges are identified alongside potential future research directions to support the development of next-generation wearable transistor applications.

Received 29th July 2025
Accepted 9th October 2025

DOI: 10.1039/d5sc05680b

rsc.li/chemical-science

[a]*Department of Chemical Engineering, National Taiwan University of Science and Technology, No. 43, Sec. 4, Keelung Rd., Da'an Dist., Taipei City 10607, Taiwan. E-mail: ycchiu@mail.ntust.edu.tw*

[b]*International School Ho Chi Minh City, 67 Đ. Nguyễn Cừ, Thảo Điền, Thủ Đức, Hồ Chí Minh, Vietnam*

[c]*Sustainable Electrochemical Energy Development Center, National Taiwan University of Science and Technology, Taipei City 10607, Taiwan*

† These authors contributed equally to this work.

Livy Laysandra

Livy Laysandra earned her PhD degree in the Department of Chemical Engineering at National Taiwan University of Science and Technology (NTUST) in 2024 under the supervision of Professor Yu-Cheng Chiu. She is currently a postdoctoral researcher in Yu-Cheng Chiu's group, focusing on designing and synthesizing multifunctional elastomers with self-healing and recyclable properties to advance sustainable polymer materials.

Dinda Bazliah

Dinda Bazliah is currently pursuing a combined master's and PhD program under the guidance of Professor Yu-Cheng Chiu in the Department of Chemical Engineering at National Taiwan University of Science and Technology (NTUST). Her research focuses on developing elastic polymers for dielectric and semiconducting layers used in thin-film transistors.

1. Introduction

The ongoing evolution of wearable electronics, particularly modern transistor devices, has imposed demanding requirements on materials. As these devices become increasingly integrated with the human body, materials are required to seamlessly combine high electrical functionality with skin-like mechanical properties to ensure both reliable operation and user comfort (Scheme 1). Furthermore, these materials must withstand mechanical fatigue, resist deformation from daily wear, and maintain stability against environmental exposures, including sweat, moisture, UV exposure, and temperature fluctuations.[1,2] Biocompatibility, low surface irritation, and breathability are equally vital for user comfort and safety, especially during long-term or continuous skin contact.[3,4] To meet these demands, researchers have focused on synthetic rubber-like polymers, commonly known as elastomers, which offer a unique combination of high elasticity[5–7] and toughness[8] along with tunable chemistry.[9,10]

This enables precise tuning of their mechanical and interfacial properties through chemical design, enabling seamless integration with electronic components in device engineering and biological environments.[11–13] Their hydrophobic nature and excellent barrier properties protect sensitive device layers from environmental ingress of water and oxygen, enhancing the longevity and reliability of wearable transistors.[14–16] Furthermore, certain rubber-like synthetic polymers possess dielectric properties that satisfy the stringent requirements of transistor devices, featuring high dielectric constants and low dielectric loss to enable efficient, low-voltage operation while minimizing

Daniel Muara Sentosa

Daniel Muara Sentosa joined Professor Yu-Cheng Chiu's Laboratory in Department of Chemical Engineering at National Taiwan University of Science and Technology in the fall of 2020 and received his BSc in the summer of 2023. He is currently pursuing a combined master and PhD degree with research focusing on stretchable, self-healing polymers and nanocomposite synthesis via microplasma.

Bui Hai Khue

Hai-Khue Bui received her MS degree from the Department of Chemical Engineering, National Taiwan University of Science and Technology (NTUST) in 2025, under the supervision of Professor Yu-Cheng Chiu. Her research interests include the synthesis of polymers and their applications in organic field-effect transistor memory.

Ayu Cahyarani Heksa

Ayu Cahyarani Heksa received her MSc degree from dual degree program collaboration of National Taiwan University of Science and Technology (NTUST) and Sepuluh Nopember Institute of Technology (ITS) in 2024 under the guidance of Professor Yu-Cheng Chiu and Professor Siti Nurkhamidah. Currently, she is pursuing her doctoral degree in the Department of Chemical Engineering at NTUST under the supervision of Professor Yu-Cheng Chiu. Her current research interests involve polysaccharide-based materials utilization for coating and edible film.

Yu-Cheng Chiu

Yu-Cheng Chiu joined the Department of Chemical Engineering at National Taiwan University of Science and Technology (Taiwan Tech). as a tenure-track assistant professor since August 2017 and has been promoted to associate professor since August 2022. Prior to joining the faculty, Yu-Cheng was a postdoc in the Zhenan Bao research group at Stanford University when he devoted on the research of intrinsically stretchable/healable semiconducting polymer and high-performance OFET by solution shearing technique. Before moving to Stanford, he received his PhD degree under the supervision from Prof. Wen-Chang Chen in December 2012 from the Chem. E. at National Taiwan University and then stayed in the same group for his first post-doctoral research until 2014. Currently, his major interests are the elastic and self-healing semiconducting materials, soft organic devices including transistor and transistor memory, and morphology characterization for polymer materials.

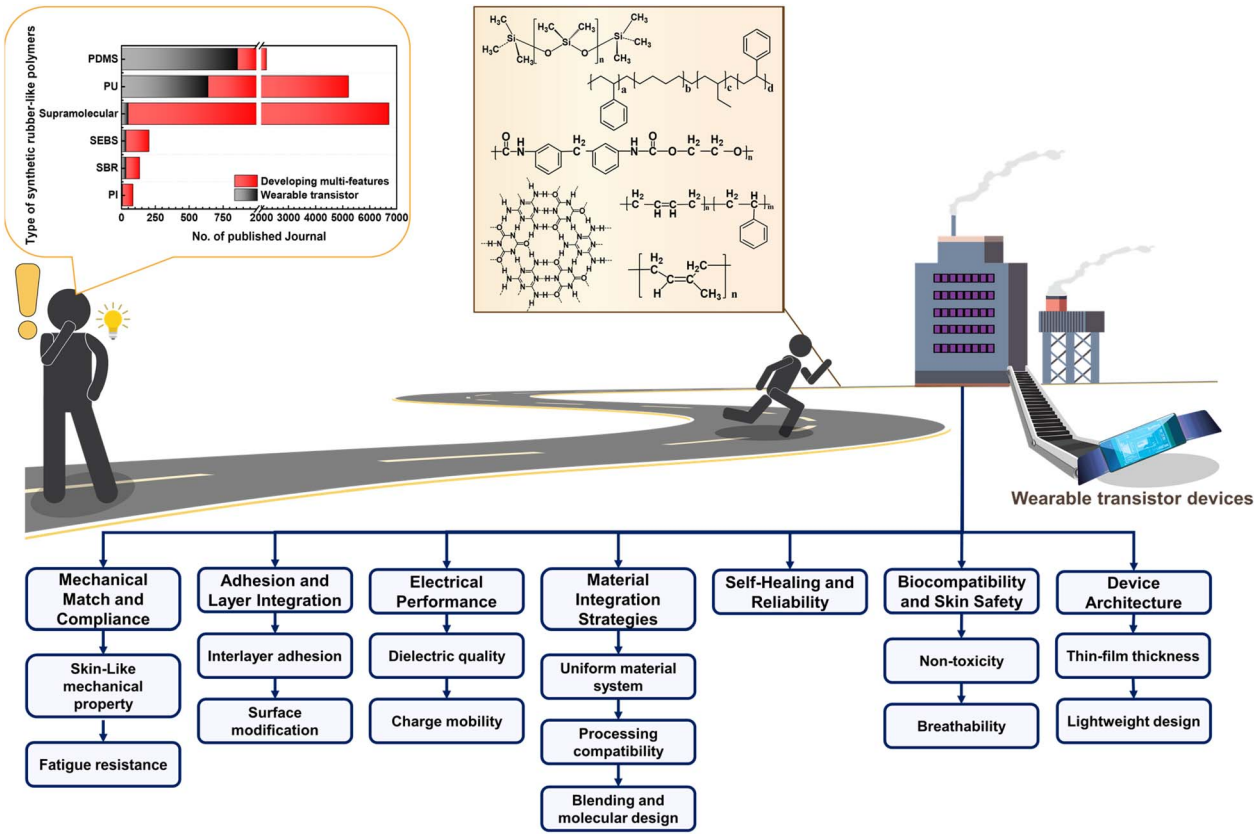

Scheme 1 Overview of rubber-like synthetic polymers: publication trends over the past 15 years (sourced from the Scopus database) comparing the number of studies focused on the development of multifunctional elastomers with those on their integration into wearable transistor devices. Representative chemical structures and diagrams highlight the current requirement to integrate elastomers into wearable transistor devices.

gate leakage, both of which are critical for stable charge transport.[17] In addition, for device reliability, elastomers that have undergone surface modification or chemical functionalization are very likely to facilitate strong interfacial adhesion with semiconducting and conductive elements.[18–22] Ultimately, rubber-like synthetic polymers provide a vital combination of properties essential for the future success of wearable transistor technologies.

Rubber-like synthetic polymers, such as polydimethylsiloxane (PDMS), polyurethane (PU), supramolecular polymers, styrene–butadiene rubber (SBR), styrene–ethylene–butylene–styrene (SEBS), and polyisoprene (PI), have opened new avenues in wearable transistor design by enabling reliable performance under mechanical stress while protecting sensitive device layers from oxygen and water ingress.[23–25] Each of these elastomers exhibits distinct advantageous properties: PDMS offers outstanding elasticity, optical transparency, and high electrical resistivity.[5,26] Its biocompatibility, crucial for continuous skin contact as demonstrated by Duffy *et al.*, who reported that PDMS does not induce cytotoxicity or skin irritation, supporting its widespread use in biomedical and microfluidic devices requiring cell or tissue contact.[26,27] These attributes make PDMS well-suited for use as a substrate, insulating dielectric, encapsulation layer, and matrix for organic semiconductors (OSCs).[18,20,28] SEBS is valued for its tissue-mimicking softness and mechanical compliance, which facilitate natural deformation and conformability to complex, dynamic surfaces, thereby enhancing device durability and processing reliability over large areas.[29,30] Additionally, SEBS offers high thermal stability and facilitates the formation of nanoconfined, phase-separated active layers with semiconducting polymers that sustain high charge mobility under mechanical strain.[29,30] PU stands out for its solvent-processable and tunable elasticity, exceptional resistance to fatigue, and easy incorporation of self-healing bonds that preserve device performance after repeated mechanical damage.[31] Beyond simple blending,[10,32] PU can be chemically integrated into the backbone or side chains of conjugated polymers, promoting stronger intermolecular interactions and controlled phase separation that result in more uniform microstructures, ultimately enhancing mechanical durability and electronic function.[33–37] Supramolecular polymers provide highly reversible non-covalent interactions that enable dynamic self-healing and stimuli-responsive behavior, allowing adaptive mechanical behavior and facile processing.[38,39] SBR serves as a stretchable dielectric owing to its mechanical compliance and elasticity, which is demonstrated by a strain to failure of 300–500% and a Young's modulus of 1–10 MPa. It also provides low-leakage insulation, with current reported as low as 10^{-9} to 10^{-11} A at 1 MV cm^{-1}. Its properties can be fine-tuned through chemical modification and

composites to meet the needs of advanced flexible circuits.[40,41] Synthetic PI features a soft, modifiable backbone, and adhesive properties.[42–49] Unlike natural rubber, synthetic PI is free of latex proteins, significantly reducing the risk of type I hypersensitivity reactions and thereby enhancing its safety profile.[50,51] When appropriately engineered, PI delivers strong electrical insulation and robust flexibility needed for reliable integration into next-generation wearable transistor.[52,53] Collectively, these polymers endure strains far above 30%, withstand moisture, abrasion, and thermal cycling, and enable irritation-free body contact, making them irreplaceable for skin-worn devices.[54]

A transformative frontier in the development of multifunctional wearable transistors is the emergence of self-healing materials. These advanced materials are capable of autonomously repairing mechanical damage, a crucial innovation poised to significantly extend device durability and maintain performance even after repeated deformation or accidental fracture, thereby addressing a key limitation of current flexible electronics.[9,55]

Self-healing mechanisms generally fall into two main categories such as covalent bonding and non-covalent bonding. Covalent self-healing relies on reversible breaking and reforming of chemical bonds to repair damage, such as Diels–Alder reactions, disulfide linkages, Schiff base formation, and boronic acid esters which typically require external stimuli like elevated temperature or light to initiate healing. In contrast, non-covalent self-healing exploits reversible dynamic intermolecular interactions including hydrogen bonding, ionic bonding, metal–ligand coordination, electrostatic interactions, π–π stacking, and van der Waals forces. These interactions often enable room-temperature (RT), rapid, and spontaneous repair without the need for external triggers.[56–60] Among rubber-like synthetic polymers mentioned above, PU and supramolecular polymers stand out due to their intrinsic chemical architectures that support effective self-healing.[31,61] PUs benefit from a combination of reversible covalent bonds, such as Diels–Alder and disulfide linkages, and dynamic non-covalent interactions including hydrogen bonding, π–π stacking, and ionic interactions. These mechanisms enable healing either through external stimuli like heat or light or spontaneously at RT.[31] Supramolecular polymers are composed of smaller molecules linked by dynamic and reversible non-covalent interactions, such as hydrogen bonding, metal–ligand coordination, and π–π stacking that facilitate spontaneous self-healing at ambient conditions.[38,61] Conversely, elastomers such as PDMS, SBR, SEBS, and PI generally lack intrinsic self-healing properties and therefore require chemical modification or incorporation of dynamic functional groups to impart self-healing functionality.[54,62,63] Integrating these self-healing abilities within transistor component, such as dielectric, substrate layers, or active layers, is critical for advancing next-generation "smart" devices that are both resilient and self-sustaining, as repeatedly demonstrated in recent advances.

While extensive research has focused on advancing the multifunctionality of rubber-like synthetic polymers through innovations in chemistry, architecture, and integration strategies[13,30,31,53,57,63] as depicted by publication trends and milestones in Scheme 1, the practical deployment of these advanced elastomers in wearable transistor devices is still at an early stage.[64] Most reported work still centers on proof-of-concept demonstrations or device prototypes, with only a handful achieving robust, long-term operation under realistic wearable conditions.[65] Distinct from earlier reviews that mainly revolve around conjugated polymers within active semiconducting layers,[12,66–71] this article systematically maps the transformative journey and multiple roles of rubber-like synthetic polymers across all layers of wearable transistor devices. We highlight not only the progress from basic substrates and dielectrics to robust integration in memory, sensors, and neuromorphic (synaptic) modules, but also delivers a clear-eyed evaluation of self-healing mechanisms, pointing out what has already been achieved and where capability gaps still limit full device autonomy. By directly contrasting this material-centric focus with prior literature and by tracing a logical progression of both successes and open challenges, this review establishes a comprehensive and actionable foundation for advancing skin-conformable, multifunctional, and resilient wearable electronics in the years ahead.

2. The revolutionary process of synthetic rubbers

This section provides a historical overview of rubber-like synthetic polymers, dating back to their transformation from early usage of simple stretchability and flexibility to modern advancements such as self-healing and their integration as functional components in transistor devices. Self-healing performance has demonstrated significant potential and has become a leading strategy to address stability and lifetime challenges in wearable transistor devices. However, integrating these materials remains challenging and must be carefully tailored to the specific transistor components. Consequently, a deep understanding of the interplay between polymer properties and device performance is essential to achieve optimal outcomes.

Beyond ensuring functional and mechanical compatibility, materials intended for direct skin contact must also demonstrate long-term biocompatibility and non-irritation to safeguard user comfort and health during prolonged wear. Accordingly, the final subsection focuses on the safety profile of these polymers, presenting evidence from *in vivo* and *in vitro* clinical studies and animal cytotoxicity tests that confirm their suitability for integration into wearable electronic systems designed for continuous skin contact. Therefore, Section 2 commences with a concise evaluation matrix that outlines critical material criteria based on their potential functionality to be applicable in the organic thin film transistor devices, including roles as semiconducting, dielectric, or substrate layers. This framework encompasses essential parameters such as mechanical modulus and elongation, charge carrier mobility, dielectric constant, breathability, processability, and biocompatibility, providing a standardized basis for systematically assessing each rubber-like synthetic polymer throughout the section.

2.1. Polydimethylsiloxane (PDMS)

The synthesis of PDMS traced back to the 1940s with the Müller–Rochow process, wherein methylchlorosilanes were generated through the reaction of elemental silicon with methyl chloride. These reactive intermediates subsequently underwent hydrolysis and polymerization, yielding flexible siloxane polymer chains.[72–74] Early commercialization attempts were hindered by significant challenges related to process scalability and the management of undesirable byproducts. Pioneering companies such as Dow Corning spearheaded efforts to optimize catalytic systems, explore alternative precursor materials, and refine purification methodologies, thereby mitigating byproduct formation and enhancing polymer quality.[2,75–78] The advent of ring-opening polymerization techniques for cyclic siloxanes in the 1970s marked a pivotal advancement, enabling precise control over polymer architecture and molecular weight distribution. This breakthrough facilitated the large-scale production of high-purity PDMS with reduced impurities, laying the groundwork for its eventual widespread adoption in flexible electronics.[79,80] Fig. 1a illustrates this historical development and key milestones of PDMS. By the late 1990s, PDMS had become a material of choice for flexible transistor substrates, owing to its exceptional elasticity, optical transparency, chemical inertness, and biocompatibility.[5,26,81] While conventional PDMS forms a dense (non-porous) material that acts as a strong barrier against gases and moisture, the fabrication of porous PDMS structures has emerged as a valuable strategy to further enhance comfort during prolonged skin contact in wearable devices. Introducing controlled porosity allows PDMS to retain its excellent mechanical flexibility and dielectric properties while permitting the passage of sweat vapor and moisture, thereby significantly improving breathability and reducing skin irritation, which is a critical factor for next-generation skin-conformal electronics.[3,26,27] Nonetheless, PDMS inherently exhibits a hydrophobic surface with low surface energy posed formidable obstacles to the uniform deposition of semiconductor layers and device stability.[11,15,82] To circumvent these limitations, advanced surface engineering strategies such as plasma treatment[83] and ultraviolet-ozone treatments[18,84,85] were employed to oxidize methyl groups ($-CH_3$) on the PDMS surface, generating hydroxyl and other polar functionalities that enhance surface wettability and facilitate subsequent chemical modifications. A quintessential example was illustrated in the work by Gu *et al.*, where PDMS substrates underwent sequential surface modification involving piranha solution treatment followed by UV-ozone exposure. The piranha solution, a potent oxidizing mixture of sulfuric acid (H_2SO_4) and hydrogen peroxide (H_2O_2), effectively converted hydrophobic moieties into hydrophilic silanol (Si–OH) groups, substantially increasing surface energy and wettability, as depicted in Fig. 1b. Subsequent UV-ozone treatment further augmented silanol density and induced the formation of a silica-like surface, stabilizing the hydrophilic state. This dual modification protocol significantly improved the affinity of the PDMS stamp for the IGZO precursor solution, enabling uniform ink adsorption and precise pattern transfer. The resulting amorphous IGZO thin-film transistors exhibited a field-effect mobility of 6 $cm^2\ V^{-1}\ s^{-1}$, an on/off current ratio of $\sim10^8$, a low leakage current of $\sim10^{-11}$ A, and a narrow hysteresis of 0.2 V.[18] These findings underscore the critical role of surface modification in transforming PDMS into a reliable, high-performance stamping substrate for thin-film transistor fabrication.

The utilization of PDMS as a substrate in stretchable transistors has naturally extended to its deployment as a dielectric layer owing to its remarkable insulating properties, including high electrical resistivity (10^{12}–10^{14} Ω cm), wide dielectric breakdown strength (250 to 635 V μm^{-1}), and low dielectric loss (0.02 and 0.036), all coupled with superior mechanical flexibility.[17] However, PDMS suffers from intrinsic limitations such as thermal instability, pronounced electrical leakage, low surface energy, and a relatively low dielectric constant (~2.8).[86] These deficiencies can be effectively ameliorated through advanced surface modification techniques, including physical mixture with nanoparticles,[87] plasma treatment,[88] and chemical treatments.[89] For instance, plasma treatment introduces polar functional moieties onto the PDMS surface, thereby augmenting wettability and fostering enhanced adhesion with organic semiconductors. Qin *et al.* elucidated that soft plasma treatment substantially increased the surface energy of PDMS while reducing its hydrophobicity, culminating in a uniform and defect-minimized dielectric–semiconductor interface.[88] The introduction of abundant –OH and SiOx groups also creates a high density of charge trapping sites at the dielectric–semiconductor interface, which further affects the electrical performance as discussed in the artificial synaptic electronic section (Fig. 1c). Collectively, these findings underscore the critical role of soft plasma surface modification and the underlying surface oxidation mechanism in transforming PDMS into a reliable, high-performance dielectric layer for flexible artificial synaptic transistor fabrication. One approach to promote the dielectric value of PDMS involves the incorporation of nanoparticles such as silver, Al_2O_3, and carbon into PDMS matrix.[20] Furthermore, the incorporation of functional coatings such as polydopamine introduces carboxyl (COOH) groups into PDMS composites. These groups engage in robust hydrogen bonding and electrostatic interactions primarily with the hydroxyl groups (OH) of silanol (Si–OH) on PDMS chains and embedded nanoparticles. These interfacial interactions intensify polarization effects, substantially elevating the dielectric constant from approximately 2.8 to values exceeding 10, while concurrently preserving dielectric stability under tensile strains ranging from 30 to 50%.[89]

Leveraging PDMS's inherent elasticity, researchers have employed it to enhance organic semiconductors (OSCs) for stretchable transistors, addressing the intrinsic brittleness of OSCs.[25] The most prevalent and effective approach involves physically blending PDMS with OSCs, wherein the elastomeric PDMS matrix confines the OSCs domains at the nanoscale.[28] This confinement acts as a flexible scaffold that absorbs mechanical strain, reduces stress concentration, and prevents crack formation within the OSCs regions. By limiting polymer chain displacement and preserving molecular ordering, the PDMS matrix maintains continuous charge transport pathways,

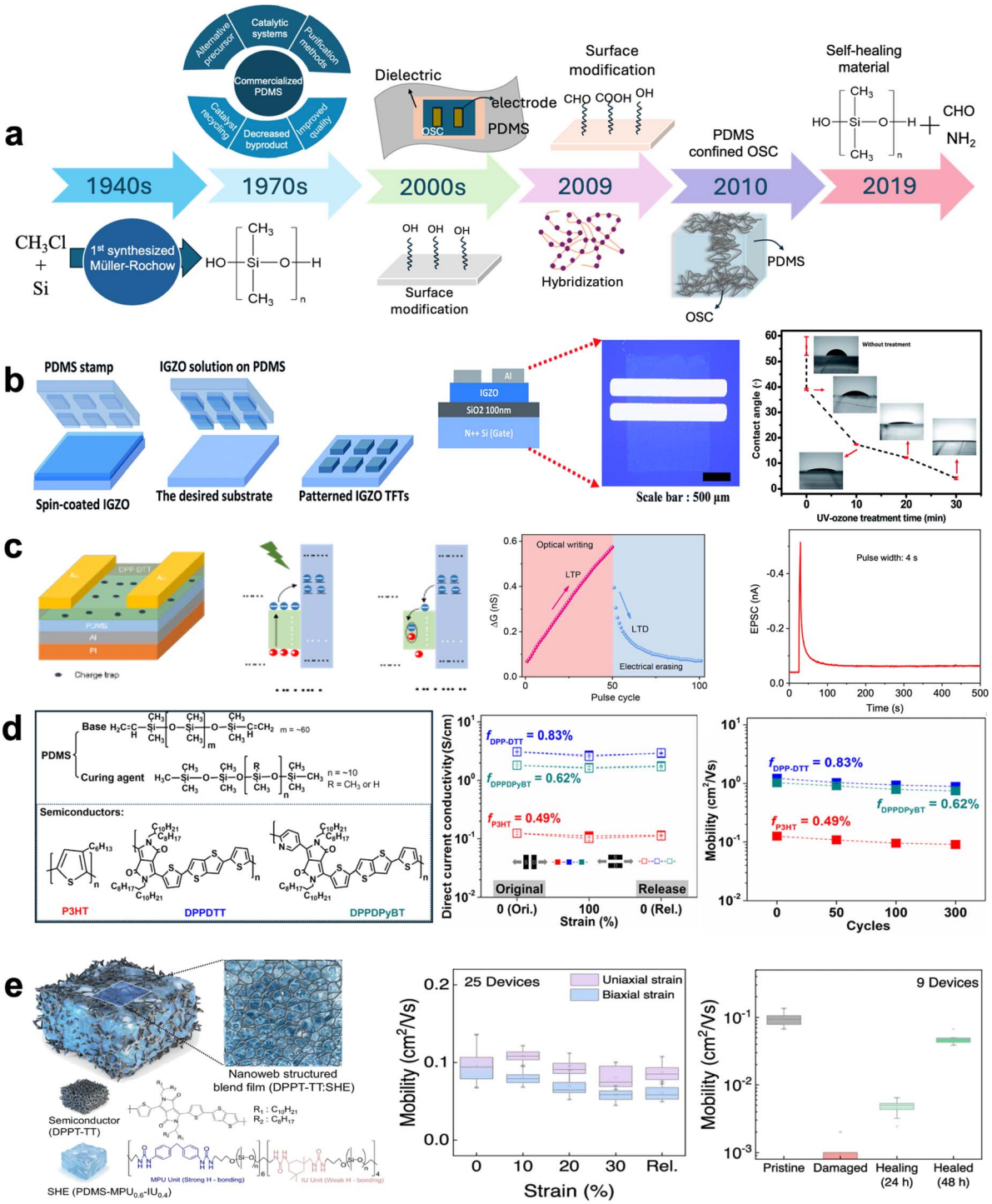

Fig. 1 Overview of PDMS evolution from its initial synthesis to advanced applications in stretchable transistor technologies. (a) Historical timeline and key milestones in PDMS synthesis, commercialization, and its integration into electronic devices, highlighting how advances in PDMS chemistry have enabled its use in transistor components and the development of self-healing capabilities. (b) Schematic of PDMS surface modification and its use as a stamping substrate for precise patterning and fabrication of high-performance thin-film transistors. (c) Strategies to enhance the dielectric properties and interfacial compatibility of PDMS *via* chemical treatments to improve device stability and performance. (d) Blending PDMS with organic semiconductors (OSCs) to form nanoscale-confined OSC domains within the PDMS matrix, resulting in high stretchability and robust charge transport under mechanical deformation, but without intrinsic self-healing capability. (e) A distinct self-healing strategy using a nanoweb-structured blend of DPPT-TT semiconductor and a PDMS-based elastomer with dual-strength hydrogen bonds, enabling rapid autonomous self-healing at RT and preserving device mobility and performance after repeated damage and strain. Adapted with permission from ref. 18 copyright 2016 Royal Society of Chemistry, ref. 88 copyright 2023 Elsevier, ref. 90 copyright 2017 American Chemical Society, and ref. 63 copyright 2024 Springer Nature.

enabling devices to endure large strains without significant degradation in electrical performance.[91,92] For example, Zhang *et al.* demonstrated that incorporating a small fraction of semiconducting polymer (<1 wt%) into a PDMS matrix yields stretchable composites that retained or even surpassed the electrical performance of pristine films.[90] This enhancement was attributed to PDMS acting as a compliant elastomeric scaffold, confining polymer domains at the nanoscale, mitigating strain localization, and suppressing crack initiation. Notably, blends with high-mobility semiconducting polymers (such as DPP-DTT and DPPDPyBT) sustained field-effect mobilities above 1 $cm^2\ V^{-1}\ s^{-1}$, even under 100% strain, while P3HT/PDMS blends achieved mobilities up to 0.17 $cm^2\ V^{-1}\ s^{-1}$ (Fig. 1d). These results indicated that the interpenetrating network structure preserved charge transport pathways despite mechanical deformation. However, compared to systems with covalently integrated architectures, such physically blended networks may still exhibit less control over microstructural organization and phase uniformity, potentially limiting further enhancements in stretchability and electronic performance.[28,90] This finding underscores that while PDMS blending effectively preserves short-range molecular ordering and mobility, achieving simultaneous optimization of high mobility and mechanical resilience requires more precise microstructural control beyond simple blending. Overall, these strategies demonstrate that physical blending with PDMS effectively maintains and improves both the mechanical integrity and electrical properties of OSCs in flexible and stretchable transistors, establishing PDMS as a foundational material for next-generation flexible electronics.

Of prime concern, although stretchable transistors can endure repeated mechanical strain during cycling, microdamage inevitably accumulates over time.[9,55] To address this, incorporating self-healing materials into PDMS has emerged as an effective strategy to impart autonomous repair capabilities. Oh *et al.* engineered PDMS-based stretchable semiconducting films by blending a DPP polymer containing PDCA units with a PDMS elastomer functionalized with PDCA ligands. Upon addition of Fe(III) ions, dynamic metal–ligand coordination bonds formed between PDCA groups in the polymer and elastomer, creating a flexible, reversible cross-linked network within the low-modulus PDMS matrix.[59] These bonds broke and reformed under strain, enabling stress relaxation and autonomous self-healing by repairing microcracks. Concurrently, nanoscale phase separation preserved interconnected semiconducting domains, maintaining continuous charge transport pathways. The composite exhibited fracture strains above 1300% and retained field-effect mobility ($\sim$0.1 $cm^2\ V^{-1}\ s^{-1}$) after repeated stretching and healing cycles, demonstrating that dynamic metal–ligand cross-linking in PDMS effectively integrates mechanical resilience with electrical functionality in stretchable transistors. Recently, Vo *et al.*[63] developed a self-healing elastomer (PDMS–$MPU_{0.6}$–$IU_{0.4}$) by reacting amine-terminated PDMS with two diisocyanates (MPU and IU), introducing dual-strength hydrogen bonds, which depicted in Fig. 1e. Strong MPU bonds provide elasticity, while weaker IU bonds dissipate energy and prevent aggregation. Subsequently, the self-healing elastomer was blending with DPP polymer to preserve the electrical performance and to impart self-healing ability to the material. This device autonomously self-heal at RT with about 80% healing efficiency after 24–48 hours and maintain stable electrical performance under strains up to 30% (Fig. 1e). The transistors exhibit an initial field-effect mobility of approximately 1.3 $cm^2\ V^{-1}\ s^{-1}$ and retain functional mobility around 0.07 $cm^2\ V^{-1}\ s^{-1}$ after 100 cycles of mechanical stretching and healing at 30% strain. Their nanoscale phase-separated morphology preserves charge transport pathways, enabling rapid recovery and long-term ambient stability without encapsulation, making them promising for wearable transistor electronics.

2.2. Polyurethane (PU)

PU was first synthesized in 1937 by Otto Bayer and his team at IG Farben in Germany, who developed the foundational diisocyanate-polyol chemistry that enabled the creation of both rigid and flexible polymers.[93] In the early 1950s, polyisocyanates were commercially available and the combination of toluene diisocyanate (TDI) with polyester polyols enabled the large-scale production of flexible polyurethane foams, rapidly expanding its use in insulation, cushioning, and automotive components. PU elastomers, which have potential self-healing properties, are generally categorized according to the dynamic bonding mechanisms, such as reversible covalent bonding, reversible non-covalent bonding, and a combination of multiple bonds as presented in Fig. 2a.[31] On the other hand, PU mechanical properties can be tuned by adjusting the NCO/OH ratio, chain extension coefficient, hard segments content, and the chain length.[94] Another researcher reported that synthesizing hydroxyl-functionalized aromatic pinacol as initiator into crosslinked-PU resulted in self-healing and recycling properties. The mechanism relied on the high bond energy of the C–C bond of pinacol as well as the hydrogen bond between hard segments and semicrystalline soft segments. Therefore, the dynamic equilibrium of pinacol enables self-healing and recycling of the polymer.[95] Further utilization in wearable electronics and sensors emerged prominently, coinciding with advances in flexible materials that could conform to human skin and body movements. The scale-up and commercialization of PU-based wearable devices accelerated after 2010, driven by the increasing demand for health monitoring and human–machine interfaces. PU primarily serves as a dielectric layer but recently has also shown potential to be applied as a semiconductor layer. One common problem occurred in transistor device is current leakage, that can be addressed by introducing a dielectric layer into transistor configuration as an insulating barrier.

For example, Li's group investigated the use of *para*-sexiphenyl (*p*-6P)/vanadyl-phthalocyanine (VOPc) and introduced a PU-based dielectric layer capable of modulating the charge flow in the device.[33] A solution-processable photosensitive PU was fabricated through a UV light cured crosslinking reaction, resulting in a reduced free volume within the dielectric layer. This reduction in free volume, combined with a non-pinhole surface morphology, led to a substantial decrease in leakage

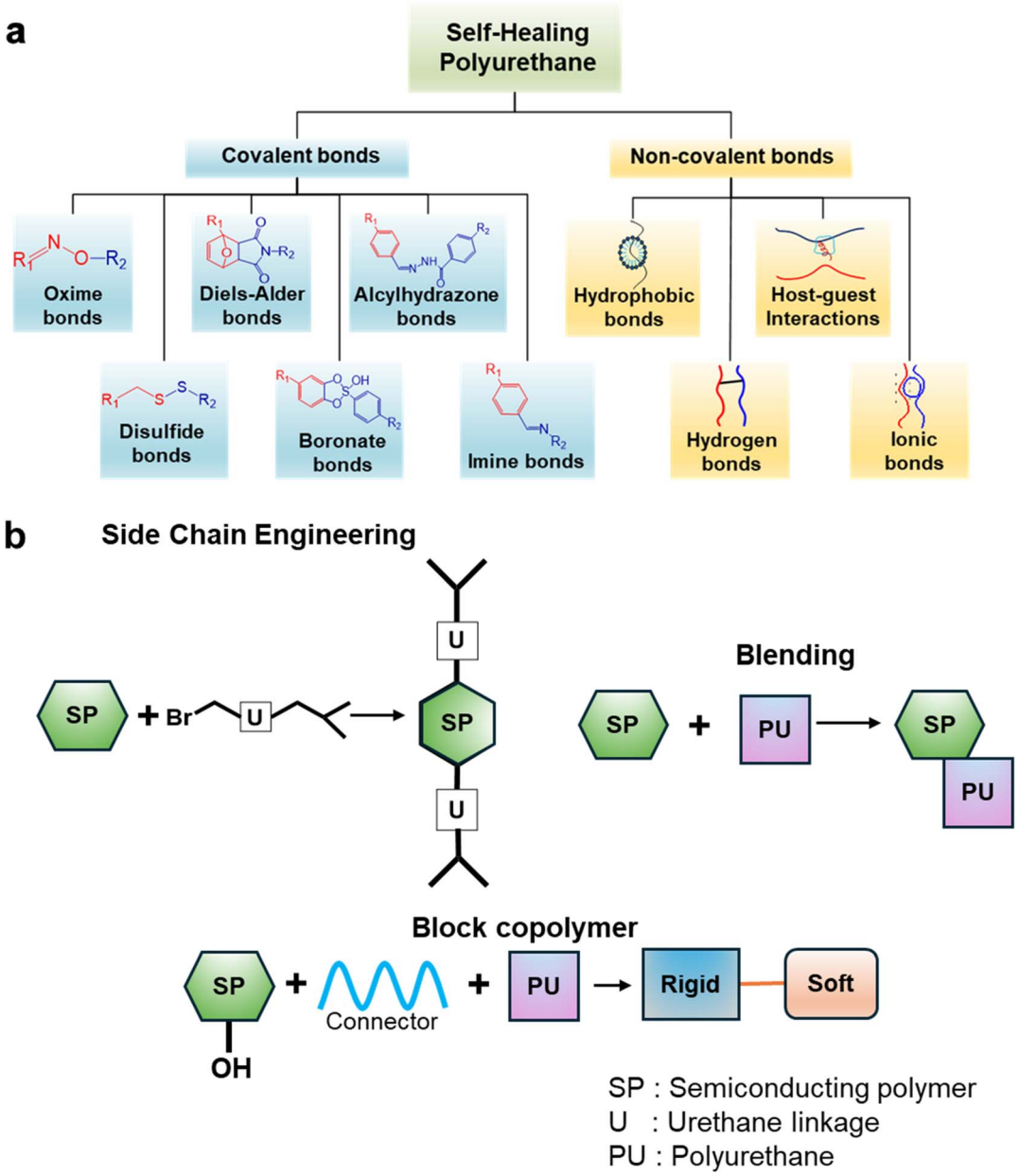

Fig. 2 Schematic overview of self-healing mechanisms in PU systems. (a) Key reversible interactions enabling healing, categorized into non-covalent (hydrophobic, hydrogen, ionic, and host-guest) and covalent (oxime, disulfide, Diels–Alder, alicyhydrazone, boronate, and imine) bond types. (b) Design strategies for fabricating stretchable and self-healing semiconducting PU, including side-chain engineering, block copolymer formation, and physical blending approaches.

current, reaching values as low as 1×10^{-5} A, while maintaining excellent device performance characterized by a mobility of 0.13 $cm^2 V^{-1} s^{-1}$ and an on/off current ratio of 10^4.[33] Barreto's group invented a high *k*-value dielectric for the purpose of PMMA alternative by applying PU material in OLET devices.[35] The synthesized PU from block copolymers with alternating soft segment based on THF and hard segment based on 4,4 methylene diphenyl diisocyanate and 1,4 butane diol resulted in a reduction in the number of traps, exhibited low operating voltage (0–10 V) enhancing V_{th} (−6.5 V), higher mobility, optical power output in the devices. Kim's group invented a self-healing polyurethane with novel functionality for fully recoverable layered sensor arrays.[96] The synthesized oxime–carbamate bond-based polyurethane (OC-PU) was fabricated through a step polymerization process by combining soft segments such as PTMG and PDMS, IPDI as hard segment, while using DMG and DETA as chain extenders and cross-linkers. The hydroxyl and aminopropyl groups at the ends of PTMG and PDMS, respectively, react with the isocyanate group of IPDI, resulting in the formation of urethane and urea groups. These newly formed groups establish numerous hydrogen bonds, creating weak interactions throughout the polymer. Such interactions

not only enhance stretchability by acting as sacrificial bonds during mechanical deformation but also facilitate the self-healing of the polymer when heated above its glass transition temperature (T_g). To further tailor the polymer's properties, DMG was introduced as a chain extender, reacting with the terminal isocyanate groups of the prepolymer to incorporate thermo-reversible oxime–carbamate bonds within the polymer chain. Each segment of the resulting polymer contributes distinct characteristics to OC-PU, collectively imparting stretchability, self-healing ability, and transparency, making it an ideal candidate for use as a soft substrate. These mechanisms demonstrated outstanding mechanical performance of OC-PU elastomer, featuring an elongation at break of 1076%, a Young's modulus of 1.2 MPa, and an impressive self-healing efficiency of 93.7% when heated to 65 °C.

To address the inherent brittleness of polymer-based semiconductors while enhancing their mobility, researchers have made significant breakthrough by implementing into two common methods including introduced PU into backbone or side chain of conjugated polymers, another way is conjugated polymers modification by using physical blending of PU and chemical cross-linking *via* urethane linkage. The implementation of applying main-chain and side-chain engineering to diketopyrrolopyrrole (DPP)-based polymers through the introduction of urethane linkages have been performed by prior researchers. For example, Lee's group enhanced the stretchability of DPP-based alternating copolymers by incorporating urethane groups into their side chains (Fig. 2b).[36]

This modification introduced long-branched urethane side chains with moderate hydrogen bonding strength, which not only improved solubility but also provided dynamic bonding that effectively dissipates mechanical stress. As a result, $PDPP_{urethane}$ thin films exhibited exceptional stretchability, sustaining up to 100% external strain without compromising electrical performance in organic transistor applications (Fig. 3a–e). Similarly, Pei's group synthesized polyurethane (PU) multiblock oligodiketopyrrolopyrrole copolymers *via* urethane linkage copolymerization (Fig. 3f) by optimizing the ratio of hard and soft domains to achieve remarkable mechanical and electronic performance, including over 300% crack onset strain, a maximum hole mobility of 0.19 $cm^2 V^{-1} s^{-1}$, and high elastic recovery (ER) under large strain of 175%.[37] Also, several researchers developed wearable and adaptive devices by incorporating carbon nanotube (CNT) and graphene into synthesized PU composites as additive resulted in enhanced tensile strength and elasticity, further improved conductivity and sensing performance properties.[10,32] These studies collectively demonstrate that urethane linkages serve as dynamic, hydrogen-bonding motifs that reinforce polymer networks, balancing mechanical flexibility with charge transport, thereby advancing the development of highly stretchable, durable semiconductor materials suitable for flexible electronics.

2.3. Supramolecular polymers

Supramolecular polymers were first synthesized rooted on the self-assembly of monomers through reversible bonds.[97] Notably, simple methods involving dissolving components in molten liquids enabled scalable production of polymers containing multiple dynamic interactions such as covalent disulfide bonds, hydrogen bonds, and metal coordination–offering low-temperature processability and autonomous repair capabilities resulting in materials with distinctive features ultrahigh stretchability, rapid self-healing ability, and reusable adhesivity.[38] Building on the dynamic and scalable supramolecular polymer systems enabled by reversible bonding, recent developments also explore how solution processing conditions control polymer self-assembly, crystallinity, and ultimately device performance. For instance, Zheng's utilized a benzodifurandione-derived oligo(*p*-phenylene vinylene) (BDOPV) polymer, characterized as a donor–acceptor (D–A) conjugated polymer featuring intricate molecular architecture and a higher number of atoms within each repeating unit. By employing a co-solvent approach, the polymer's solution-state configuration was manipulated to promote one-dimensional rod-like self-assembly in good solvents, while two-dimensional lamellar structures predominated in poor solvents.[98] Recognizing the correlation between solution-state configurations and solid-state morphologies, the solution environment was precisely controlled to produce films exhibiting enhanced crystallinity without compromising interdomain connectivity. Consequently, this optimized film demonstrated a nearly twofold increase in electron mobility, reaching 3.2 $cm^2 V^{-1} s^{-1}$. The improved crystallinity was attributed to the enhanced polymer aggregation triggered by the presence of the poor solvent in the mixed solvent system. Beyond solution-state polymer assemblies, supramolecular interactions also play a crucial role in dispersing carbon nanotubes and influencing device-level electrical behavior. Several researchers further employed single-walled carbon nanotube (SWCNT) as electrode and semiconducting layer. For example, Chortos's group employed SWCNTs of varying diameters to investigate the factors that restrict charge transport in all-carbon stretchable transistors using low-capacitance nonpolar dielectric materials.[99] SWCNTs were dispersed by utilizing a supramolecular polymer created *via* hydrogen bonding between didodecylfluorene units. Centrifugation was performed afterwards, causing the metallic SWCNTs to sediment into a pellet while the semiconducting SWCNTs remained suspended in the solution. The study showed that polar groups on the surface enhance the adhesion of the SWCNTs. On the other hand, these polar groups may serve as trap sites, leading to hysteresis due to charge trapping during the gate voltage sweep. Additionally, the presence of polar surface groups can cause a shift in the threshold voltage. This effect is further intensified because polar groups tend to attract dopants like oxygen and water. Among the evaluated SWCNT sources, those with a maximum diameter of 1.5 nm exhibited the highest performance, achieving a mobility of 15.4 $cm^2 V^{-1} s^{-1}$ and an on/off ratio $>10^3$ in stretchable transistors. Devices featuring a large band gap demonstrated greater sensitivity to strain due to a strong dependence on dielectric thickness, while contact-limited devices were significantly less affected by strain.

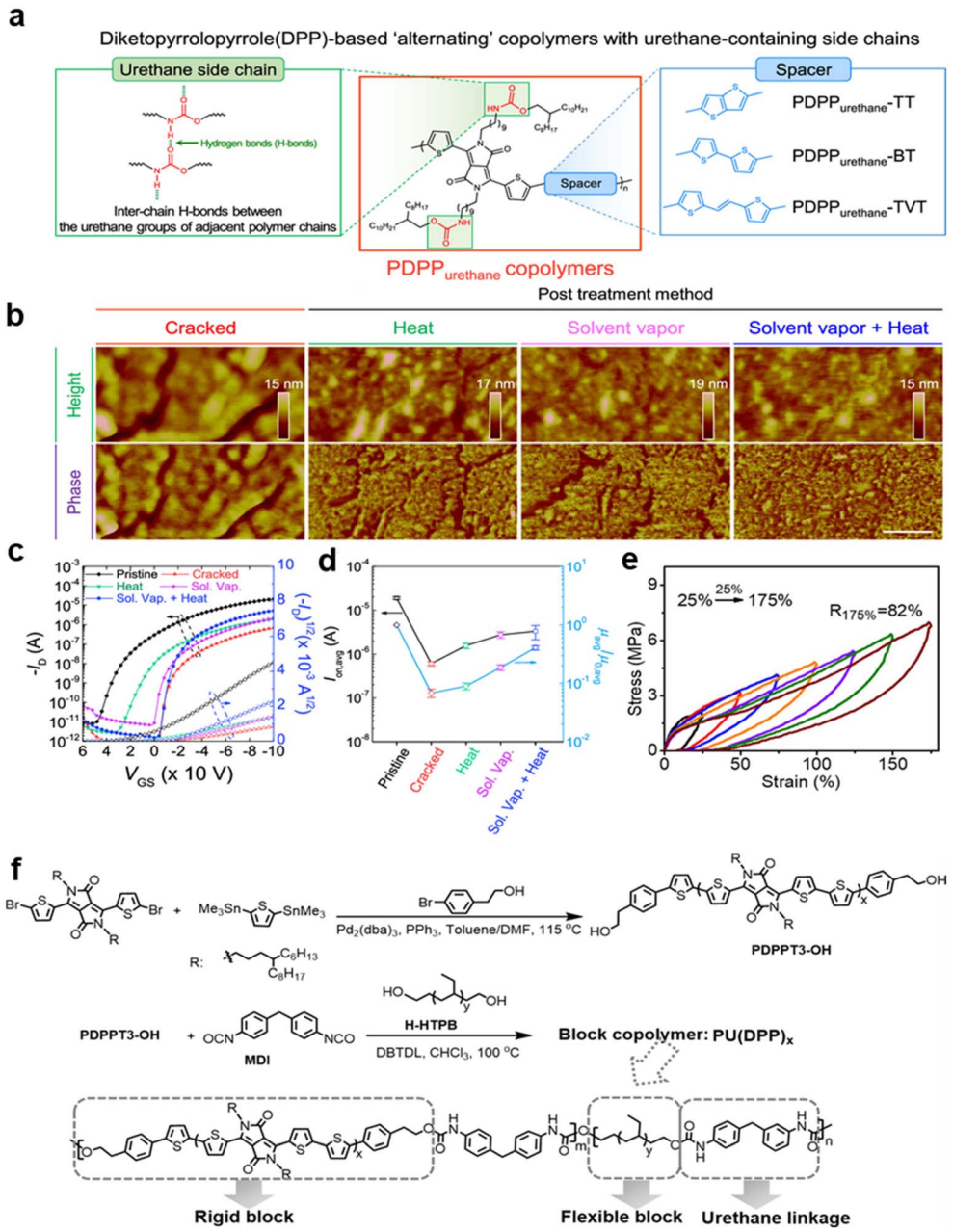

Fig. 3 (a) Molecular structures of PDPPurethane copolymers, (b) AFM height and phase images of the cracked thin films of PDPPurethane-TVT by 10 cycles of stretching with 130% strain and the self-healed thin films of PDPPurethane-TVT based on various post-treatments (*i.e.*, heat, solvent vapor, solvent vapor + heat), (c) transfer characteristics and (d) average on-current ($I_{on,avg}$) and relative hole mobility (average mobility/average mobility from a pristine thin film, $\mu_{avg}/\mu_{0,avg}$) of the cracked and healed films of PDPPurethane-TVT using various post-treatments, (e) ER under individual strain from 25% to 175% with load–unload cycles (f) synthetic route to the polyurethane block copolymers PU(DPP)$_x$, ref. 36, and 37 copyright 2020 & 2022 American Chemical Society.

Then, the exploitation of supramolecular polymers evolved into stretchable and flexible materials. The breakthrough innovation was initiated by Zhang's group that exploited Thioctic Acid (TA) synthesized into poly(TA-DIB-Fe) copolymer featured supramolecular polymeric materials with dynamic covalent disulfide bonds, noncovalent H-bonds, and iron(III)–carboxylate coordinative bonds.[38] The synthesis mechanisms relied on one-pot reaction of molten TA liquid, 1,3-diisopropenylbenzene (DIB), and iron(III) chloride ($FeCl_3$). Upon TA heating, the five-membered ring containing the disulfide bond undergoes thermally initiated ring-opening polymerization driven by dynamic disulfide exchange. During the subsequent cooling, the material transitions into a fluidic liquid characterized by a linear covalent backbone, while carboxylic side chains simultaneously dimerize through hydrogen bonding to efficiently cross-link the linear poly(TA). The addition of DIB quenches the terminal diradicals, further strengthening the network through covalent cross-linking.

Finally, introducing $FeCl_3$ partially replaces the weaker hydrogen bonds, enhancing the overall stability of the structure. The synthesized material demonstrated excellent stretchability and mechanical strength ([TA-to-iron(III) molar ratio of 18 000 : 1] for a strain of 15 000%.) due to the presence of three types of dynamic chemical bonds such as dynamic covalent disulfide bonds, hydrogen bonds, and iron(III)–carboxylate coordinative bonds. These bonds enable the network to stretch through a hierarchical energy dissipation mechanism. Additionally, the dry network contains a high density of cross-linking sites, resulting in highly folded polymer chains that facilitate easier chain sliding by reducing the distances between chains. Furthermore, the abundance of carboxylic groups in the poly(TA-DIB-Fe) copolymer promotes hydrogen bonding with polyhydric surfaces, making this copolymer a promising candidate for surface adhesive applications.

Furthermore, Yoon's group demonstrated a wearable ion-sensing platform constructed from a bio-derived supramolecular polymer network engineered with dynamic hydrogen-bonding motifs.[100] The material structure was developed by applying a durable supramolecular polymer based on esterified-CA/SA/CHDM coating onto the surface of carbon fiber thread (CFT) electrodes as presented in Fig. 4a. Anchored onto the potentiometric ion-sensing thread, this polymer layer endowed the system with inherent self-healing properties (Fig. 4b and c). The moderate cross-link density of citric acid facilitates the formation of a diffusible, pseudo-tetra-armed three-dimensional network. Moreover, the presence of unreacted carboxylic acid and hydroxyl groups enables intermolecular hydrogen bonding, which drives supramolecular self-assembly and promotes self-healing. Succinic acid plays a vital role by preventing excessive cross-linking, thereby achieving a balance between mechanical strength and healing efficiency. Finally,

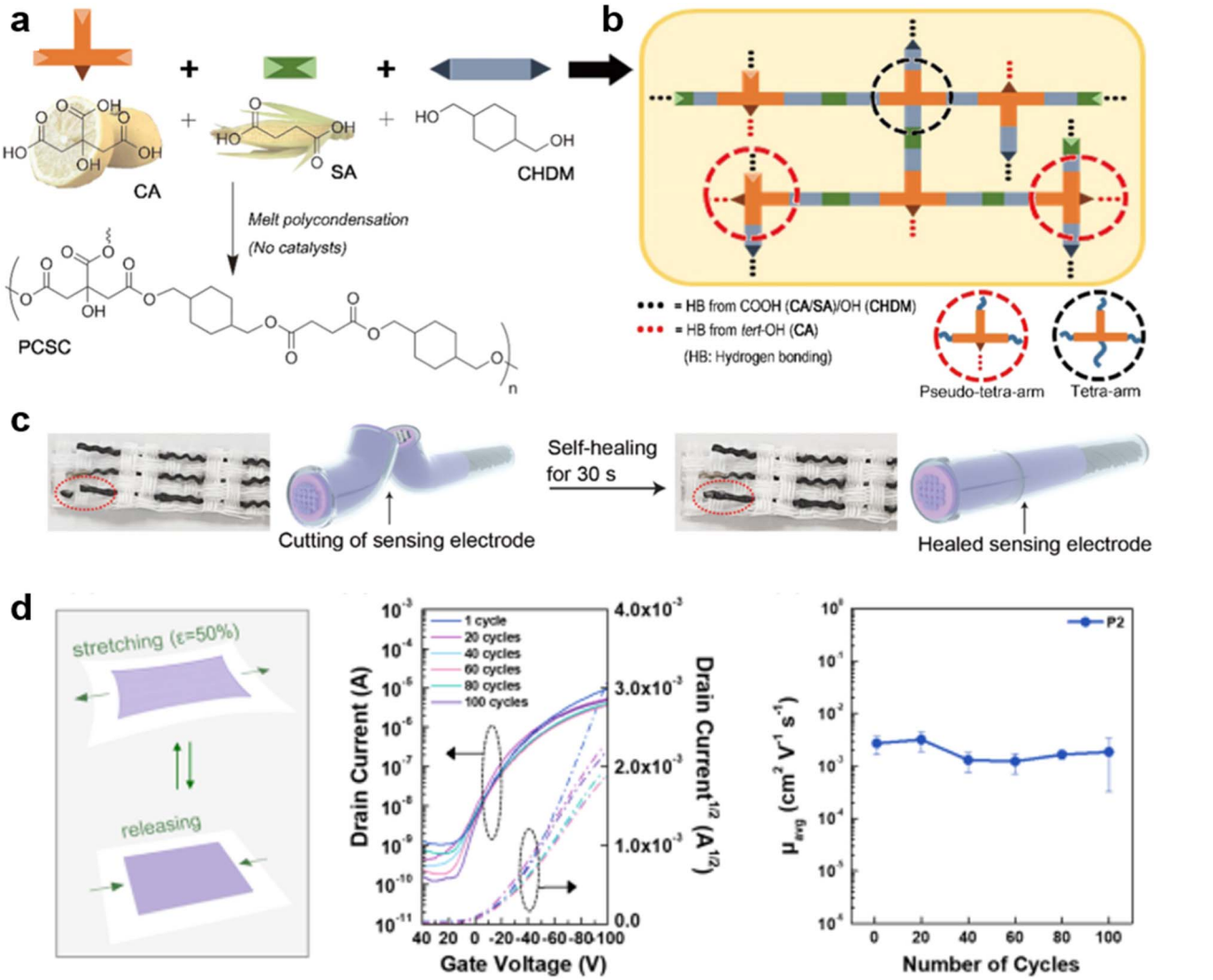

Fig. 4 (a) Synthesis of self-healable supramolecular polymer (PCSC), (b) illustration of chemical structure of PCSC and self-healing *via* hydrogen bonding, (c) photographs and schematic diagrams depicting the ion-sensing electrodes before cutting and after healing, (d) repeated stretching/releasing tests and their impact on PS_{161}–Zn–$P3HT_{187}$. The schematic illustrates the 50% strain cycle. Transfer curves and corresponding mobility changes of PS_{161}–Zn–$P3HT_{187}$ are shown after 1, 20, 40, 60, 80, and 100 cycles, with strain applied parallel to the charge transport direction, ref. 61 and 100 copyright 2019 & 2022 American Chemical Society.

the reversible conformational transitions between the *e*,*e-trans* and *a*,*a-trans* isomers of the cyclohexylene ring in CHDM impart flexibility to the polymer chains, enhancing chain mobility without sacrificing mechanical integrity. Consequently, this wearable sweat-sensor system enabling seamless textile integration while achieving > 97% mechanical restoration within 30 seconds at 25 °C. Another study by Wu's group discussed applied the coordination-driven self-assembly strategy to simplify the creation of stretchable polymer semiconductors.[61] The metallo-supramolecular diblock copolymers were constructed *via* dynamically linking polystyrene (PS) and poly(3-hexylthiophene) (P3HT) blocks through zinc-mediated bonds, resulted in two block copolymers with varied PS chain lengths. Both materials matched the electrical performance of pure P3HT in relaxed states but excelled under strain. The incorporation of an additional PS block significantly improves the deformability of semiconducting polymers. This improvement arises due to the amorphous coil chains within the PS block can absorb external strain and delay the initiation of cracks. Due to their disordered, amorphous structure, these coil chains provide ample space for chain mobility, allowing the material to endure greater strain without substantially impairing charge transport. Moreover, the dynamic metal–ligand coordination bonds linking the rigid rod and flexible coil segments facilitate chain alignment under mechanical stress. This enhances stretchability by increasing the polymer's modulus, expanding the amorphous domain, and preserving moderate to high charge mobility through interchain hopping. In contrast, blending experiments using P3HT and terpyridine-modified PS without zinc complexation were conducted to assess the role of amorphous PS alone. These findings highlight that block copolymer architectures outperform blends in achieving the desired combination of stretchability and charge transport for flexible electronics. Treatments with a longer PS segment, maintained mobility from 5.48×10^{-3} to 1.40×10^{-3} $cm^2\ V^{-1}\ s^{-1}$ even at 100% stretching and survived 100 stretch–release cycles at 50% strain Fig. 4d. The enhanced stretchability and minimal mobility loss stem from the flexible PS chains dissipating strain energy, while the P3HT preserved charge transport. This metallo-supramolecular approach effectively balances mechanical resilience and electrical stability, offering a scalable route for durable wearable electronics.

2.4. Styrene butadiene rubber (SBR)

In the late 1920s, Walter Bock and Eduard Tschunkur successfully synthesized SBR through an emulsion polymerization process by combining a balanced proportion of styrene and butadiene, free-radical initiators (*e.g.* potassium persulfate), emulsifiers and chain transfer agents to control polymer growth. Both cold emulsion (5 °C) and hot emulsion polymerization (50–60 °C) can be performed, allowing flexibility in production conditions.[101] The resulting copolymer typically contains 10–25% styrene and 75–90% butadiene, with molecular weights between 100 000 and 300 000 g mol^{-1}, optimized to deliver strong mechanical properties such as elasticity and abrasion resistance.

Over the decades, SBR and related block copolymers like styrene–butadiene–styrene (SBS) have found new life in wearable electronics attributed to their excellent elasticity and durability. Early studies by Helaly's group demonstrated that inorganic fillers such as lead silicate and burnt mazote boiler deposits notably enhance the vulcanization rate, tensile strength, and abrasion resistance of SBR, while fillers like aluminium oxide and ilmenite reduce the dielectric constant, tailoring the composite's electrical insulation characteristics.[102] Building on this foundation, a paper-form solid electrolyte combining $Rb_4Cu_{16}I_7Cl_{13}$ was fabricated with SBR achieved high ionic conductivity (3×10^{-3} S cm^{-1}) and improved damp resistance at an optimal 65 vol% SBR content, marking an early integration of SBR in electrochemical devices. Comparable electrical conductivities of PU to polyaniline (PANI) was furtherly reported, highlighting the growing interest in conductive polymer composites.[103] The field advanced markedly by Lee's group that reported the fabrication of highly stretchable conductive fibers embedding silver nanowires and nanoparticles within a SBS elastomer matrix *via* wet spinning and *in situ* silver (Ag) reduction.[104] The achieved outstanding properties such as electrical conductivity (2450 S cm^{-1}), exceptional elongation at break (900%) and stable conductivity retention under strain enabled real-time human motion detection in smart gloves (Fig. 5a and b). Further innovations by Wang's group involved utilizing SBS combined with few-layer graphene to create highly sensitive, stretchable strain sensors. Fabricating process was applied through wet-spinning method relied on strong interfacial interactions.[105] The resulting SBS/FLG fiber-based strain sensor demonstrated outstanding performance, featuring a broad workable strain range exceeding 110% and exceptional sensitivity, with a gauge factor of 160 at 50% strain and an impressive 2546 at 100% strain and the stability of conductive graphene networks were analyzed (Fig. 5c). Moreover, numerous approaches in enhancing electromechanical properties have been reported by incorporating CNT as fillers. The reinforcement suggested through π-stacking interactions between the aromatic π-electrons in SBR and the delocalized π-electrons in CNTs (Fig. 5d–g).[106–110]

In terms of native physical properties, both SBR and SBS are inherently dense, elastic materials that lack inherent porosity or breathability, limiting their ability to permit air or water vapor transmission under normal conditions.[111,112] When used in direct contact with skin, such limitations can lead to sweat accumulation and discomfort during prolonged wear. To address these challenges, SBS requires structural modification through advanced processing techniques that generate porous architectures or nanosheet forms.[113] These engineered variants exhibit markedly enhanced water vapor permeability, in some cases surpassing the natural skin's water vapor transmission rate (WVTR), thereby improving skin comfort and reducing moisture buildup. The introduction of porosity is typically achieved through nanoscale phase separation techniques or the incorporation of fiber-like fillers that form interconnected networks, promoting moisture diffusion while maintaining the elastomer's mechanical integrity.[114] Importantly, unlike natural rubber latex, SBR and SBS do not contain latex proteins known

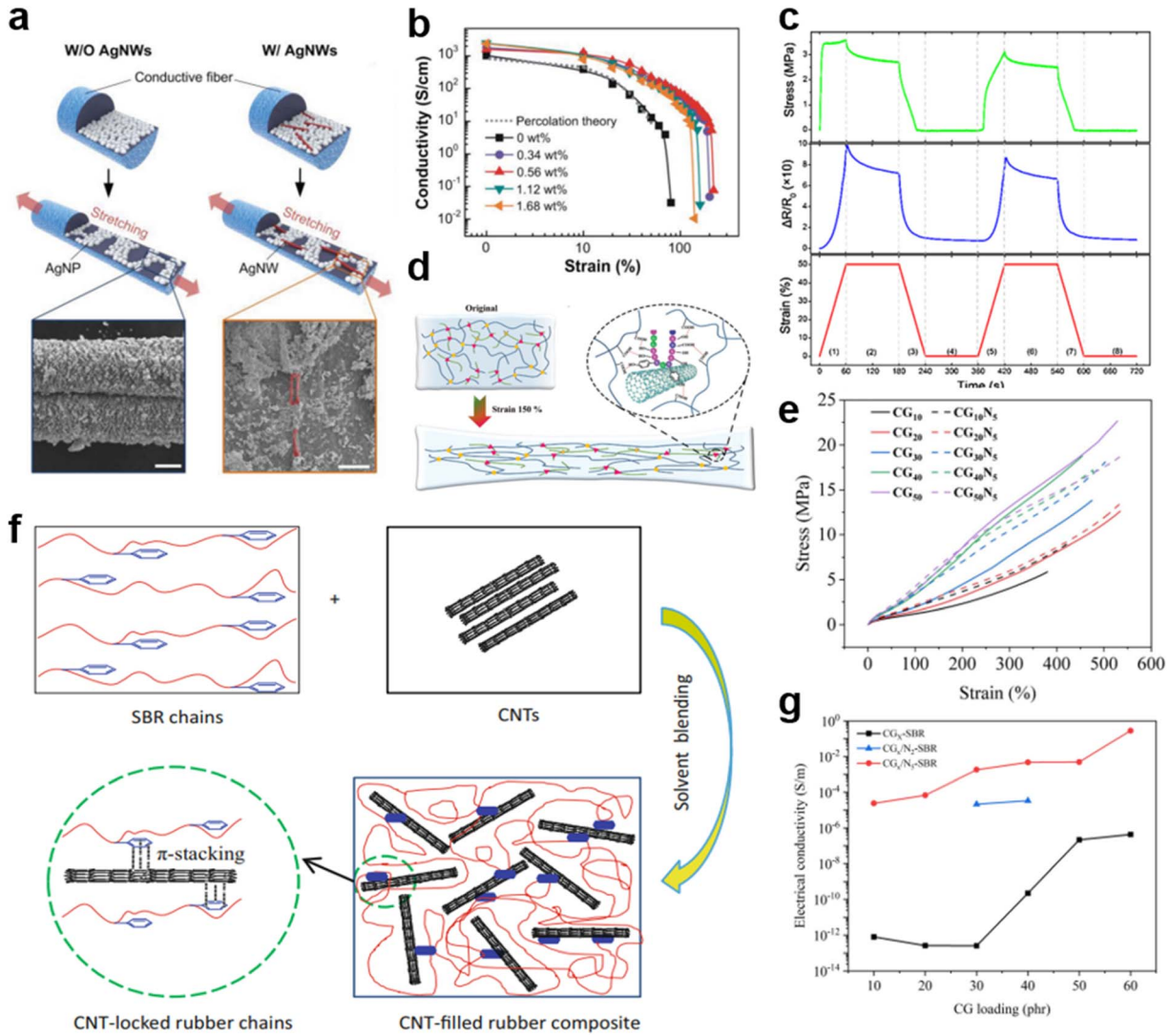

Fig. 5 (a) Representation of morphological and structural changes in Ag nanowires (AgNWs) and Ag nanoparticles (AgNPs) within the composite fiber matrix under mechanical strain. (Inset, left navy-bordered box: SEM image of the AgNP-incorporated SBS fiber without AgNWs subjected to 50% tensile strain, highlighting nanoparticle distribution and fiber deformation) strain, (b) variation in electrical conductivity of fibers produced with different filler concentrations as a function of applied, (c) variation of stress and $\Delta R/R$ in SBS/3G fibers during cyclic stretching–releasing at 50% strain for the initial two cycles, with numbered regions indicating stretching, releasing, and relaxation phases, (d) schematic illustration of the XSBR/SSCNT sensor nanostructure depicting its configuration before and after the application of a stretching force, (e) stress–strain curves for CGx-SBR, CGxN2-SBR, and CGxN5-SBR composites, where *x* represents the varying phr of fillers. CG: cryptocrystalline graphite, SBR: styrene butadiene rubber, (f) illustration of the molecular-level interactions between a rubber matrix and carbon nanotube (CNT) fillers, highlighting the role of π−π stacking in enhancing composite structure and properties, (g) electrical conductivity variations with different CG filler loadings in CG-SBR, CGxN2-SBR, and CGxN5-SBR composites, ref. 104 copyright 2015 John Wiley & Sons, ref. 105 copyright 2018 Elsevier, ref. 108 copyright 2022 John Wiley & Sons, ref. 109 and 110 copyright 2024 John Wiley & Sons.

to trigger type I hypersensitivity reactions, offering a low risk of allergic responses and improving their suitability for skin-contact applications.[115] Through careful material design and processing, these modified synthetic rubbers meet the comfort requirements for human skin interfacing devices, balancing durability, flexibility, allergenic safety, and breathability. These findings highlight the promising potential of styrene–butadiene-based materials for use in wearable transistor devices.

2.5. Styrene ethylene butylene styrene (SEBS)

The synthesis and application of SEBS as a functional elastomer have significantly advanced since its introduction in the 1970s. Initially researched and developed by Shell, industrial production of SEBS commenced in 1971 with its commercialization and later expanded through acquisition by Kraton.[116] The synthesize of SEBS was achieved through anionic polymerization of styrene and butadiene, followed by catalytic hydrogenation to transform the butadiene mid-block into a saturated ethylene/butylene segment, thereby enhancing the polymer's

thermal and oxidative stability. Overcoming early challenges in achieving uniform hydrogenation and controlling copolymer morphology involved innovations in catalyst systems and processing techniques.[117–120] The unique triblock structure of SEBS combines mechanical strength from the PS end blocks and elasticity from the ethylene/butylene mid-block, rendering it suitable for diverse applications, including adhesives, encapsulants, and flexible substrates.[6,121] Moreover, engineering porous SEBS architectures can offer substantial benefits for skin-contact wearable devices. By introducing controlled porosity using methods, such as phase separation or template leaching, SEBS substrates allow sweat vapor to permeate through the material, significantly improving breathability and reducing skin irritation during prolonged wear. This modification preserves the elastomer's characteristic tissue, like softness and flexibility, enabling long-term, comfortable integration with the skin.[14,21,122] By 2010, SEBS began to be explored for use as a substrate in transistors, focusing on plasma treatment to enhance adhesion and modify its hydrophobic and hydrophilic properties for improved electronic performance.[14] A significant milestone was achieved in 2025 when Ye *et al.* introduced a surfactant-functionalized SEBS substrate, providing an effective alternative to traditional plasma treatments for surface modification. Incorporating surfactants such as Span 80 or Tween 80 transformed the naturally hydrophobic SEBS surface into a stable hydrophilic one, eliminating the necessity for additional treatments (Fig. 6a). This advancement enabled direct circuit and mask printing on SEBS substrates while enhancing wettability and adhesion. Moreover, the surfactant-functionalized SEBS retained crucial characteristics such as tissue-like Young's modulus, flexibility, transparency, biocompatibility, hydrolytic stability, and heat resistance. These modifications significantly improved the interface properties between SEBS substrates and conductive layers, essential for effective charge transport and mechanical robustness in electronic devices.[21]

With the recognition of SEBS as a viable substrate material in organic and flexible electronics, its applications expanded to include its use as a dielectric layer due to its superior mechanical flexibility, chemical stability, and ease of processing.[121] Since the mid-2010s, with a relatively low dielectric constant of approximately 2.1 to 2.2, SEBS has been employed as a gate dielectric in stretchable transistors and flexible devices.[123] The dielectric performance of SEBS can be significantly enhanced through the incorporation of fillers such as graphite or titanium dioxide nanoparticles, which increase the

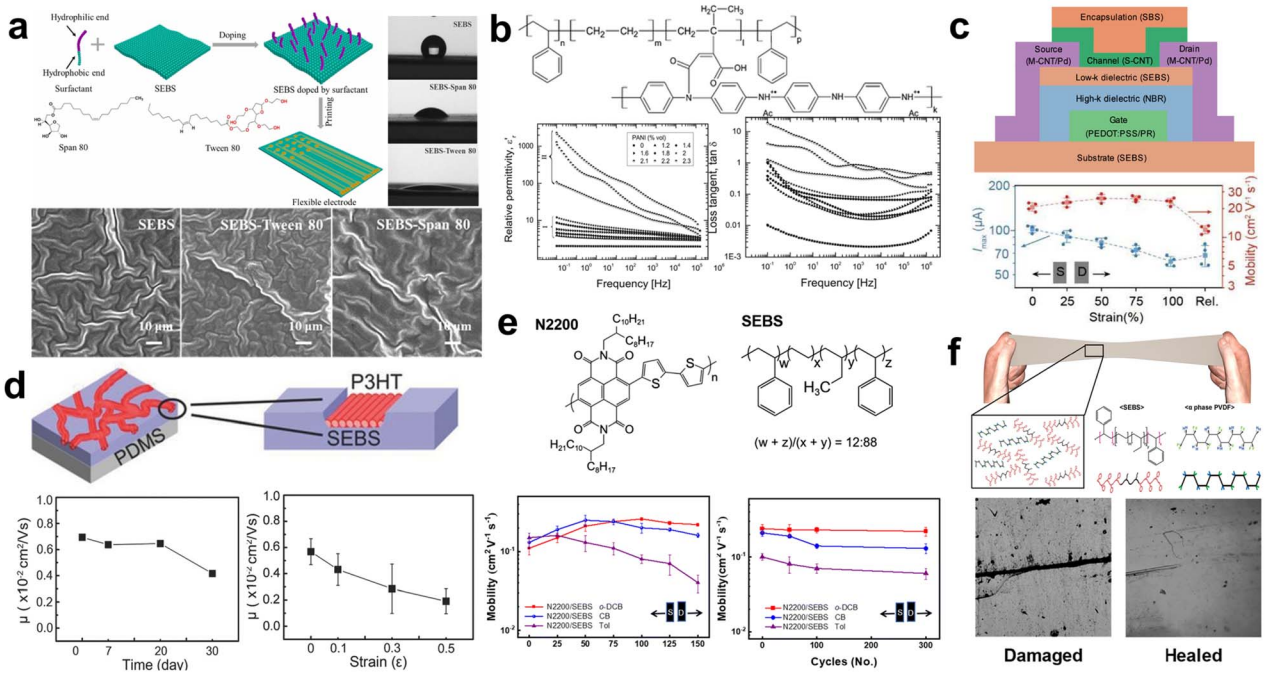

Fig. 6 SEBS-based elastomeric components for stretchable and flexible transistor devices. (a) Strategies to improve SEBS hydrophilicity by surfactant modification (Tween 80, Span 80), as shown in schematic and SEM images. (b) Chemical structures and dielectric properties of SEBS composites, demonstrating their effectiveness as gate dielectrics with stable, enhanced permittivity across frequencies. (c) Application of low-*k* SEBS dielectric crosslinked with an azide-based agent, providing solvent resistance and mechanical robustness, which ensures stable electrical performance under strain. (d) Encapsulation of P3HT with SEBS on a PDMS substrate, enhancing air stability and maintaining electrical performance during stretching. (e) Blending N2200 with SEBS suppresses excessive crystallization and aggregation, resulting in improved charge mobility and operational stability across different solvents and repeated mechanical cycling. (f) Schematic of the preparation and physical crosslinking mechanism of self-healing SEBS/paraffin composite phase change materials, alongside photographs showing the material's self-healing after being cut and reheated. Reproduced with permission from ref. 21 copyright 2025 Elsevier, ref. 124 copyright 2020 Royal Society of Chemistry, ref. 127 copyright 2024 American Chemical Society, ref. 66 copyright 2015 John Wiley & Sons, ref. 128 copyright 2023 Royal Society of Chemistry, and ref. 129 copyright 2024 The Korean Ceramic Society.

dielectric constant while maintaining flexibility. Notable advancements include chemically grafting maleic anhydride (MA) onto the SEBS backbone to form a grafted copolymer (SEBS-*g*-MA), which elevated the dielectric permittivity by up to 470% compared to neat SEBS, as shown in Fig. 6b. This enhancement arises from the introduction of polar MA groups that facilitate dipolar polarization within the elastomer, thus reducing the operating voltage required for electroactive polymer actuators.[124] Improvement of solvent resistance and mechanical robustness in SEBS can be achieved by chemically crosslinking SEBS dielectrics, which is pivotal for stable multilayer device fabrication.[125,126] Recent research by Zhong *et al.* developed azide-based photo-crosslinking to form covalent crosslinks within the SEBS network upon ultraviolet (254 nm) exposure. This approach yielded a dielectric layer with a low dielectric constant (~2.3), exceptional elasticity, and improved solvent resistance. Subsequent patterning *via* oxygen plasma etching enhanced adhesion with overlapping layers, resulting in transistors fabricated with SEBS dielectrics exhibiting high carrier mobilities up to 20 $cm^2 V^{-1} s^{-1}$ under 100% strain while retaining optical transparency (Fig. 6c). The integration of SEBS as a dielectric material combines mechanical flexibility with electrical efficiency, positioning it as a critical enabler for high-performance, intrinsically stretchable integrated circuits.[127] This evolution reflects a broader trend in flexible electronics research, leveraging SEBS's unique combination of elasticity, thermal stability, and tunable dielectric properties. By serving multiple crucial roles, from substrate to dielectric layer, SEBS contributes significantly to advancing the development of robust, wearable, and biocompatible electronic systems, paving the way for innovative digital applications in the future.

While molecular tailoring strategies such as covalent grafting, block copolymerization, and supramolecular assembly are common in the broader field of OSCs engineering, these approaches have not been widely applied to SEBS as a direct chemical modifier. Consequently, blending remains the primary method for utilizing SEBS to tailor the mechanical and electrical properties of OSCs films for stretchable electronics. In this widely adopted approach, SEBS is mixed with conjugated polymers to form composite films that exhibit a nanoconfined morphology: the SEBS matrix imparts elasticity and mechanical robustness, while the OSCs domains maintain efficient charge transport.[130] Early studies dating back to 2015 demonstrated blends of SEBS with P3HT, achieving electron mobilities of approximately 0.4 $cm^2 V^{-1} s^{-1}$ after 30 days of air exposure, and preserving up to 33% of mobility after 50% strain stretching (Fig. 6d).[66] More recent work by Zhang *et al.*[128] focused on blending the conjugated polymer N2200 with SEBS (Fig. 6e), where the elastomer weakens the strong intermolecular interactions within N2200, suppressing excessive crystallization and large aggregate formation. This interaction promotes the development of a finely interpenetrating nanofibril network with smaller fibril sizes during extended film-forming times. The SEBS matrix provides mechanical elasticity and accommodates strain, enabling the nanofibril network to maintain continuous charge transport pathways even under large deformation. This controlled morphology results in stretchable transistors exhibiting electron mobilities around 0.1–0.2 $cm^2 V^{-1} s^{-1}$ that remain stable under strains up to 100% even after repeated stretching cycles. The synergy between weakened polymer interactions and elastomer blending is thus critical for achieving durable, high-performance stretchable organic transistors (Fig. 6e).

Recent researcher has advanced the self-healing capabilities of SEBS elastomers by exploiting physical cross-linking mechanism. Zhang *et al.*[30] developed self-healing SEBS/paraffin composite phase change materials (C-PCMs) using a one-step plate vulcanization method based on physical entanglement. In this system, the self-healing effect arises when the material is damaged and subsequently heated: the PS segments in SEBS melt, enabling both SEBS polymer chains and paraffin to flow and re-entangle, effectively closing fissures. Upon cooling, the structure locks back into place, restoring the material's integrity. The optimal composite, containing 85 wt% paraffin, demonstrated high elasticity (with elongation up to 1160% after healing) and robust thermal stability. This reversible mechanism allows the composite to recover its shape and mechanical properties after damage, making it particularly suitable for flexible and wearable thermal applications. This mechanism allows the material to recover its shape and mechanical properties after damage, making it suitable for flexible and wearable thermal applications. Building on this approach, Yoon *et al.*[129] created highly stretchable and self-healing composite films by blending elastic SEBS with high-dielectric PVDF through a solution-based process. Here, the self-healing behavior is attributed to physical cross-linking within the SEBS matrix and the maintenance of an amorphous PVDF phase, which together enable the polymer chains to regain mobility upon heating. When the film is cut and the pieces are pressed together and heated at 70 °C for 2 hours, the cut surfaces fuse seamlessly, demonstrating intrinsic self-healing capability. After this thermal treatment, the healed film could withstand 576% strain, compared to the original 1600% strain of the pristine film (Fig. 6f). FTIR analysis confirmed the absence of new chemical bonds between SEBS and PVDF, indicating that the self-healing is governed solely by reversible physical interactions and chain mobility, with SEBS playing a key role in preventing PVDF crystallization and maintaining its amorphous character.

2.6. Polyisoprene (PI)

As presented in Fig. 7, over a century ago, isoprene was first isolated from natural rubber by pyrolysis and subsequently polymerized into *trans*-1,4-PI through treatment with hydrochloric acid in 1879, where HCl acted both as initiator (proton source) and as a provider of the counter-anion (Cl^-).[131] The process begins with protonation of the monomer to form an allylic carbocation intermediate. This carbocation attacks another isoprene molecule, preferentially forming *trans*-1,4 linkages as a result of steric and electronic effects that stabilize the transition state. Advances in catalyst technology enabled the production of *cis*-1,4-PI through stereospecific polymerization using Ziegler–Natta catalysts by Goodyear Tire & Rubber

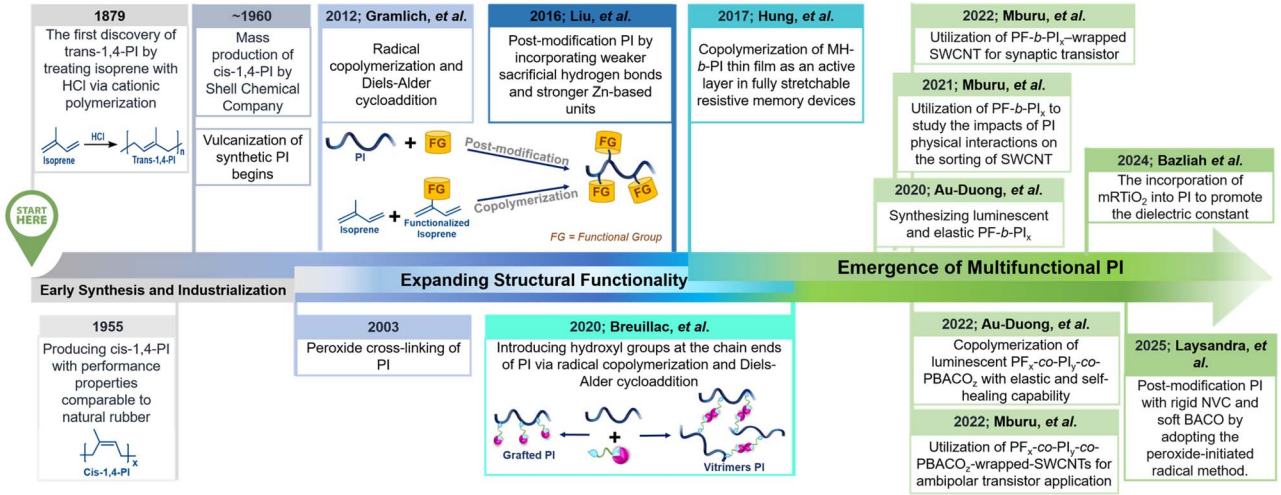

Fig. 7 A timeline illustrating the development of PI, highlighting key milestones from its early synthesis to its current use in stretchable transistor devices.

Company in the mid-1950s with properties comparable to natural rubber, marking a significant milestone for synthetic elastomers.[131,132] Shortly thereafter, Shell Chemical Company initiated the first commercial production of stereoregular PI with over 90% cis content using a lithium catalyst between 1959 and 1960.[132] These stereoregular PI was then vulcanized or hydrogenated to further enhance their mechanical properties for widespread use in industrial commodities such as tires, rubber bands, tubes, and gloves.[133] While early PI synthesis focused on replicating the natural rubber structure (primarily *cis*-1,4-PI), advances in polymerization methods and catalyst technologies have enabled the incorporation of functional monomers and other compounds. These modifications have expanded the properties and contributions of *cis*-1,4-PI beyond traditional uses, paving the way for its integration into stretchable and flexible transistor devices.[13,134] Owing to their inherent unsaturated hydrocarbon backbones and reactive diene structure, PI can also undergo diverse chemical transformations, including cycloaddition, electrophilic/nucleophilic addition, radical polymerization, post-modifications, and coordinated catalytic addition (Fig. 7).[42–49]

Modifications of PI not only enhance their physical and mechanical properties but also allow researchers to engineer advanced PI derivatives with additional tailored functionalities, thereby expanding their suitability for wearable device applications.[13,19,43,44,62,134,135] For instance, Hung *et al.* synthesized carbohydrate-*block*-polyisoprene (MH-*b*-PI$_n$) *via* copper(I)-catalyzed azide–alkyne cycloaddition (CuAAC), commonly referred to as "click" reaction (Fig. 8a).[19] This approach involved coupling alkyne-functionalized maltoheptaose (MH–C≡CH) with azide-terminated PI (PI$_n$–N$_3$), resulting in a stable triazole linkage between the two blocks. Prior to the click reaction, PI chains were functionalized at their chain ends by halogenation followed by nucleophilic substitution with sodium azide, yielding PI$_n$–N$_3$. This strategy allowed precise control over the block copolymer architecture, combining the flexibility of PI with the functional properties of the carbohydrate segment. The resulting MH-*b*-PI exhibited well-controllable memory performance, including write-once-read-many-times (WORM), flash, and dynamic-random-access-memory (DRAM) by their self-assembled nanostructures. Note that the detailed mechanism underlying the MH-*b*-PI$_n$-based memory behavior will be discussed in a subsequent section.

Building upon earlier advances, Chiu's group further propelled the multifunctionality of PI-based materials by synthesizing poly[2,7-(9,9-dioctylfluorene)]-*block*-polyisoprene (PF-*b*-PI$_x$) block copolymers through a dual-strategy approach, that included Suzuki coupling for the rigid PF rod segment and reversible addition–fragmentation chain transfer (RAFT) polymerization for the growth rubber-like PI coil segment.[43] This methodology enables precise control over molecular architecture and molecular weight, resulting in materials that synergistically combine stable luminescence, elasticity, and electronic functionality. Post-synthesis vulcanization transformed the conjugated-based PI copolymer PF-*b*-PI$_{1.8}$, which has the longest PI chain length in this study (molecular weight 16 400 g mol^{-1}), into bulk or film materials capable of stretching up to 150% without crack formation. The cross-linked networks are also capable of yielding free-standing films with nanoscale thickness, exhibiting exceptional elasticity and tough mechanical strength, maintained high photoluminescence quantum yield (PLQY) stability over 1000 stretching cycles at 150% strain. Leveraging these insights, Mburu *et al.* investigated the role of physically bonded PI in the selective sorting and stabilization of semiconducting SWCNTs using PF$_x$-*b*-PI$_y$ block copolymers with a constant low molecular weight of 12 000 g mol^{-1} for the PF segment and varying PI chain lengths.[134] The appeal of SWCNTs lies in their superior and tunable electrical properties, making them ideal candidates for low-cost, high-performance transistor and memory device applications.[13,134,136–138] However, this enticing performance critically depends on the uniformity and isolation of individual

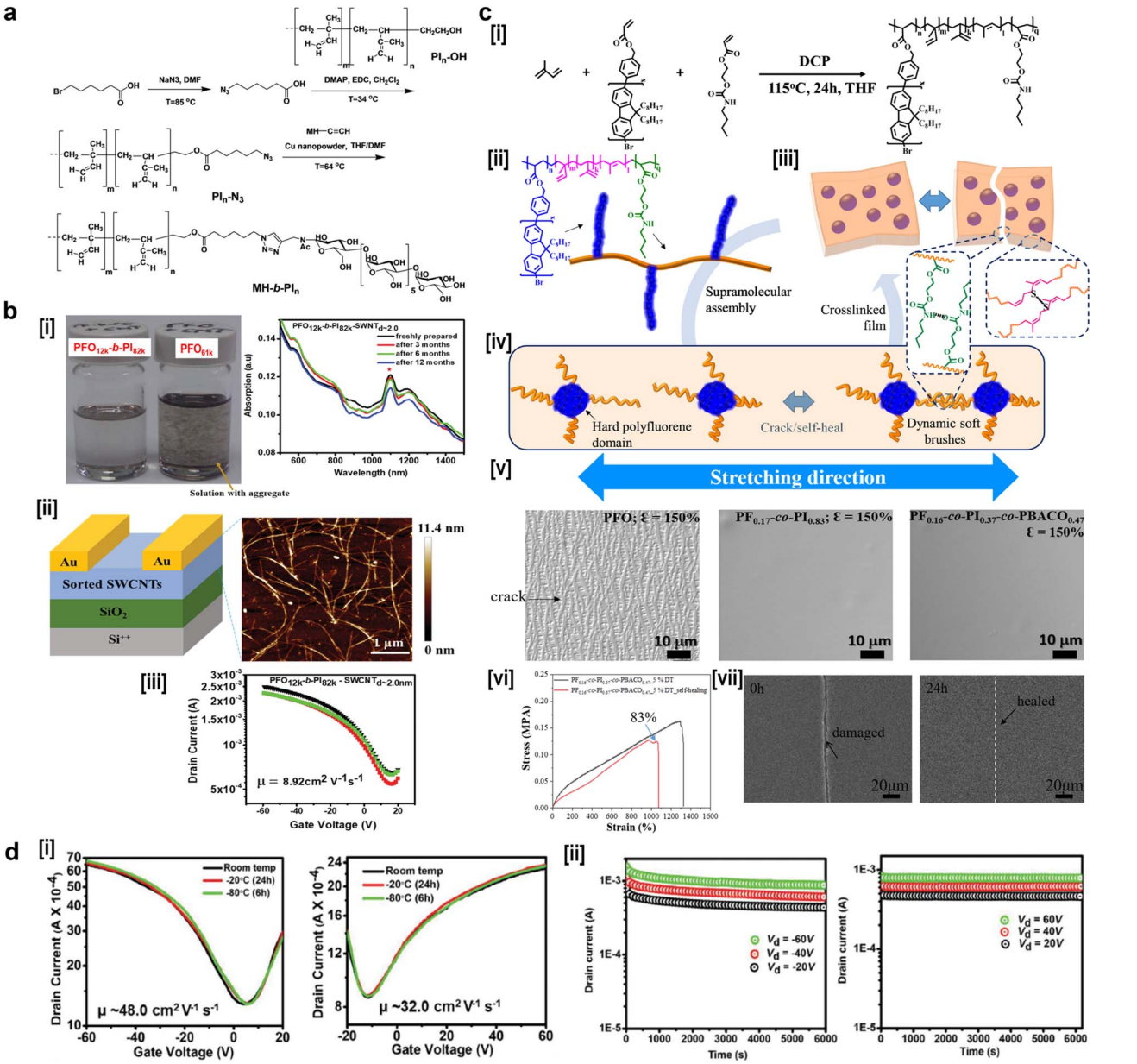

Fig. 8 (a) The synthesis routes of MH-*b*-PI$_n$ block copolymers for stretchable resistive memory device application. (b) SWCNTs-thin film transistor fabrication: [i] stability and dispersion study based on photograph image and UV-spectra, [ii] schematic of BGTC transistor configuration and AFM image of SWCNTs sorted by PFO$_{12K}$-*b*-PI$_{82K}$, and [iii] I_D–V_G transfer curve of the device using PFO$_{12K}$-*b*-PI$_{82K}$-dispersed sc-SWCNTs (diameter ≤ 2.0 nm) as the semiconducting layer. (c) Molecular design of the intrinsically elastic and self-healing luminescent PF$_x$-*co*-PI$_y$-*co*-PBACO$_z$: [i] synthetic scheme; [ii] branched copolymer with soft PI-*co*-PBACO backbone (blue) and rigid PF branches (orange); [iii] self-assembled into a two-phase nanostructure; [iv] elasticity tuning *via* DT cross-linking (gray spheres) and hydrogen bonding (dotted lines), [vi] OM images of the PF, PF$_{0.17}$-*co*-PI$_{0.83}$, and PF$_{0.16}$-*co*-PI$_{0.37}$-*co*-PBACO$_{0.47}$ thin films under 150% strain, and [vii] investigation RT self-healing performance of the PF$_{0.16}$-*co*-PI$_{0.37}$-*co*-PBACO$_{0.47}$ film based on tensile test and SEM images before (0 h) and after (24 h) self-healing. (d) The [i] (I_D–V_G) transfer curves and [ii] retention stability of p-type and n-type PFO$_{0.16}$-*co*-PI$_{0.36}$-*co*-PBACO$_{0.48}$-sc-SWCNTs respectively, where the retention tests were performed at gate voltages of ±60 V. Reprinted with permission from ref. 19. copyright 2017 John Wiley & Sons., ref. 134 copyright 2021 John Wiley & Sons, ref. 62 copyright 2022 American Chemical Society, ref. 139 copyright 2022 John Wiley & Sons.

nanotubes. SWCNTs naturally tend to aggregate into bundles due to the van der Waals (VDWs) and π–π interactions, which can cause electrical short circuits, reduce carrier mobility, and degrade device reliability. Proper dispersion breaks these bundles into isolated nanotubes, enabling consistent and efficient charge transport pathways necessary for high-performance FETs and memory devices. Moreover, well-dispersed SWCNTs ensure uniform film morphology, reduce defect density, and enhance semiconducting purity, all contributing to improved device stability, reproducibility, and longevity. The PI segment facilitates selective dispersion of SWCNTs in organic solvent through weak VDWs and π–π

interactions mediated by its hydrocarbon and double bond backbone, while simultaneously providing steric barriers among their inter-tubes that effectively prevent the reaggregation of the sorted SWCNTs. Meanwhile, the PF segment ensures strong π–π stacking with SWCNTs. These findings demonstrate that longer PI chains (82 000 g mol^{-1}) markedly enhance sorting efficiency and maintain dispersion stability, as evidenced by the sustained solution transparency and consistent UV-vis absorption profiles over a one-year period (Fig. 8b). By employing a bottom-gate top-contact (BGTC) transistor design, it was confirmed that the synergistic interactions yield high electronic performance, achieving hole mobility of 8.92 cm^2 V^{-1} s^{-1} (Fig. 8b).

The same research group subsequently employed PF_x-*b*-PI_y (with molecular weights of 12 000 g mol^{-1} for PF and 82 000 g mol^{-1} for PI segment)-wrapped-SWCNTs for the fabrication of a high-performance synaptic transistor.[13] Thin-film transistor integrates SWCNTs as both the semiconductor channel and electret layer, significantly simplifying device architecture and fabrication. The simple-structured synaptic TFT device exhibits both high charge carrier mobility (≈11.3 cm^2 V^{-1} s^{-1}), output current (10^{-4} to 10^{-3} A), and a large memory window (>70 V), while the photoactive fluorene block enables effective photonic modulation. This dual electrical and optical control allows the device to mimic key biological synaptic functions, including long-term potentiation (LTP), long-term depression (Ltd), excitatory postsynaptic current (EPSC), inhibitory postsynaptic current, PPF, STDP, and SRDP, thereby functioning as a fully modulated photonic/electrical synaptic transistor. This approach effectively overcomes critical limitations of previous synaptic devices, including limited charge storage (essential for maintaining stable and adequate charge retention), low current output (which can restrict device performance and signal-to-noise ratio, thereby limiting practical applicability), and complex fabrication (as the complicated manufacturing processes reduce scalability and increase manufacturing cost, hindering widespread adoption). Moreover, it presents a promising strategy for neuromorphic computing applications that integrate optical and electrical stimuli for multifunctional information processing.

Another noteworthy additional functionality is the incorporation of intrinsic self-healing capabilities into PI, thereby enhancing durability and extending functional longevity. In 2022, Chiu's group achieved a significant breakthrough by synthesizing a semiconducting branched copolymer featuring a soft segment composed of PI and poly(2-[[(butylamino) carbonyl]oxy]ethyl acrylate) (PBACO) that contains pendant hydrogen bond donor/acceptor groups, combined with a hard branch derived from PF (Fig. 8c).[62] A series of synthesis procedures began from vinyl-functionalized hydroxyl-terminated polyfluorene (PFO) *via* esterification to produce vinyl-terminated PF, continued with copolymerization *via* free-radical polymerization (FRP) to yield PF_x-*co*-PI_y-*co*-$PBACO_z$, and finally, thin film fabrication through sulfur vulcanization using 1,9-nonanedithiol (DT) as a covalent cross-linker (Fig. 8c). The $PF_{0.17}$-*co*-$PI_{0.83}$ and $PF_{0.16}$-*co*-$PI_{0.37}$-*co*-$PBACO_{0.47}$ thin films on PDMS substrates exhibited improved deformability, maintaining exceptionally smooth surfaces under mechanical strain of 150%, in contrast to PFO thin film, which fractured under similar conditions (Fig. 8c). These results highlight the role of PI as an effective stretchability-enhancing component. Additionally, due to PBACO acting as the self-healing component based on dynamic H-bonding interactions between the –NH group and a lone electron pair on the C=O group, the cross-linked $PF_{0.16}$-*co*-$PI_{0.37}$-*co*-$PBACO_{0.47}$_5 wt% DT with a low T_g of −17 °C achieves a self-healing efficiency of 83% within 24 h, with complete restoration confirmed by the absence of cut marks in SEM images (Fig. 8c).

Expanding on the principle that π–π stacking interactions between conjugated polymers and SWCNTs are essential for effective dispersion and selective sorting of semiconducting nanotubes, copolymers designed for this purpose generally incorporate conjugated segments with high molecular weights exceeding 10 000 g mol^{-1} in their backbones to strengthen these interactions.[13,134,136,137] Conversely, low molecular weight conjugated polymers tend to be ineffective for sorting due to their insufficient interaction with SWCNTs.[134,137,140] Taking interest in the combination molecular structure of PF_x-*co*-PI_y-*co*-$PBACO_z$, Mburu *et al.* investigate the synergistic effects of VDWs and hydrogen bonding interactions for enhancing the sorting of SWCNTs with long shelf life and high stability at low temperatures (4, −20, and −80 °C).[139] To elucidate the role of the PI and H-bond-containing PBACO segment, a low-molecular-weight vinyl-PFO (∼4500 g mol^{-1}) was incorporated as a side chain, while PI_y-*co*-$PBACO_z$ formed the main backbone. Although $PFO_{0.17}$-*co*-$PI_{0.83}$ copolymer showed limited sorting due to the short PI chain (∼210 units), the inclusion of PBACO significantly improved sorting efficiency. The system successfully isolated SWCNTs with diameters up to 1.17 nm, maintaining dispersion stability without aggregation for over one year at low temperatures. Additionally, ambipolar transistors fabricated from these solutions exhibited average charge carrier mobilities of 48 cm^2 V^{-1} s^{-1} (p-type) and 32 cm^2 V^{-1} s^{-1} (n-type), with retention stability exceeding 6000 seconds (Fig. 8d). The positive outcomes observed are attributed to the PI-PBACO moiety, which facilitates H-bond-driven supramolecular structures that enhance sorting efficiency and create stronger repulsive forces to prevent nanotube reaggregation. This research reveals that even when integrating low molecular weight PF as side chains, the presence of linear groups featuring physical interactions such as VDW and H-bonds, effectively enhances the sorting and stability of SWCNTs.

While the mechanical flexibility of PI could be beneficial for flexible substrates or encapsulation layers, their application as dielectric layers in transistor devices is generally not recommended due to inadequate dielectric properties, including low dielectric constant, limited breakdown strength, and high leakage current. These limitations stem from the non-polar, long chain hydrocarbon nature of PI's polymer backbone, which lacks significant polarity and aromatic groups. To address these limitations, Chiu's group utilized a commercial *cis*-1,4-PI with a high molecular weight of 250 000 g mol^{-1} grafted onto modified rutile titanium dioxide ($mRTiO_2$) nanoparticles as an insulating material.[62] $mRTiO_2$ were pretreated

with a coupling agent to enhance interfacial adhesion and prevent aggregation. Subsequently, rubber composite films were fabricated *via* sulfur vulcanization. The resulting modified composite films exhibited excellent elasticity, sustaining 50 loading–unloading cycles without residual strain. Importantly, the incorporation of $mRTiO_2$ nanoparticles significantly increased the dielectric constant from 2.12 to 12.93.

Later, Chiu's group sought a simpler, one-step approach using peroxide-initiated radical modification to directly incorporate rigid and soft functional monomers into the PI main chain, successfully converting the typical low-viscosity fluid of commercial *cis*-1,4-PI (molecular weight 35 000) into a solid film that exhibits RT self-healing capability based on dynamic non-covalent interactions, such as hydrogen bonds and π–π stacking, while maintaining high elasticity and stretchability (over 1000% strain).[44] Considering the excellent hydrophobic properties of PI and NVC compound, the radically modified PI exhibits remarkable mechanical stability, with tensile strength only slightly reduced from 2.91 to 2.89 MPa and elongation at break reaching up to 1200%, while this modified PI demonstrates effective self-healing, maintaining a healing efficiency of 95% even after immersion in water at 25 °C for 24 hours. The water-insensitive nature of PI and NVC can effectively disrupt interactions between water molecules and the active sites of BACO functional groups, thereby preserving its self-healing capability in aqueous environments. The reaction mechanism initiates with the homolytic cleavage of the weak O–O bond in dicumyl peroxide (DCP) under thermal or high-energy conditions, forming two cumyl radicals. These radicals subsequently undergo beta-scission to produce methyl radicals, which efficiently abstract allylic hydrogens from PI, generating polymer radicals. During the alkyl radical termination step, the PI radicals couple with other radical species, forming covalent bonds that modify the polymer backbone. Importantly, the resulting modified PI retains a linear architecture without additional covalent cross-linking, enabling efficient recycling through simple dissolution and remolding processes, thus supporting sustainable device fabrication. Given that the commercial chemicals used are widely available, easily sourced, and require straightforward preparation, this strategy holds significant promising route for large-scale industrial manufacturing.

Despite numerous researchers have successfully synthesized PI with self-healing properties, to the best of our knowledge, only a limited number of researchers have explored the application of PI-based materials in thin film transistor device fabrication, and their use has generally been confined to individual stretchable layers within other rigid components.[13,62,135,137] This partial integration means that PI-based materials have not yet been employed to create fully stretchable and self-healable thin film transistor devices. As a comprehensive overview, Table 1 summarizes recent advancements in PI-based self-healing materials from the past decade, covering synthetic methods, healing mechanisms, mechanical and self-healing performances. Interestingly, a notable advancement was reported by Wang *et al.* in 2022, who synthesized self-healing PI through a catalyst-controlled polymerization of isoprene using rare earth catalysts, specifically a half-sandwich scandium complex.[141] This method represents a significant breakthrough, as the self-healing properties arise entirely from the inherent PI structure itself, without requiring additional self-healing components. This advancement highlights the potential for designing self-healing polymers that depend solely on the intrinsic characteristics of PI, thereby advancing the field of self-healing materials. This method produced PIs with a controlled microstructure consisting of an approximately 70/30 ratio of 3,4- to *cis*-1,4-microstructures. The resulting polymer exhibited excellent self-healing properties at RT within 48 h without any external intervention, attributed to nanoscale heterogeneities formed by microphase separation of the relatively hard 3,4-segments dispersed within a flexible *cis*-1,4-segment matrix, which act as reversible physical cross-linking points enabling spontaneous repair (Table 1). Hydrogenated versions of this PI also showed similar self-healing and mechanical performance, demonstrating the broad applicability of this approach.

2.7. Biocompatibility assessment

Rubber-like synthetic polymers intrinsically possess remarkable elasticity and toughness, characterized by a low Young's modulus that closely approximates the mechanical compliance of biological tissues. This mechanical compatibility facilitates their harmonious integration with living environments. The cytotoxicity test is a fundamental component of biocompatibility assessment for medical devices and biomaterials, conducted in accordance with the ISO 10993 standard.[153] This standard specifies the protocols and acceptance criteria used to evaluate whether a medical device meets essential biocompatibility requirements.[153] As presented in Fig. 9a, numerous studies have assessed the biocompatibility of synthetic rubber-like materials in animal models, with PDMS emerging as the most extensively investigated elastomer implant material for both humans and animals. This prominence is due to PDMS's long-term bio-stability, chemical inertness, manufacturability, gas permeability, and its ability to minimize strain-induced wrinkling owing to its low Young's modulus.[154] *In vivo* studies by Jensen *et al.*, demonstrated that subcutaneously implanted PDMS in rats elicited minimal inflammatory response and no tissue necrosis, with histological scores comparable to those of established non-toxic reference materials in accordance with ISO 10993 guidelines.6. Moreover, plasma-treated PDMS further improved tissue integration by producing thinner, more adherent, and well-vascularized capsules without exacerbating inflammation.[155] Complementing these findings, Fig. 9b presents an evaluation of PDMS compounds on differentiated PC12 neuronal cells derived from rats confirming that bulk PDMS, as commonly used in cochlear implants, is biocompatible with neuronal cells and supports its safety for biomedical applications.[156] Building on the biocompatibility of PDMS, Minev *et al.* developed a soft PDMS-based neural implant for subdural insertion in rats (Fig. 9c).[157] These flexible devices were compared with stiff polyimide implants to assess long-term biointegrability, using ladder walking tests to evaluate hindlimb motor function. Rats implanted with the soft PDMS

Table 1 Recent advancements in PI-based self-healing materials

No.	PI-based material	Full name	Self-healing mechanism	Mechanical properties[a]			Self-healing conditions		Self-healing efficiency[b]	Ref./year
				Stress (MPa)	Strain (%)	Toughness (MJ m^{-3})	Time	External stimuli		
1	PhDT5-S2.5A1	Polyisoprene rubber vulcanized with benzene-1,4-dithiol (PhDT) to form a dynamic crosslinked network rich in polysulfide bonds (PhDT = benzene-1,4-dithiol modifier, S2.5 = 2.5 phr sulfur, $A1 = 1$ phr accelerator)	Thermal-induced dynamic exchange of polysulfide bonds	6.41	1068	23.47	40 min	170 °C	90%	142/2025
2	*Rm*-PI/m_1_n_2	Radically modified *cis*-1,4-polyisoprene with *N*-vinylcarbazole and 2-([[(butylamino)carbonyl]oxy] ethyl acrylate) segments	Hydrogen bond from BACO and π–π stacking from NVC	2.91	1087	25.27	24 h	Not required	93% (macroscale) 98% (nanoscale) 95% (underwater)	44/2025
3	SIS-D0.5-B5	Poly(styrene-*b*-isoprene-*b*-styrene) vitrimeric elastomer crosslinked with di-vinyl boronic ester *via* dicumyl peroxide (DCP)-initiated radical grafting	Intrinsic self-healing *via* reversible dynamic boronic ester (B–O) covalent bonds.	~13	~850	—	6 h	100 °C	40%	143/2024
4	75Na–25Mg	Polyisoprene ionomer with 2.3 mol% carboxyl groups randomly distributed along the chain, co-neutralized with Na^+ and Mg^{2+} ions	Intrinsic self-healing *via* ionic crosslinks and ion-hopping	~9	~1000	—	24 h	45 °C	100%	144/2024
5	PI/STA-5	Polyisoprene crosslinked with 5 phr sulfur-rich copolymer STA (sulfur-thioctic acid (TA) copolymer)	The dynamic covalent network	24.2	~714	—	6 h	120 °C	95% (based on tensile strength recovery) 83.3% (based on mechanical strain recovery)	145/2024
6	B-PIP-0.65	Terminally hydroxyl-functionalized polyisoprene crosslinked with bis(6-membered cyclic carbonate) (bCC), forming a nanophase-separated vitrimeric rubber	Dynamic carbonate bonds and nanophase reinforcement *via* ring-opening crosslinking of bCC	~22	~800	~60	1 min	80 °C	91% (based on tensile strength recovery)	146/2023
7	$PI_{0.83}$-*co*-$PBACO_{0.17}$-QDs	Polyisoprene-*co*-poly(2-[[(butylamino) carbonyl]oxy]ethyl acrylate) with $CsPbBr_3$ quantum dots	Hydrogen bonding from PBACO and ionic interactions between BACO's Lewis base carbonyl (C=O) and Pb^{2+} in $CsPbBr_3$ QDs	0.15	486	—	24 h	Not required	90% (based on tensile strength recovery)	147/2022
8	P4	Polyisoprene with a microstructure of ~70/30 3,4-/*cis*-1,4-units, synthesized using a rare-earth (scandium) catalyst	Nanoscale self-assembly of hard segments formed by 3,4-units, which act as reversible physical cross-links, while the soft *cis*-1,4-PI allows	~1.5	2200	—	48 h	Not required	100%	141/2022

Table 1 (*Contd.*)

No.	PI-based material	Full name	Self-healing mechanism	Mechanical properties[a]			Self-healing conditions		Self-healing efficiency[b]	Ref./year
				Stress (MPa)	Strain (%)	Toughness (MJ m^{-3})	Time	External stimuli		
			chain mobility and reformation of the physical network at ambient conditions							
9	$PF_{0.16}$-*co*-$PI_{0.37}$-*co*-$PBACO_{0.47}$_5%DT	Poly[2,7-(9,9-dioctylfluorene)]-*co*-polyisoprene-*co*-poly(2-[[(butylamino) carbonyl]oxy]ethyl acrylate) copolymer, crosslinked *via* vulcanization process using 5 wt% 1,9-nonanedithiol	Hydrogen bonding in the BACO segments	0.167	1290	1.07	24 h	Not required	83% (based on mechanical strain recovery)	62/2022
10	T5P5 (TPI : PEW = 50 : 50)	*Trans*-1,4-polyisoprene/polyethylene wax composites	Thermal-triggered chain mobility, diffusion, and recrystallization	14.18	431	—	30 min and 5 days	120 °C and 10 MPa pressure for 30 min continue with RT for 5 days	21% (based on tensile strength recovery)	148/2022
11	PI–PHEA RC elastomer with 1 mol% crosslinker	Polyisoprene–poly(2-hydroxyethyl acrylate) elastomer crosslinked with β-cyclodextrin trimer *via* rotaxa-polymerization (RC elastomer)	Multiple hydrogen bonds and sliding cross-links	9.79	887.48	43.40	24 h	60 °C	84% (based on mechanical strain recovery)	149/2020
12	CPI-90Na	Blended *cis*-polyisoprene-based ionic elastomer where 90% of the carboxyl group was neutralized with sodium	Ionic crosslinks	∼11	∼1600	∼50	48 h	Not required	80%	150/2020
13	PI2(1.4)85Na	Polyisoprene modified with carboxyl group and partially neutralized with sodium (molecular weight index: 2; mol% carboxyl groups: 1.4; % Na^+ neutralization: 85)	Ionic crosslinks and network rearrangement *via* ion-hopping	∼13	∼1600	—	64 h	Not required	88%	151/2020
14	B-4A-PIP	Block terminally tetra-alanine-functionalized PI	Hydrogen-bonding interactions among the tetra-analine units	15	890	43.6	1 h	Not required	100% (based on tensile strength recovery)	49/2018
15	ZnATA-4/8	PI grafted with 3-amino-1,2,4-triazole (ATA), coordinated with Zn^{2+} ions (4/8 = Zn^{2+} to ATA molar ratio)	Dual-dynamic network consisting of multiple hydrogen bonds and Zn-triazole coordination bonds	21	∼900	60	24 h	80 °C	74% (based on tensile strength recovery) and 71%	152/2017

[a] The use of symbol "∼" in the mechanical stress, strain, and toughness values were derived through visual analysis of the graphical data presented in the reference journal due to the lack of tabulated data. [b] Unless otherwise stated, the self-healing efficiency percentage is calculated by comparing the tensile toughness before and after the healing process. Reported values are rounded to the nearest whole number.

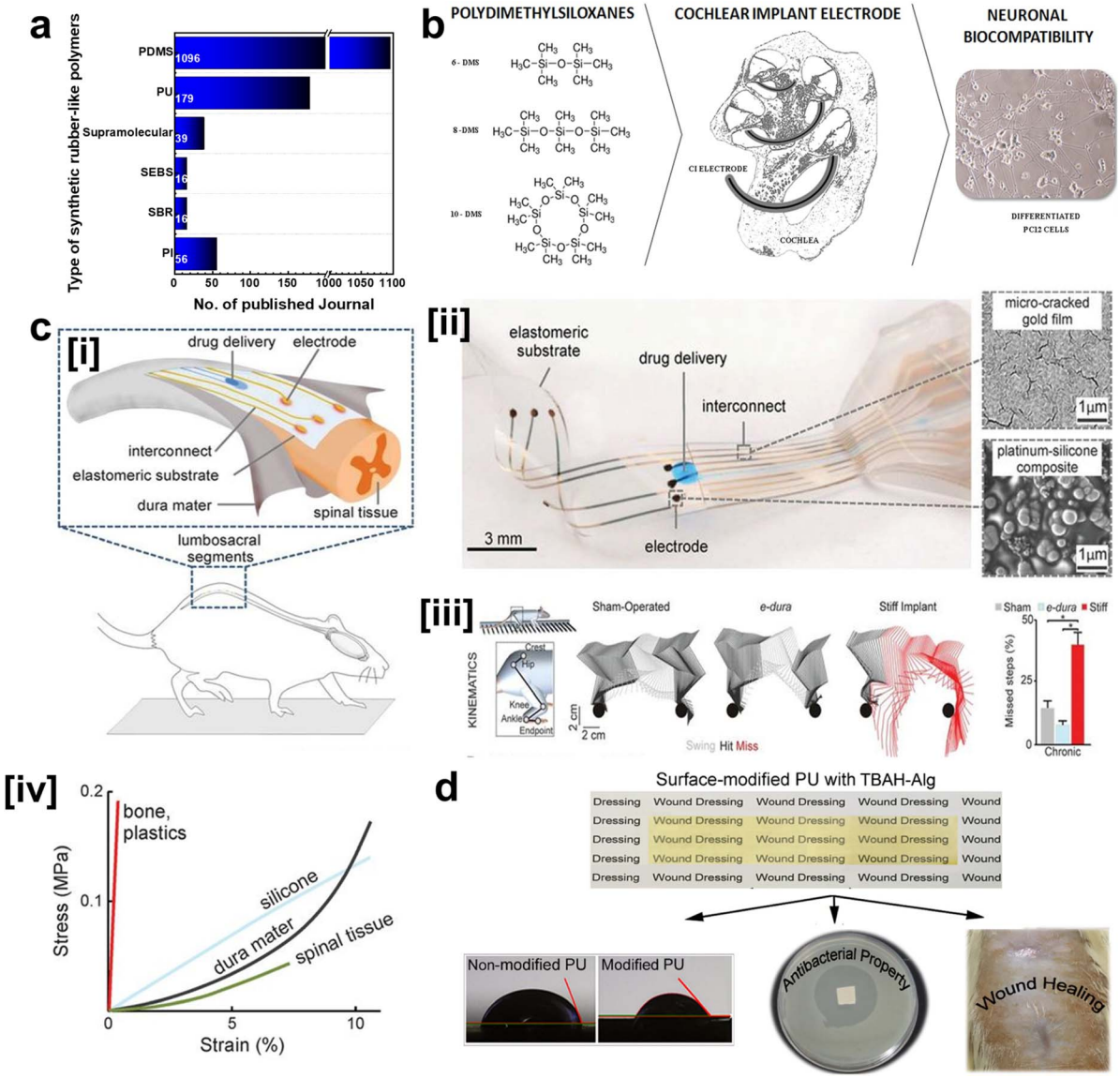

Fig. 9 (a) Number of studies on synthetic rubber-like polymers evaluated for *in vivo* and *in vitro* biocompatibility over the past 15 years (sourced from the Scopus database). (b) Safety evaluation of three types of PDMS compounds (hexadimethylsiloxane, octamethyltrisiloxane, decamethylcyclopentasiloxane) on an *in vitro* neural cell model (PC12) (c) a soft neural implant fabricated from PDMS is designed for subdural placement in rats: [i] schematic of the elastic device implant positioned in rats for biocompatibility testing; [ii] photographs of a soft PDMS-based device with the scanning electron micrographs of the gold film and the platinum–silicone composite; [iii] hindlimb movement analysis and proportion of missed steps averaged in the ladder walking test at 6 weeks in rats; and [iv] stress–strain curves comparing the mechanical properties of spinal tissues, dura mater, and implant materials. (d) Photograph of a transparent PU wound dressing that possesses antibacterial activity. Reprinted with permission from ref. 156 copyright 2019 Elsevier, ref. 157 copyright 2015 American Association for the *Advancement of Science*, ref. 159 copyright 2019 American Chemical Society.

devices exhibited normal motor function and showed no signs of chronic inflammation for up to six weeks, demonstrating the advantages of mechanical compliance in implant design (Fig. 9c). A comparative analysis of the mechanical properties of spinal tissues, including the dura mater, alongside various implant materials such as bone plastics and silicone, highlights the importance of matching implant mechanics to the specific anatomical environment.[157]

Genneri *et al.* examined the skin compatibility of SEBS-based patches *via* an *in vitro* skin permeation study with ibuprofen as a model drug.[158] The study employed modified Franz cells under occlusive conditions on pig ear skin, which is widely recognized as a suitable model due to its similar histological structure and permeability to human skin. Adhesive peel strength and tack were carefully optimized to minimize skin damage or irritation upon removal, ensuring gentle yet effective adhesion. Extending the scope to wound healing applications, Salekdeh *et al.* investigated a surface-modified cationic polyurethane (CPU) wound dressing and tested its cytocompatibility (Fig. 9d).[159] The modified CPU significantly enhanced wound healing in both non-infected and infected full-thickness rodent models. In the non-infected rat model, it accelerated wound closure, promoted

organized collagen deposition, and stimulated angiogenesis while reducing inflammation compared to the commercial Tegaderm dressing. In the infected mouse model, histological analysis demonstrated improved fibroplasia and vascularization, confirming superior skin regeneration capabilities relative to standard clinical dressings. Collectively, these studies highlight the excellent biocompatibility and functional advantages of rubber-like synthetic polymers. Their easy-to-tailor mechanical properties combined with excellent biocompatibility, make these materials highly promising for biomedical devices and wound care, offering enhanced integration and performance beyond current clinical standards.

3. Emerging frontiers in wearable transistor technologies

The preceding section reviewed the historical progression of the evolution of rubber-like polymers, tracing their development from laboratory-scale synthesis to commercial manufacturing. It further explored the advancement of multifunctional polymers tailored for integration into one of the device component, including semiconductor, dielectrics, and substrates layers. In this section, we shift focus to cutting-edge advancements, with particular emphasis on the development of fully stretchable rubber transistors. The first subsection, titled "Rubbery transistors," critically examines the electrical performance, mechanical robustness, and operational stability of these devices under various forms of mechanical deformation. The second section namely "Skin-conformable wearable sensor platform" highlights researchers' goal to develop transistor devices that closely replicate human skin, not only in mechanical behaviors but also in self-healing and sensory functions. This approach is inspired by the skin's ability to sense heat, pressure, strain, and other stimuli when subjected to temperature changes, touch, or deformation. This biomimicry also aims to enhance long-term comfort, as devices that physically resemble skin are more comfortable and better suited for prolonged wear directly on the body. The third and fourth subsections focus on "Artificial synaptic electronics" and "Memory devices", which are distinguished from conventional rubbery transistors by their unique functionalities. Artificial synaptic devices replicate biological synapse functions, sustaining synaptic plasticity and consistent performance under repeated mechanical deformation, thus enabling brain-inspired computing and adaptive sensing. Memory devices prioritize flexible data storage with tailored polymers and device architectures that ensure high stability, low power consumption, and mechanical durability, supporting reliable long-term information retention in wearable applications. These advanced functionalities extend beyond standard transistor performance by integrating bioinspired processing and robust data retention within mechanically demanding environments.

3.1. Rubbery transistors

In recent decades, electronic devices have become an integral part of daily life, with applications expanding from traditional rigid systems to flexible and stretchable devices. These advanced devices can accommodate large deformations and conform to curved surfaces, enabling innovations in fields such as robotics,[160,161] prosthetics,[162,163] and wearable biomedical instruments.[164–166] To support this, early efforts in developing wearable transistor devices have primarily concentrated on ensuring stability of electrical performance under repeated mechanical strain and physical stress.[167,168] In the scope of stretchable transistor, many types of materials and methodologies are used to achieve these prominent factors, *i.e.* ion gels[169] or physically-modified wrinkled active layer.[170] However, these materials cannot comprise to be considered "fully stretchable", as their operability for stretchable transistors was less than 30% applied strain due to surging leakage current increase. Considering their mechanical properties and high flexibility, rubber-like synthetic polymers have become a staple option to create fully stretchable transistors, with the main goal of maintaining stable electrical performance under repeated mechanical strain and physical stress.

One of the early breakthroughs in stretchable transistor was reported in 2015 by Chortos *et al.* through development of a flexible and durable transistor capable of operating under intense physical conditions (Fig. 10a). The stretchability of fabricated device is attributed to thermoplastic polyurethane (TPU) dielectric and substrate, complimented by CNT electrodes and semiconductor. Unlike conventional metal electrodes and rigid semiconductors, the fabrication process of this device involved transferring unsorted CNT into TPU substrate, followed by integration of source–drain (unsorted CNT) and semiconductor layers (CNTs sorted with poly(3-dodecylthiophene)) onto a TPU dielectric. These components were then merged together to form a fully stretchable top-contact bottom-gate transistor ($\mu = 0.18 \pm 0.03$ cm^2 V^{-1} s^{-1}). The introduction of stretchable material into the transistor allows its operation up to 100% strain for 1000 cycles, while also maintaining its functionality under pressure (until 75 kPa), after sudden impact with hammer, and punctured by needle. Despite this trait, electron mobility continues to decline as the stretching length increases ($\mu_{100\%\ \text{stretching}} = \sim 60\%\ \mu_{\text{original}}$ [perpendicular to channel direction]; $\mu_{100\%\ \text{stretching}} = \sim 52\%\ \mu_{\text{original}}$ [parallel to channel direction]) with minimal recovery afterward ($\mu_{\text{recovery}} = \sim 75\%$ and $\sim 60\%\ \mu_{\text{original}}$, respectively), likely due to irreversible damage to the CNT semiconductor that hinders charge transport.[167] In 2016, Cai *et al.* also designed a stretchable transistor consist of CNT electrodes, SWCNT semiconductor, $BaTiO_3$/PDMS hybrid dielectric on PDMS substrate *via* all-printing method (Fig. 10b). The fabricated device provided 4 cm^2 V^{-1} s^{-1} average mobility. However, its performance dropped significantly after stretching ($\mu_{50\%\ \text{strain parallel}} = 65\%$ of original; $\mu_{50\%\ \text{strain perpendicular}} = 75\%$ of original), especially on repeated cycles ($\mu_{1000\ \text{cycle parallel}}$).[171] This issue of first generational fully rubber transistor was present considering lack of treatment and modification to counter morphology changes during stretching. Therefore, integration of elastomers into fully stretchable devices would finds its way beyond substrate or dielectric materials in future researches.

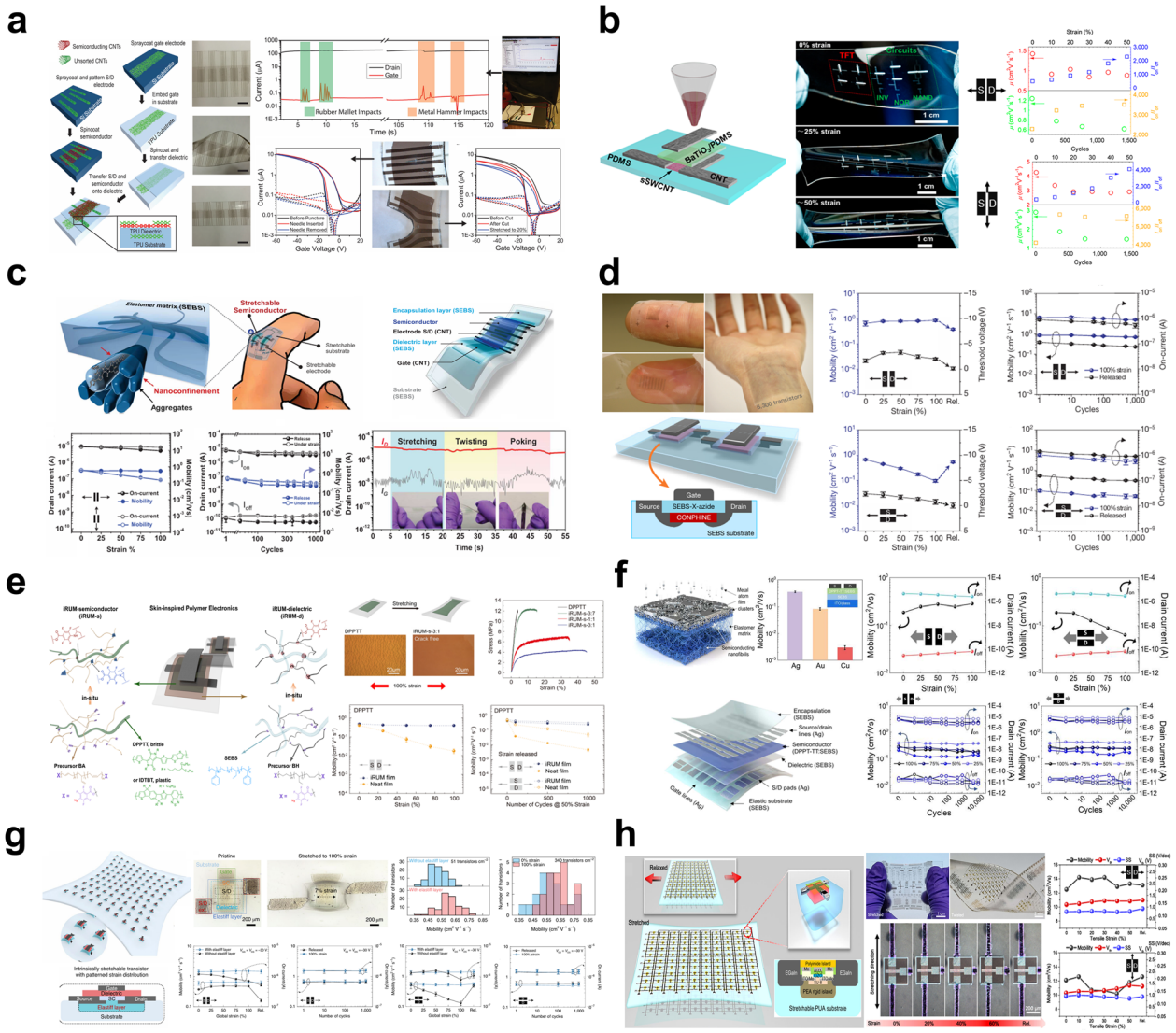

Fig. 10 Progresses on development of fully-stretchable transistors (a) stretchable transistor employing carbon nanotube semiconductor and electrodes on TPU substrate and (b) PDMS substrate. (c) Nanoconfinement method (CONPHINE) in fully-stretchable transistor by employing SEBS with conjugated polymer semiconductor. (d) Scalable fabrication of CONPHINE-based fully-stretchable transistor (e) *in situ* rubber matrix formation (iRUM) for conjugated polymer semiconductor using perfluorophenyl azide (PFPA) end-capped polybutadiene (BA) to improve stretchability of semiconducting and dielectric layer. (f) Development of stretchable metal electrode by Ag metallization on fully-stretchable devices. (g) Introduction of separated stiff and elastic regions on stretchable semiconductor to minimize stretching on active site. (h) MOSFET fabrication on stiff region with stretchable substrate to induce stretchability on MOSFET. Reprinted with permission from ref. 167 copyright 2015 John Wiley & Sons., ref. 171 copyright 2016 American Chemical Society, ref. 173 copyright 2017 American Association for the *Advancement of Science*, ref. 126 copyright 2018 American Association for the *Advancement of Science*, ref. 176 copyright 2021 Springer Nature, ref. 177 copyright 2022 American Association for the *Advancement of Science*, and ref. 178, and 179 copyright 2021 & 2024 Springer Nature.

Stable operation in extreme mechanical conditions has become the primary focus fully-stretchable transistor development. Hence, countering morphological changes while maintaining stable charge transfer of the semiconducting layers is highly crucial.[172] This issue can be solved through developments of intrinsically-modified stretchable electronic materials, providing a stable transport channel during stretching without any irreversible deformation. Hence, introduction of elastomers in this section would be very beneficial to introduce material stretchability into the active layer while retaining decent electrical properties. Xu *et al.* discovered nanoconfinement method of conjugated semiconducting polymers (Fig. 10c) to reduce semiconducting polymer nanofiber diameter to be less than 50 nm, reducing material crystallinity and improving its ductility. This method, termed "CONPHINE", was achieved through addition of SEBS to provide nanoconfinement effect while maintaining high aggregation, resulting in high stretchability and charge transport. The first COPHINE polymer semiconductor was made using DPPT-TT conjugated polymer with SEBS elastomer. Resulting CONPHINE film was proven to display similar transfer properties with neat DPPT-TT while maintaining a stable mobility during stretching in a bottom-contact bottom-gate device with SiO_2 dielectric ($\mu_{original} = 1.32$ $cm^2\ V^{-1}\ s^{-1}$, $\mu_{100\%\ stretching} = 1.08\ cm^2\ V^{-1}\ s^{-1}$), suggesting that

SEBS addition in the active layer retains electrical performance of the DPPT-TT. In fact, the film still operable upon stretching up to 200% ($\mu_{200\%\ \text{stretching}} = 0.33\ \text{cm}^2\ \text{V}^{-1}\ \text{s}^{-1}$), indicating its maintained charge transport pathways even in extreme mechanical conditions. This outstanding result leads to fabrication of fully-stretchable device composed of CONPHINE film active layer with CNT electrodes and SEBS dielectric and substrate. The stretchable device was presented with average mobility of 0.59 $\text{cm}^2\ \text{V}^{-1}\ \text{s}^{-1}$ ($\mu_{100\%\ \text{stretching}} = 0.55\ \text{cm}^2\ \text{V}^{-1}\ \text{s}^{-1}$) with high transparency, durable, and excellent conformability for skin application. The CONPHINE nanoconfinement method was also demonstrated with other conjugated polymers (P-29-DPPDTSE, PffBT4T-2DT, P(DPP2TTVT), PTDPPTFT4) with maintained electrical properties while improving its high stretchability.[173] Considering broad variation of main-chain groups with outstanding mobility, the use of DPP-based conjugated polymer also presents as an ideal example of semiconducting polymer to be used with this methodology and promotes many CONPHINE semiconductors the upcoming studies.[126,174,175]

As an advanced semiconductor material with ease of fabrication, Wang *et al.* utilized CONPHINE-based semiconductor layer for a scalable stretchable OFET production *via* patterning method. To achieve this, Wang *et al.* utilizes elastomer dielectric of SEBS to be crosslinked using azide-based crosslinker to increase solvent-resistivity, enabling high-scale COPHINE semiconductor (DPP2TTVT-PDCA with SEBS) patterning *via* etching method and finished by CNT electrodes *via* masking. The stretchable device was modified up to an impressive total of 6300 transistors in 4.4 × 4.4 cm^2 with high transparency and conformity for use in human skin (Fig. 10d). The fabricated stretchable device shows a high charge mobility during stretching to 100% (average $0.821 \pm 0.105\ \text{cm}^2\ \text{V}^{-1}\ \text{s}^{-1}$ for dense array; average 1.37 $\text{cm}^2\ \text{V}^{-1}\ \text{s}^{-1}$ for less-dense array) with no current hysteresis, high $I_{\text{on/off}}$ (10^4), and low leakage. The feasibility of this method was demonstrated by fabrication of a series of stretchable circuits, such as inverter using pseudo-CMOS design, universal logic gate with NAND design, and amplifier using self-feedback design with stable operation even during stretching.[126] This has set a staple standard for fully-stretchable transistors in the following researches: durable transistor (low hysteresis and leakage) with minimal decrease of transfer properties during stretching. Aside from CONPHINE method, Zheng *et al.* designed *in situ* rubber matrix formation (iRUM) mechanism to achieve target properties for both semiconducting and dielectric layer (Fig. 10e) while embedding high stretchability. iRUM precursor based on perfluorophenyl azide (PFPA) end-capped polybutadiene (BA) was employed alongside poly-thieno[3,2-*b*]thiophene-diketopyrrolopyrrole (DPPTT) as semiconducting layers with following considerations: (1) BA provide flexible backbone with compatible surface properties with semiconducting polymer for proper blending. (2) PFPA enables self-crosslinking with BA (azide/C=C cycloaddition) or with polymer semiconductor (azide/C–H insertion) (3) maintained charge transport pathways from polymer semiconductor aggregation due to higher BA self-crosslinking rate. Controlling precursor and semiconductor is highly crucial to maintain stable mobility by balancing reactivity of azide/C=C and azide/C–H insertion to produced crosslinking-induced elasticity without disrupting chain packing and aggregation. iRUM semiconductor (iRUM-s) was able to maintain ~1 $\text{cm}^2\ \text{V}^{-1}\ \text{s}^{-1}$ mobility in conventional Si MOSFET and 0.5 $\text{cm}^2\ \text{V}^{-1}\ \text{s}^{-1}$ in stretchable OFET using CNT gate and source/drain electrode and PDMS dielectric. Moreover, cyclic durability of stretchable semiconductor enables high-retention transfer properties despite stretching to 100% strain and cycled 1000 times at 50% strain. In addition, iRUM approach applied for SEBS dielectric results in high crosslinking density to increase flexibility, solvent resistance, and photo-patternable of semiconductors. This leads to application into fully patterned elastic transistor with iRUM-approached semiconductor and dielectric to realize feasibility of producing robust elastic electronics. A resulting 0.4 $\text{cm}^2\ \text{V}^{-1}\ \text{s}^{-1}$ mobility was obtained with stable performance after 1000 stretching cycles at 50% strain.[176]

At first glance, integration of elastomers for fully stretchable devices are driven solely by material stretchability, flexibility, and toughness. However, elastomers offer more traits beyond their mechanical properties, including ease of processing, hydrophobicity, chemical stability in ambient conditions, and ease of modifications on the elastomers itself. Ease of elastomers processing enables Xu *et al.* to perform solution searing on CONPHINE-based stretchable transistors using micro-structured line blades in order to align its semiconducting polymer chains, hence increasing its electrical performance. This method was tested using COPHINE-formed stretchable DPPDTSE semiconductor and its results are compared with conventional method of spin-coating. Fabricated on fully stretchable transistors with CNT electrode and SEBS dielectric, solution-sheared (SS) COPHINE-film exhibited higher mobility than spin-coated COPHINE-film[173] ($\mu_{\text{SS-COPHINE}} = 1.5\ \text{cm}^2\ \text{V}^{-1}\ \text{s}^{-1}$; $\mu_{\text{SC-COPHINE}} = 1.01\ \text{cm}^2\ \text{V}^{-1}\ \text{s}^{-1}$). The directional ordered structure of SS-COPHINE-film was based on shearing direction during fabrication, which is parallel to the charge transport direction. This influences its transfer properties during stretching, where slight mobility decrease was observed during stretching perpendicular to transfer direction while no significant changes were observed during parallel stretches. This device also provides stable transport even until 1000 cycles, which largely attributed to fabrication of CONPHINE active layer themself. The ease of elastomer's processing in this manner was also highly scalable into large scale production of high-performance fully-stretchable transistors.[180,181] Aside from material processing, rubber-like synthetic polymers also able to provide excellent support for metal diffusion to fabricate stretchable metal-based electrode. Although metal electrodes are known to possess high conductivity, they are less common to be applied in fully-stretchable transistors considering its poor stretchability and higher contact resistance compared to CNT- or graphene-based electrodes.[182,183] Some researches opted to add elastomers in metal-based electrode materials to embed stretchability for electrode materials (*i.e.* AuNP-AgNWs/PDMS,[184] AgNW-PUA[185]), although they resulted in inferior conductivity than pristine condition and requires additional processability compare to bulk metal form. In 2022, Kim *et al.*

explores Ag metallization in elastomer-based fully-stretchable transistor to design highly flexible electrode without compromising much of its conductivity. Ag metallization was found to create metal-elastic intermixing region when deposited onto soft rubber–semiconductor, such as CONPHINE layer, that resulted from diffusion of Ag metal on the rubber–semiconductor interface, resulting in high elasticity in Ag electrode with enhanced stability during stretching (Fig. 10f). The success of its fabrication also possibly supported by high toughness of rubber materials itself by retaining its shape without any physical deformation upon metal diffusion. Based on this result, 5 × 5 fully stretchable transistor array was fabricated using DPPT-TT:SEBS nanoconfined semiconductor, SEBS dielectric, and Ag electrodes, with average mobility of 0.288 $cm^2 V^{-1} s^{-1}$. Moreover, transistor mobility only showed a slight decrease upon strain while performs similarly to pristine condition after multiple cycles.[177] Compared to other common electrodes for fully stretchable transistors, Ag possess the highest electricity among metals with higher processability compared to SWCNTs. Therefore, Ag may present as suitable alternative electrodes for future rubber-based fully-stretchable devices with high performance and lower costs. Another beneficial trait of elastomers and rubber materials' application in stretchable devices are ease of material modification, such as structural customization and crosslinking methods. This trait inspires the unique design of stretchable transistor by introducing stiff and elastic regions, where each focus on retaining electrical performance and device stretchability, respectively. When applied using different types of material, stiff and elastic region's interconnections are prone to failure due to the large modulus mismatch during stretch. To tackle this, Wang *et al.* designed separated region of active areas in multi array transistor using different PS concentration in SEBS (Fig. 10g).[178] Elastiff layer, as the stiff active region, was achieved *via* crosslinking of rigid SEBS (67 vol% PS) that are prepared on soft SEBS (12 vol% PS) to prevent substantial strain at active layer during device stretching. The use of rigid SEBS as Elastiff layer also enables strong adhesion into the SEBS substrate to prevent interconnection failure upon stretching. Fully stretchable transistor was fabricated by preparation of COPHINE semiconductor,[173] azide-crosslinked SEBS dielectric and CNT source/drain electron on Si/SiO^2 with dextran sacrificial layer, followed by patterning of rigid SEBS and laminated with soft SEBS substrate. Transistor fabrication was completed after removal of sacrificial layer for transferring device fully into SEBS substrate and masking CNT gate. Fabrication of transistor with the stiff regions results in similar mobility value (0.62 ± 0.08 $cm^2 V^{-1} s^{-1}$) compared to device with same structure without stiff region (0.51 ± 0.06 $cm^2 V^{-1} s^{-1}$). The layer between Elastiff and substrate region proved to be tear-free after stretching to 100% from strong adhesion between each layer. Moreover, the distinct capabilities of this methodology can be exhibited through minimized stretching of active region (7% strain on the active region) upon 100% of entire device stretch. The minimized strain leads to decrease in morphological changes that preserve charge pathways for efficient transfer, as proven by preserved mobility under strain compare to non-strain-patterned device with the same structure. Considering the differential in the stiff/elastic layouts, the mechanical stability of this design relies heavily on device size, inter-device distances, and stiff layer thickness. The success of this design enables fabrication of stretchable devices without compromising active site's stretchability for electrical performance or *vice versa*, enabling more combinations between stretchable substrate and rigid transistors. Given this success, fabrications of stretchable non-organic transistor can be realized on rigid regions (active site) on a stretchable substrate to achieve high mobility with stable performance upon stretching. Kang *et al.* succeeded to design a stretchable MOSFET by implementing polyepoxy acrylate (PEA) rigid islands formation in flexible polyurethane acrylate (PUA) substrate *via* acrylic crosslinking (Fig. 10h).[179] To fabricate a stretchable metal oxide transistor, metal oxide transistor and circuits are firstly fabricated on photopatterned PI layer, prepared as covering layer. Molybdenum (Mo) gate electrode was deposited on patterned PI, followed by *a*-Al_2O_3 dielectric layer, *a*-IGZO semiconductor, and flexible eutectic–galliumindium stretchable electrode. Then, EA-based resin was cured into PEA *via* photolithography method and laminated by PUA by UV curing. In the field of stretchable transistors, it is noteworthy that the use of metal oxide materials is not highly considered due to their inability to stretch or deliver consistent transfer properties upon stretching. In contrary, this design provides a stable base for stretchable MOSFET design as this fabricated device able to stretch up to 60% strain with high recoverability with minimal stretch in the active site due to synergistic effect of common acrylate group of PUA and PEA in providing strong intramolecular covalent bonding. The use of metal-oxide semiconductor enables carrier mobility of 12.5 $cm^2 V^{-1} s^{-1}$, a considerably high value as a stretchable transistor, with maintained value upon stretching in repeated cycles. While it is reported that threshold voltage shift was observed upon repeated cycles due to change of average spacing of metal oxide lattice, this pose to be a minimal concern since it occurs after extensive cycling times (10 000 times stretching to 30% strain). Owing to their mechanical performance and potential for high mobility transistor fabrication, stretchable transistors based on rigid-elastic architecture offer promising pathways to achieve high-performance transistors with excellent stretchability.

3.2. Skin-conformable wearable sensor platform

Building on extensive research in stretchable materials, the field of stretchable electronics has made significant advancements, particularly in strain-tolerant sensors. Rubber-like synthetic polymer materials have emerged as particularly advantageous for skin-integrated sensing applications due to their intrinsic hydrophobicity, superior mechanical robustness, and favorable conformability to the complex contours of human skin. Over time, numerous stretchable sensors have been fabricated utilizing diverse rubber-like synthetic polymer substrates, notably PDMS,[16,186,187] PU,[188] and SEBS,[126,189,190] each offering distinct physicochemical properties that contribute to device performance and durability. The developing methods to

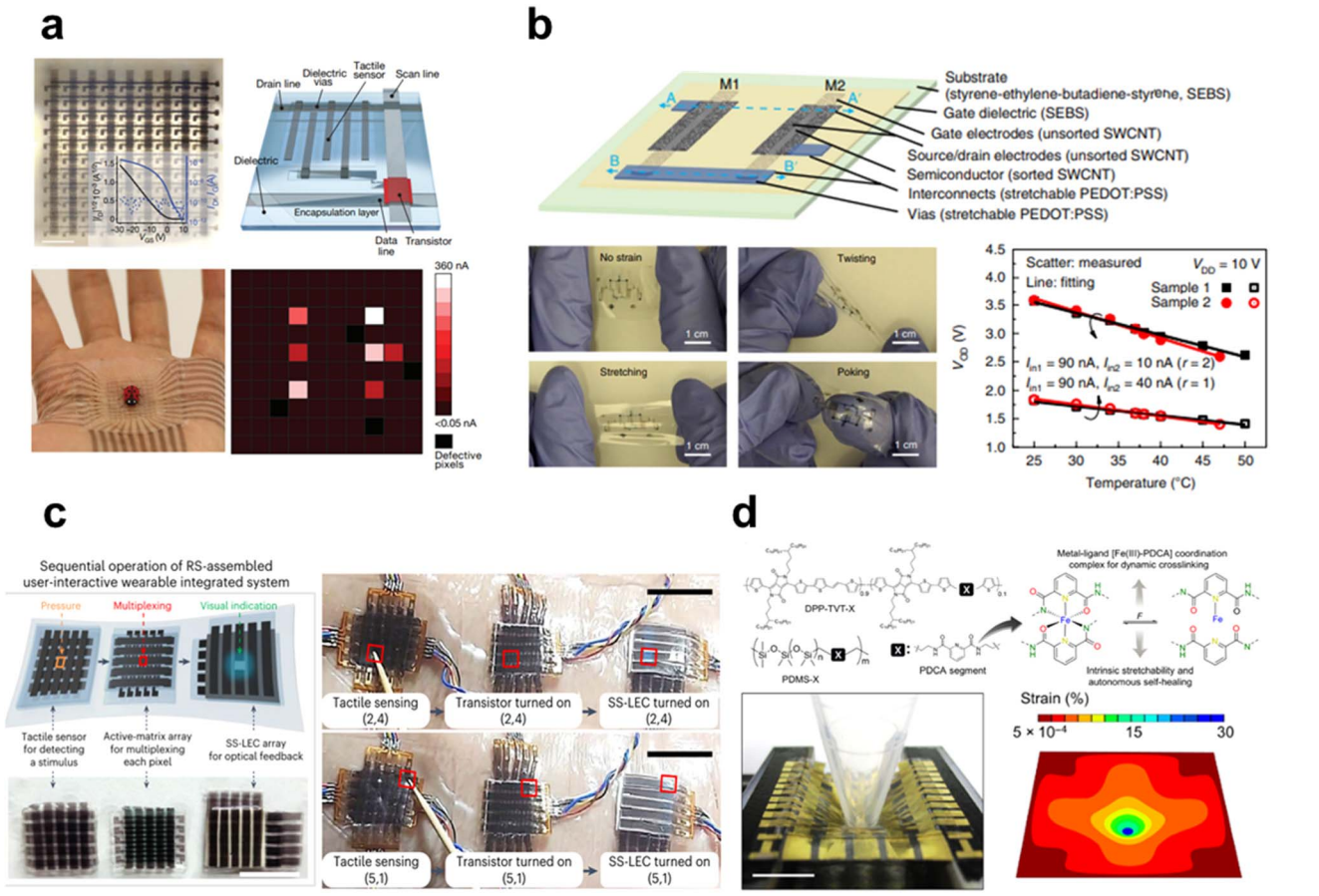

Fig. 11 Rubber-based wearable sensors based on material characteristics. Fully-stretchable skin-conformable sensors: (a) tactile sensor arrays based on COPHINE semiconductors with SEBS substrate. (b) Temperature sensor using SWCNT-based transistor on SEBS.; self-healable sensors: (c) fully self-healable e-skin system using nanoconfinement of DPP-DTT with PDMS-$MPU_{0.4}$-$IU_{0.6}$ elastomer. (d) Strain sensor utilizing metal–ligand self-healing mechanism of DPP-TVT-PDCA elastomer. Reprinted with permission from ref. 126 copyright 2018 American Association for the *Advancement of Science*, ref. 190 and 192 copyright 2018 & 2025 Springer Nature, and ref. 59 copyright 2019 Association for the *Advancement of Science*.

produce stretchable electronics also enables numerous wearable sensor types based on their stimuli; being temperature, pressure, strain, light, or even magnetic fields through active site choice of materials.[186,191] In 2018, Wang *et al.* reported the fabrication of tactile sensor array based on the prior design of fully- stretchable transistor using CONPHINE semiconductor and azide-x-SEBS dielectric materials (Fig. 11a). Fabricated on skin-conformable SEBS substrate, the 10 × 10 sensor array utilizes CNT electrode with tactile sensor and used to accurately detect object placed on the sensor array.[126] In the same year, Zhu *et al.* fabricate a stretchable temperature sensor using SWCNT transistor on SEBS substrate (Fig. 11b). The mechanism of temperature sensing was observation through changes of output voltage (V_{OD}) in different temperatures without strain-induced voltage shift.[190] Hence, fabricated sensor not only display detailed and accurate temperature-sensing capabilities, but also operational during various mechanical stretching. These findings serve as pathways for future stretchable sensor design, as the demands for skin electronics increased for many mechanically-demanding activities, such as sport or robotics.

Considering the complexity of skin movements during activities, it would be inevitable for applied skin sensors to be damaged overtime. At times, focusing on material durability by introducing more covalent complexes or stiff material addition would significantly increase hardness of material and would be uncomfortable for skin during use. As a way to tackle damaged applied skin-sensor, self-healing mechanism would be introduced on rubber-like synthetic polymers. The main appeal of stretchable and self-healing material for e-skin application is to retain high toughness and durability while employing self-healing characteristics. There are two types of self-healing mechanism: intrinsic self-healing or employing healing agents. The use of additional healing agents is commonly achieved using microcapsules that are designed to broke and release healing agents upon rupture. However, this healing mechanism is generally considered inferior to intrinsic self-healing since it is ineffective for repeated damage at the same location.[193,194] Considering the need of material longevity and continuous skin movements during activities, intrinsic self-healing materials are more preferred for skin electronics applications.

In polymer science, intrinsic self-healing mechanisms are achieved through covalent (Diels–Alder, amine reactions, boroxine reactions) or non-covalent bonding (hydrogen bonds, metal–ligands interactions, π–π interactions) between functional groups.[168] Unlike covalent bonding, non-covalent-based self-healing mechanism are usually preferred for wearable devices considering no significant changes on the material properties after self-healing. Employing rubber materials with self-healing mechanism generally includes self-healing moiety main chain/network. In 2018, Bao's group design a supramolecular elastomer network of PDMS-$MPU_{0.4}$-$IU_{0.6}$, where MPU and IU constructs linkages from strong and weak hydrogen bonds, respectively. The complimentary properties between rubber and self-healing moieties results in elastomer that combines high modulus and strain capacity with highly efficient autonomous self-healing ability.[195] Based on these results, PDMS-$MPU_{0.4}$-$IU_{0.6}$ supramolecular elastomers demonstrate strong potential as material for e-skin sensors as exemplified through fully-stretchable e-skin system fabrication by Jang *et al.* A user-interactive wearable integrated e-skin system of self-healable strain sensor, LEC module, and equipped with additional fully stretchable and self-healable TFT switch module was designed using PDMS-$MPU_{0.4}$-$IU_{0.6}$-DPP-DTT as nano-confinement matrix of DPP-DTT into self-healing semiconducting layer (Fig. 11c). The 5 × 5 configuration of sensor, transistor, and LEC array enables tracking of specific sensing location on the strain sensor by tracing change in resistance in specific spot when pressed.[192] Another type skin-like material as wearable sensor was made by employing modified PDMS and DPP-TVT using PDCA, as demonstrated by Oh *et al.* This idea was initiated from previous report on self-healable semiconductor DPP-TVT-PDCA by Oh *et al.*, providing self-healing capability and moderate elasticity through addition of PDCA while preserving charge transfer properties of DPP-TVT.[196] Utilized as an active matrix in strain-sensing array, PDMS-PDCA was introduced to provide dynamic crosslinking into the self-healable semiconductor. To provide autonomous healing capability and stretchability, metal–ligand coordination complexes between Fe(III) ion to PDCA ligand are utilized to provide dynamic crosslinking between PDCA moieties (Fe–$N_{pyridyl}$, Fe–N_{amido}, Fe–O_{amido}). With this modification, the self-healing semiconductor exhibits a gradual decline in mobility and normalized on-current with increasing strain, but both properties show notable recovery upon strain release. In addition, material's mobility is able to recover from 0.047 ± 0.013 to 0.028 ± 0.047 $cm^2 V^{-1} s^{-1}$ after being cut and healed due to self-healing mechanism from intrinsic semiconducting material design. Based on this result, a transistor array was fabricated using Au electrodes with SEBS dielectric, substrate, and encapsulation layer. Considering the change of normalized on current upon strain and usability in low drain voltage (−5 V), the skin-like stretchable transistor acts perfectly as wearable sensor to detect applied strain (Fig. 11d).[59] Through these advancements, wearable sensors' developments have been revolutionized into skin-like devices that open a pathway for numerous self-healing rubber application in the future.

3.3. Artificial synaptic electronics

The advancement of electronic devices is increasingly directed toward emulating the human brain's functions through synaptic devices capable of replicating complex behaviors such as spike-timing-dependent plasticity (STDP). In STDP, synaptic strength dynamically adapts based on the precise timing of electrical spikes, enabling learning and memory processes.[197–199] Among various neuromorphic approaches, synaptic transistors have emerged as a particularly promising platform due to their transistor-based architecture, which offers inherent tunability, scalability, and compatibility with existing semiconductor technologies.[67,69,200] Early synaptic transistors developed in the 1990s by Shibata and Ohmi were based on traditional metal-oxide-semiconductor (MOS) technology, using silicon and silicon dioxide as the gate insulator.[201] These devices relied on charge storage and electronic modulation within solid-state materials to emulate synaptic functions but did not involve ionic conduction. A major breakthrough came in 2010 with the Nanoparticle Organic Memory Field-Effect Transistor (NOMFET) developed by Vuillaume's group.[202] This hybrid organic/inorganic device combined pentacene with embedded gold nanoparticles to explicitly mimic synaptic plasticity through charge trapping and release, reproducing key synaptic behaviors such as short-term plasticity and spike-dependent conductance modulation. Following this, metal oxide-based synaptic transistors using materials like IGZO and ZnO emerged in the early 2010s, leveraging oxygen vacancy migration and ion dynamics to achieve gradual and reversible conductance changes, enabling more biomimetic synaptic functions.[203,204] Around 2013, ionic liquid-gated synaptic transistors were introduced, employing ion migration within ionic liquids to modulate channel conductance in a highly analogue and energy-efficient manner.[12,205] This approach closely mimics biological neurotransmission by enabling reversible and tunable synaptic weight changes at low voltages, further advancing the field toward realistic neuromorphic computing devices. However, these advancements still could not meet the requirements for stretchable devices due to their rigidity and lack of mechanical flexibility, limiting their application in wearable or bio-integrated electronics.

Early substrates used for soft electronics in synaptic transistors included polycarbonate, polyethylene terephthalate (PET),[209,210] polyethylene naphthalate (PEN),[211] and polyimide (PI),[88] chosen for their flexibility and chemical resistance. Nevertheless, these materials have limitations, as transparency, thermal resistance, and especially stretchability, which are crucial to preserving device performance under strain in soft electronics.[212] In 2018, Lee *et al.* addressed these challenges by fabricating a fused FT4-DPP conjugated polymer blended with PEO to form nanowire channels, CNT electrodes, and a high-capacitance ion gel electrolyte, as provided in Fig. 12a. All device components were integrated onto a highly stretchable SEBS substrate, which was specifically chosen for its exceptional elasticity and mechanical durability. The SEBS substrate enabled the device to endure repeated and extreme deformations while preserving stable electrical and synaptic

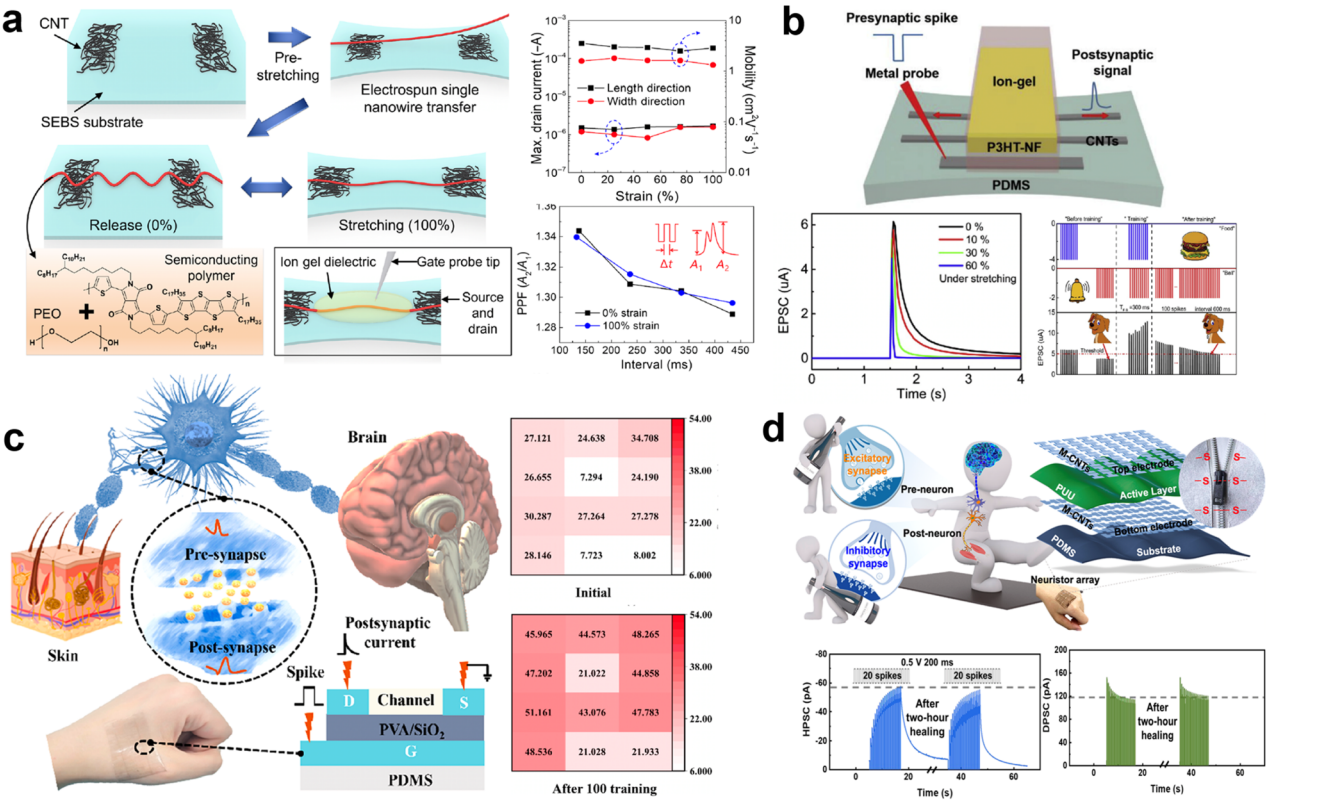

Fig. 12 Schematic illustrations and experimental results demonstrating the design and performance of stretchable synaptic (neuromorphic) transistors for wearable and bio-integrated electronics. (a) The fabrication process and mechanical robustness of a stretchable transistor based on a SEBS elastomer substrate and carbon nanotube (CNT) network, showing stable charge transport and device mobility under up to 100% strain. (b) Structure and function of an ion-gel gated synaptic transistor on a PDMS substrate, showing the emulation of synaptic behavior through presynaptic spikes and postsynaptic current responses, with reliable operation maintained during mechanical stretching. (c) Conceptual illustration of artificial synapses interfacing between electronic skin and the brain, including a device structure based on PVA/SiO_2 gel and PDMS, and data tables showing synaptic weight changes before and after training. (d) Illustration of a flexible neuromorphic array featuring both excitatory and inhibitory synapses, highlighting self-healing properties and the retention of synaptic function and signal transmission after mechanical damage and subsequent healing. Reprinted with permission from ref. 29 copyright 2018 American Association for the *Advancement of Science*, ref. 206 copyright 2020 Elsevier, ref. 207 copyright 2022 American Chemical Society, and ref. 208 copyright 2023 American Chemical Society.

performance, a critical requirement for soft robotics and wearable bioelectronics. Mechanistically, optical signals across a broad spectrum were detected by a self-powered organic photodetector, which generated voltage spikes that served as presynaptic inputs to the synaptic transistor. These spikes induced rapid anion migration within the ion gel electrolyte, transiently increasing channel conductivity and producing EPSCs. The device reliably demonstrated short-term synaptic plasticity, including PPF, spike-timing-dependent plasticity, and dynamic filtering, closely mimicking biological synaptic responses. Importantly, the robust mechanical properties of SEBS ensure that these synaptic behaviors and key performance metrics, such as carrier mobility (>1 $cm^2 V^{-1} s^{-1}$) and PPF ratio ($A2/A1$ = 1.34 at 120 ms), were maintained even under substantial strain and after repeated cycling (Fig. 12a).[29] This integration enabled the system to translate patterned optical signals into distinct synaptic outputs for optical wireless communication, and to actuate a polymer-based artificial muscle, directly emulating muscle contraction in response to neural activity. Thus, the use of SEBS is pivotal, not only for mechanical compliance but also for enabling reliable and high-performance operation of the integrated sensorimotor synapse in applications ranging from soft robotics to next-generation electronic prosthetics.

Importantly, in 2020 Wang *et al.* systematically showed for the first time that key synaptic parameters such as learning, memory, and decay constants can be modulated by varying the degree of mechanical strain. Introducing a stretchable synaptic transistor that uniquely combines wavy P3HT-NF as the semiconductor, a soft ion-gel dielectric (PAN/LiTFSI in EC/PC), and compliant CNT electrodes, all built on a PDMS elastomer substrate, as visualized in Fig. 12b. This all-organic, multicomponent system was engineered to accommodate substantial mechanical deformation without microcracking or delamination. The wavy morphology of the P3HT-NF film, formed *via* a lamination and transfer process, allowing the semiconductor to stretch and relax in tandem with the substrate to preserve both structural and electronic integrity. The CNT electrodes, embedded within the PDMS, maintain low-resistance contacts even when the device is bent or stretched. The ion-gel layer ensured efficient ion transport during operation and remains intact under strain. When a gate voltage pulse was applied, ions

migrate within the gel and modulate the channel conductivity, generating EPSCs that mimic the function of biological synapses. Notably, after stretching to 60% and releasing, the device still produced robust EPSC peaks (~13.2 μA) and maintained stable PPF ratios, indicating reliable learning and memory functions (Fig. 11b).[206] The study further revealed that mechanical strain can be used as a tunable parameter, increasing deformation alters ion transport dynamics and channel geometry to allow precise adjustment of synaptic parameters. This synergy of soft, stretchable materials and carefully engineered device architecture provides both mechanical resilience and functional adaptability, closely paralleling the behavior of biological neural tissue. As a result, these devices offer new possibilities for the development of neuromorphic electronics in wearable, implantable, and soft robotic systems, where flexibility and adaptability are paramount.

Recent research on artificial synaptic electronics is increasingly focusing on integrating self-healing capabilities into synaptic transistors. Incorporating self-healing materials into synaptic transistors not only enhances their mechanical robustness but also preserves synaptic performance after physical damage.[213–215] Although still in early stages, self-healing synaptic devices hold promise for extending device lifetime and enabling more resilient neuromorphic systems that better emulate the regenerative nature of biological tissues. For instance, Wang *et al.* developed a stretchable neuromorphic electronic skin (STRM-NES) by integrating S-CNT electrodes as the active channel, a PVA/SiO_2 ion-conducting hydrogel, and a PDMS elastomeric substrate, achieving robust synaptic functionalities with rapid self-healing and excellent mechanical durability. The synaptic behavior originated from proton migration within the PVA hydrogel, where abundant hydroxyl (–OH) groups formed dynamic hydrogen bonds, facilitating efficient proton conduction *via* a Grotthuss-type hopping mechanism (Fig. 12c). These dynamic hydrogen bonds also endowed the PVA hydrogel with autonomous self-healing capability, allowing the polymer network to rapidly recover its ionic pathways and mechanical integrity within 10 minutes after mechanical damage or burning. Meanwhile, the PDMS substrate acted as a rubber-like synthetic polymer, providing exceptional elasticity, conformal adhesion to skin, and mechanical support that enabled stable device operation under repeated deformation, including 1000 stretching cycles at 30% strain and tensile deformation up to 50%. The multilayer device maintained stable paired-pulse facilitation (PPF) ratios (~1.9) and consistent excitatory and inhibitory postsynaptic current (EPSC/IPSC) responses throughout mechanical cycling, demonstrating reliable neuromorphic plasticity.[207] Although the study did not delve into molecular design parameters or interfacial chemistry between PDMS and PVA, the effective integration of these polymers highlights a practical approach to achieving multifunctional, flexible neuromorphic devices. This work exemplifies how combining ionically conductive, self-healing hydrogels with elastomeric substrates can meet the stringent mechanical and functional demands of wearable electronics, consistent with recent advances in polymer-based electronic skins that leverage dynamic bonding and elastomeric matrices for durability and adaptability.

In 2023 Qiu *et al.* designed a bilingual bidirectional stretchable self-healing neuristor (BBSSN) array featuring a layered architecture composed of M-CNT electrodes, a PU ion-conducting layer, and a PDMS skin-like substrate, which assembled *via* van der Waals integration to ensure intimate interfacial contact and mechanical robustness (Fig. 12d). The PU ion gel exhibited a low glass transition temperature and high polymer chain mobility, enabling exceptional stretchability exceeding 1000% tensile strain and autonomous self-healing after severe mechanical damage. PDMS provided conformal adhesion and mechanical support critical for wearable applications. The device operated through the migration of mobile ions within the PU layer in response to presynaptic electrical pulses. These ions accumulated at the interface with the semiconductor channel, modulating the local electric field and transiently altering channel conductivity, which produced reversible changes in PSC. This ion redistribution dynamically enabled both excitatory (potentiation) and inhibitory (depression) synaptic behaviors under the same stimulus, governed by the direction and extent of ion migration and electrostatic coupling between ions and charge carriers. The BBSSN array maintained stable synaptic operation under 50% strain and achieved an ionic conductivity of 4.4×10^{-4} S cm^{-1} (Fig. 12d).[208] Functionally, it demonstrated robust four-quadrant information processing, spike rate-dependent plasticity, proprioceptive feedback, and rapid automated refresh of synaptic states. Notably, the device exhibited autonomous self-healing, fully restoring both structural integrity and synaptic function within 2 hours after mechanical damage. These features positioned the BBSSN as a promising platform for resilient, flexible neuromorphic systems and wearable bioelectronics capable of adaptive, bidirectional signal processing.

Rubber-like synthetic polymers play a crucial role in synaptic transistor devices, primarily serving as flexible and deformable substrates[29,207] or encapsulation layers[208] that provide mechanical resilience and ensure stable device operation under various strains. Although their use as active synaptic layers remain less common due to challenges such as low charge carrier mobility,[23,130] poor electrical conductivity,[184,185] and complex ion transport,[148] elastomers are indispensable for maintaining the mechanical integrity and durability of these devices. Consequently, current research combines these elastomer supports with semiconducting polymers[208] or composites[207] to optimize synaptic functions. Looking ahead, advancing novel rubber-like polymers or composites with enhanced electrical performance and tunable ion/electron transport will be essential. Such innovations will enable synaptic devices where both substrates and active layers deliver robust mechanical compliance alongside superior synaptic behavior, paving the way toward versatile, self-healing neuromorphic electronic skins.

3.4. Memory devices

Memory transistors denote a significant evolution beyond traditional voltage-controlled switches through the

incorporation of a charge-storage layer such as a floating gate, charge-trapping dielectric, or nanocrystal ensemble that facilitates the non-volatile retention of electrical charges. This architectural modification enables the device to preserve its programmed electronic state in the absence of power, distinguishing it from conventional transistors that lose stored information upon power removal.[216–218] The foundational concept of the memory transistor was realized with the pioneering work of Kahng and Sze at Bell Laboratories in 1967, who introduced the floating-gate MOSFET.[219] This device integrated a conductive floating gate capable of reliably trapping and retaining charge carriers, thereby establishing the basis for flash memory and related non-volatile memory technologies. These systems critically depend on stable charge retention and rapid switching kinetics, properties intimately linked to the chemical composition and interfacial engineering of the charge-storage materials, which remain active areas of research within materials chemistry and device physics.[68,220,221] Early memory devices primarily relied on inorganic materials and rigid substrates, focusing on optimizing charge-trapping layers such as floating gates, charge-trapping dielectrics, and nanocrystal layers to enhance data retention, switching speed, and endurance.[222,223] Advances in materials chemistry and interface engineering have enabled improvements in device stability, reduced leakage currents, and enhanced programming/erasing cycles, which are critical for high-performance memory applications including flash memory and emerging neuromorphic systems.[224] In addition, organic and hybrid memory transistors have attracted attention due to their potential for low-cost fabrication, mechanical flexibility, and tunable electronic properties. These devices incorporate semiconducting polymers and organic dielectrics, offering chemical versatility to tailor charge transport and trapping behaviors.[203,221,225,226] Innovations such as photo crosslinkers and molecular switches have further enabled dynamic control over memory states, expanding the functional scope of memory transistors beyond traditional inorganic systems.[227–229] Despite these advancements, conventional memory transistors have largely remained limited by their mechanical rigidity, constraining their integration into flexible and wearable electronics. The challenge lies in maintaining reliable charge storage and fast switching under mechanical deformation, which requires new materials and device architectures that combine electronic performance with mechanical compliance.[230,231]

Recent research has increasingly targeted the development of stretchable memory transistors that utilize elastomeric materials, which impart intrinsic stretchability and conformability. These materials enable devices to sustain repeated mechanical strain while preserving memory functions, a critical requirement for wearable and soft electronic applications.[232,233] Early prototypes of non-volatile memory devices have been embedded into stretchable electronic applications, in which a WORM organic memories or nanoparticle-based resistive-change memory elements were fabricated on stretchable elastomers. Among the pioneering studies, Jung *et al.* fabricated flexible organic ferroelectric non-volatile memory thin-film transistors (OFMTs) on a stretchable PDMS elastomer substrate, using poly(vinylidene-trifluoroethylene) as the ferroelectric gate insulator and poly(9,9-dioctylfluorene-*co*-bithiophene) as the semiconducting channel, as displayed in Fig. 12a. The device structure features a top-gate/bottom-contact configuration, and the entire fabrication process was adapted for compatibility with the elastic PDMS substrate. The use of PDMS is particularly beneficial for preserving electrical performance under mechanical deformation because its intrinsic elasticity and low Young's modulus allow the device layers to flex and stretch without introducing significant mechanical stress or cracks, thus maintaining interface integrity and device operation even when bent to a radius as small as 0.6 cm. As a result, the memory transistors maintained high performance, showing a carrier mobility of 5×10^{-2} cm^2 V^{-1} s^{-1}, an on/off ratio of 7.5×10^3, and a memory on/off ratio of 1.5×10^3 (retaining 20 after 2000 s) with minimal change during bending tests (Fig. 13a).[85] These results highlight the feasibility of integrating non-volatile memory functionality into future stretchable and wearable electronic systems, with PDMS substrates playing a critical role in enabling robust device flexibility and reliability.

In 2017, Hung *et al.*[19] reported the synthesis of MH-*b*-PI copolymers *via* a copper(I)-catalyzed azide–alkyne "click" reaction, combining the charge-trapping capability of the carbohydrate-based MH with the elasticity of the PI (Fig. 13b). As a synthetic rubber with a low Tg of −72 °C, PI imparted outstanding stretchability and resilience, allowing thin film memory devices to withstand strains up to 100% without cracking, and maintained stable ON/OFF current ratios above 10^6 and set voltages around −2 V even after 500 cycles at 40% strain. Electrically, PI served as an insulating soft matrix that spatially separated the MH domains' primary charge-trapping sites due to their abundant hydroxyl groups, enabling the self-assembly of well-defined nanostructures such as vertical or horizontal cylinders and spheres. The resulting morphology directly tuned the memory mode, such as vertical cylinders favoured non-volatile WORM operation with high retention, horizontal cylinders enabled rewritable Flash-type behavior, and spherical domains led to volatile DRAM-like operation, as indicated in Fig. 13b. The insulating nature of PI confined trapped charges within the MH domains, stabilizing memory states and minimizing leakage currents, while its elasticity preserved both the nanostructure and charge-trapping functionality under mechanical deformation, which is crucial for reliable operation in stretchable and wearable electronics. While this study primarily focuses on the design and function of stretchable memory materials, the MH-*b*-PI copolymer system can indeed be regarded as a form of memory transistor, bridging the gap between polymer chemistry and flexible transistor technology. This highlights its significant potential for advancing eco-friendly, mechanically robust, and high-performance wearable electronics.

Expanding on these foundational advances, Nam *et al.* introduced a new approach to stretchable memory by creating the first intrinsically stretchable floating-gate memory transistor specifically designed for electronic skin applications. Their device incorporated a blend of a semiconducting polymer

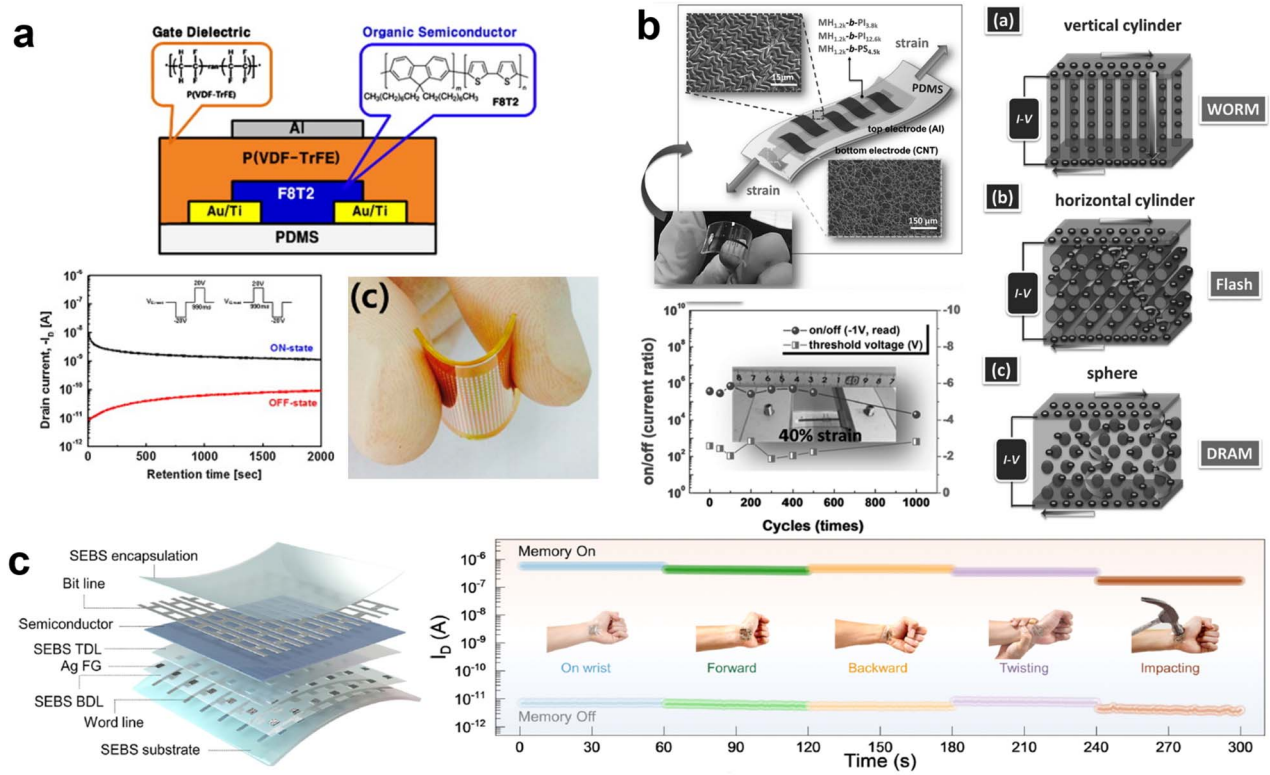

Fig. 13 Flexible and stretchable organic memory devices. (a) Schematic illustration and retention performance of a flexible organic memory transistor using a PVDF-TrFE gate dielectric and F8T2 organic semiconductor on a PDMS substrate. The retention plot shows stable ON and OFF states over time. (b) Stretchable memory device based on MH-b-PI copolymer with CNT bottom and Al top electrodes on PDMS, showing stable on/off current ratio and threshold voltage under 40% strain. Self-assembled nanostructures (vertical cylinder, horizontal cylinder, sphere) enable WORM, Flash, and DRAM memory modes, respectively. (c) Layered architecture of a fully stretchable memory array with SEBS encapsulation, and demonstration of robust memory operation (ON/OFF states) under various mechanical deformations, including wearing, stretching, twisting, and impact. Reproduced with permission from ref. 85 copyright 2025 Elsevier, ref. 19 copyright 2017 John Wiley & Sons, and ref. 234 copyright 2024 American Chemical Society.

(DPPT-TT) and an elastomer (SEBS) for the channel, and used Ag nanoparticles embedded in an elastomeric dielectric as a stretchable floating gate. Unlike previous resistive memories, this field-effect transistor (FET) architecture enabled non-destructive readout, high on/off ratios, and long retention times. The device was fabricated in a top-contact, bottom-gate configuration and implemented as a 7 × 7 active-matrix array, where each memory cell was addressable *via* patterned stretchable bit and word lines (Fig. 13c). Memory writing was achieved by a dual-stimulus mechanism: under simultaneous visible-to-NIR light illumination and positive gate bias, electrons were injected into the Ag nanoparticle floating gate *via* Fowler–Nordheim tunnelling and stably trapped, enabling robust WORM operation. While DPPT-TT does not exhibit typical photoactive semiconductor behavior, its broad optical absorption enabled effective light-assisted programming. The combined use of light and voltage as programming stimuli provided an additional layer of data security, preventing erasure by either stimulus alone. The device achieved a high on/off ratio ($>10^5$), a large memory window (17 V), and long retention time (10^6 s), all maintained under 50% uniaxial or 30% biaxial strain and after 1000 stretching cycles.[234] This impressive mechanical durability arises from the effects of the nanoconfined polymer morphology between DPP and SEBS, the favorable alignment of energy bands, and the elastic, patterned device structure. Together, these factors enable reliable, deformation-insensitive data storage, making the system highly promising for secure, long-term memory applications in wearable and electronic skin devices. This section not only emphasizes that rubber-like synthetic polymers are commonly used as substrates or mechanical supports, but also highlights their incorporation or modification with memory-active materials, enabling elastomers to provide mechanical resilience within the overall device architecture and maintain memory performance under mechanical stress.

The fabrication process and material selection for each layer in transistor devices critically influence not only electrical performance, but also mechanical durability, environmental stability, interfacial compatibility, and biocompatibility. For instance, electrical performance depends on the purity, morphology, and interface quality of materials, all governed by processing methods.[235] Mechanical durability is affected by the flexibility of the materials and the robustness of interfaces, which determine whether the device can withstand repeated bending, stretching, or twisting without cracking or delaminating.[236] Environmental stability is enhanced by choosing

Table 2 List of materials and fabrication method for each device components in wearable transistor devices[b]

	Material					Fabrication method					
No	Source/drain	Semiconductor	Dielectric	Gate	Substrate	Source/drain	Semiconductor	Dielectric	Gate	Substrate	Ref.
1	CNTs	Sorted CNTs	TPU	CNTs	TPU	Spray-coated on SiO_2, then transferred	Spin-coated	Spin-coated on SiO_2, then transferred	Spray-coated on SiO_2, then transferred	Casted on glass slides	167
2	CNTs	Sorted CNTs	PDMS/$BaTiO_3$	CNTs	PDMS	Printed	Drop-casted	Printed and cured	Printed	Prepared[a]	171
3	CNTs	CONPHINE film (DPPT-TT/SEBS)	SEBS	CNTs	SEBS	Spray-coated on SiO_2, patterned with O_2 etching, then transferred	Spin-coated and annealed on SiO_2, then transferred	Spin-coated on SiO_2, then transferred	Spray-coated on SiO_2, patterned with O_2 etching, then transferred	Casted on glass slides	173
4	CNTs	CONPHINE film (DPPT-TT/SEBS)	SEBS-x-azide	CNTs	SEBS	Spray-coated	Etched into dielectric layer	Spin-coat and UV-cured	Spray-coated	Prepared[a], laminated onto device	126
5	CNTs	iRUM-s (BA/DPPTT)	PDMS	CNTs	PDMS	Spray-coated	Spin-coated and annealed on SiO_2	Spin-coated	Spray-coated	Spin-coated onto gate layer	176
	CNTs	iRUM-s (BA/DPPTT)	iRUM-d (BH/SEBS)	CNTs	SEBS	Spray-coated	Spin-coated on dielectric layer and photo-crosslinked	Spin-coated and photo-crosslinked on SiO_2	Spray-coated on dielectric	Prepared[a], laminated into device	
6	Ag	CONPHNE film (DPPT-TT/SEBS)	SEBS	Ag	SEBS	Thermal evaporated	Spin-coated on SiO_2, then transferred	Spin-coated on SiO_2, then transferred	Thermal evaporated	Prepared[a]	177
7	CNTs	CONPHINE film (DPPDTSE/SEBS)	SEBS-x-azide	CNTs	Rigid SEBS; soft SEBS	Spray-coated	Spin-coated and annealing	Spin-coating and photo-crosslink in SiO_2	Spray-coat	Printed (rigid SEBS); laminated on device (soft SEBS)	178
8	SWCNTs	Sorted SWCNTs	SEBS	SWCNTs	SEBS	Photolithography on SiO_2	Dry-etched on source and drain pattern	Spin-coated on SiO_2, then transferred	Photolithography on SiO_2, then transferred	Casted on glass slide, then transferred	190
9	SWCNT/PDMS-$MPU_{0.4}$-$IU_{0.6}$	DPP-DTT/PDMS-$MPU_{0.4}$-$IU_{0.6}$	PDMS-$MPU_{0.4}$-$IU_{0.6}$	SWCNT/PDMS-$MPU_{0.4}$-$IU_{0.6}$	PDMS-$MPU_{0.4}$-$IU_{0.6}$	Spray-coated onto self-healing film, then assembled	Spray-coated onto SiO_2 and self-healing solution was poured on top, then assembled	Spin-coated on SiO_2, then assembled	Spin-coated on SiO_2, then assembled	Spray-coated onto self-healing film, then assembled	192
10	Au	DPP-TVT-PDCA	PDMS	Au	SEBS	Thermal evaporated	Coated on SiO_2, then transferred	Spin-coated on SiO_2, then transferred	Thermal evaporated	Prepared[a]	59
11	SWCNTs	FT4-DPP/PEO	PS-PMMA-PS/([EMIM][TFSI])	Probe tip (NA)	SEBS	Spray-coated on SiO_2, then transferred	Electro spinned to form NW, then placed on substrate	Drop-casted	NA	Prepared[a]	29
12	CNTs	Wavy P3HT-NF	LiTFSI/PAN	CNTs	PDMS	Spray-coated on SiO_2, then transferred	Spin-coated on dielectric, then transferred	Spin-coated on SiO_2, then transferred	Spray-coated, then transferred	Spin-coated	206

Table 2 (*Contd.*)

No	Material					Fabrication method					Ref.
	Source/drain	Semiconductor	Dielectric	Gate	Substrate	Source/drain	Semiconductor	Dielectric	Gate	Substrate	
13	M-CNTs	S-CNTs	PVA/SiO_2	M-CNTs	PDMS	Spin-coated on SiO_2, patterned with photolithography & O_2 etching	Spin-coated	PVA was spin-coated, then SiO_2 deposited on top	Spin-coated, patterned with photolithography & O_2 etching	Spin-coated	207
14	M-CNTs	PU		NA	PDMS	Spin-coat, patterned with photolithography & O_2 etching	Spin-coated		NA	Spin-coated	208
15	Au/Ti	F8T2	P(VDF-TrFE)	Al	PDMS	e-beam evaporation	Spin-coated	Spin-coated	Evaporated	Prepared[a]	85

[a] Detailed discussion of the preparation method is absent in the original journal reference. [b] NA: the component is not inherently part of the device.

materials and encapsulation methods that protect sensitive components from moisture, oxygen, UV light, and temperature fluctuations, thus extending device lifetime.[237,238] Interfacial compatibility is essential for reliable operation, as mismatched mechanical or chemical properties between layers can lead to poor adhesion and inefficient charge transfer.[235,239] Finally, for wearable and skin-conformable transistor devices, biocompatibility is essential.[238] The materials used must be safe for direct skin contact, should not cause irritation or allergic reactions, and also provide comfort and breathability for the wearer. Collectively, these factors underscore the importance of thoughtful material selection and fabrication strategy in advancing the functionality, reliability, and application scope of modern next generation transistor technologies. Accordingly, Table 2 provides a detailed overview of the materials employed and the corresponding fabrication techniques applied to assemble each component layer in rubbery transistors, skin-conformable sensor transistors, artificial synaptic transistors, and memory devices. This summary is important as it offers a clear overview of current manufacturing methods, aiding the identification of effective material and process combinations to optimize the functionality and reliability of transistor devices.

4. Progress and challenges in mass production of skin-like electronic devices

Given the increasing popularity of wearable devices (*i.e.* smartwatches and fitness trackers), the demand for electronic skin technology has also increased significantly and even expanding into other electronics fields. Leading electronic companies, such as Samsung Electronics, have actively invested in research and commercialization of skin-like electronic devices into the market. One research in particular was stretchable active-matrix organic light-emitting-diode (AMOLED) by Samsung Electronics, serving as one of their major targets in commercializing flexible devices.[240] Moreover, Samsung Electronics has been a key industry partner supporting the renowned Professor Zhenan Bao's research group at Stanford University since around 2010s, with a focus on developing stretchable and skin-like electronic devices for applications including wearable technology, microLED driving, and advanced health monitoring interfaces, according to the record of co-published paper.[127,213,241–247] This partnership has leveraged Bao's expertise in molecular design and fabrication processes to pioneer new materials and devices for soft robotics, implantable electronics, and flexible semiconductors. Notable advancements include the creation of stretchable electrodes and high-performance transistors, circuits, and light-emitting devices that combine electronic functionality with mechanical deformability. Samsung's commitment to flexible technologies is exemplified by their first commercial launch of bendable smartphones with the Samsung Galaxy Fold, which was officially released beginning in September 2019. These devices incorporate ultrathin glass and polymer layers, representing a significant breakthrough in flexible electronics that has driven

Table 3 Comprehensive summary of advances in multifunctional rubber-like synthetic polymers for wearable transistor applications

No.	Synthetic elastomer	Structural functionality	Additional properties	Component in devices[a]	Practical advance in devices[b]	Ref.
1	2 PDMS	PDMS	—	Substrate	Rubbery transistor	171 and 176
					Rubbery synaptic transistor	206
					Skin-like wearable synaptic devices	207 and 208
					Rubbery memory device	85
				Dielectric layer	Skin-like wearable sensor device	59
		PDMS-UV ozone treatments	Hydrophilic	Substrate	Rubbery transistor	18
		PDMS-plasma treatment	Hydrophilic	Charge storage	NA	88
		PDMS/blending/ polydopamine	Dielectric constant	Dielectric layer	NA	89
		PDMS/blending/$BaTiO_3$	High k dielectric	Dielectric layer	Rubbery transistor	171
		PDMS-MPU-IU	Self-healing	Substrate and dielectric layer	Skin-like wearable sensor device	192
		PDMS/blended/DPP-DTT/ DPPDPyBT/P3HT	Semiconducting	Semiconductor layer	Rubbery transistor	90
		PDMS-PDCA/blending/DPP	Self-healing & semiconducting	Semiconductor layer	Skin-like wearable sensor device	59
		PDMS-MPU-IU/blending/DPP	Self-healing & semiconducting	Semiconductor layer	Skin-like wearable transistor	63
					Skin-like wearable sensor device	192
2	PU	Hydroxyl-terminated polybutadiene	Hydrophobic	Not yet	NA	94
		PU/hydroxyl-functionalized/ aromatic pinacol	Self-healing and recycling	Not yet	NA	95
		PU-photocrosslinked	Photosensitive, charge flow modulator	Dielectric layer	NA	33
		PU/rrP3HT	Low polarity	Dielectric layer	NA	34
		PU/C8-BTBT	High k dielectric	Dielectric layer	NA	35
		PU/one-pot synthesis/oxime carbamate (OC)	Self-healing, hydrophobic	Substrate and dielectric layer	Skin-like wearable sensor device	96
		PU/copolymerization/ multiblock oligodiketopyrrolopyrrole	Semiconducting	Semiconductor layer	Rubbery transistor	36
		Urethane-side engineered-DPP	Semiconducting	Semiconductor layer	Rubbery transistor	37
3	Thermoplastic PU (TPU)	TPU/blending/rGO/CNT	Conducting & sensing	Sensor	Wearable sensor device	32
		TPU/dispersed/GN/MWCNTs	Sensing	Sensor	Wearable sensor device	10
4	Donor–acceptor supramolecular polymers	BDOPV-2T blending	Semiconducting	Semiconductor layer	NA	98
5	Supramolecular polymers	SWNT/didodecylfluorene dispersed	Electrode	Source and drain electrodes	NA	99
		poly(TA-DIB-Fe) copolymerization	—	Not yet	NA	38

Table 3 (*Contd.*)

No.	Synthetic elastomer	Structural functionality	Additional properties	Component in devices[a]	Practical advance in devices[b]	Ref.
6	PCSC (supramolecular self-healing polymer)	CA/SA/CHDM esterification	Sensing	Sensor	Skin-like wearable sensor device	100
7	Metallo-supramolecular diblock copolymers	PS_{161}–Zn–$P3HT_{187}$ coupling reaction	Semiconducting, stretchable, self-healing	Semiconductor layer	Rubbery transistor	61
8	SBR	SBR/embedded/AgNW	Conducting & strain-sensing	Sensor	Wearable sensor device	104
		SBR/FLG-wet spinning	Strain-sensing	Sensor	Wearable sensor device	105
		SBR/blending/CNT	Sensing	Sensor	Wearable sensor device	109
		SBR/reinforced/CG/MWCNT	Conducting	Not yet	NA	110
9	Carboxylic SBR (XSBR)	XSBR/crosslink/SSCNT	Sensing	Sensor	Wearable sensor device	108
10	14 SEBS	Pristine	—	Substrate	Rubbery transistor	126, 173 and 176–178
					Wearable sensor device	190
					Skin-like wearable sensor device	59
					Wearable synaptic device	29
				Dielectric	Rubbery transistor	173 and 177
					Wearable sensor device	190
		SEBS/Functionalized/Tween 80	Hydrophilic	Substrate	Rubbery transistor	21
		SEBS/grafting/MA	Dielectric constant	Dielectric layer	NA	124
		SEBS/photo-crosslinking	Photopatternability	Dielectric layer	Rubbery transistor	126, 127, 176 and 178
		SEBS/blending/P3HT	Semiconducting	Semiconductor layer	Rubbery transistor	66
		SEBS/blending/N2200	Semiconducting	Semiconductor layer	Rubbery transistor	128
		SEBS/blending/DPPT-TT	Semiconducting	Semiconductor layer	Rubbery transistor	126, 173 and 177
		SEBS/blending/DPPDTSE	Semiconducting	Semiconductor layer	Rubbery transistor	178
		SEBS/physical crosslink/ Paraffin	Self-healing	Not yet	NA	30
		SEBS/physical crosslink/PVDF	Self-healing	Dielectric layer	NA	129
11	PI	MH-*b*-PI	Charge storage	Charge storage layer	Wearable memory device	19
		PF-*b*-PI	Luminescence	Luminescence layer	NA	43
		PF-*b*-PI/blending/SWCNT	Semiconducting & charge storage	Semiconductor layer & charge storage layer	NA	134
		PI/wrapped/SWCNT	Semiconducting & charge storage	Semiconductor layer & charge storage layer	NA	13
		PF_x-*co*-PI_y-*co*-$PBACO_z$	Self-healing	Not yet	NA	62
		PF_x-*co*-PI_y-*co*-$PBACO_z$/ blending/SWCNT	Semiconducting & self-healing	Semiconductor layer	NA	137 and 139
		PI/grafting/*m*$RTIO_2$	Dielectric constant	Dielectric layer	NA	62
		Radically modified PI with NVC and BACO	Self-healing, recyclable	Not yet	NA	44

[a] Not yet: the material has not been applied as a component in transistor devices. [b] NA: the material has been used as one component in a stretchable device; however, not all device components are stretchable.

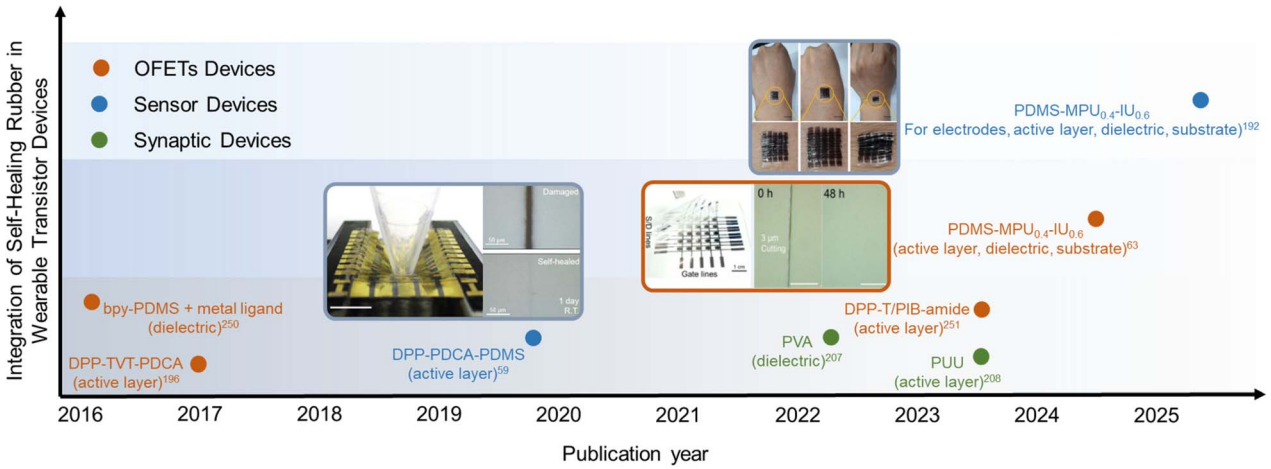

Fig. 14 Reported self-healing rubber material integration in wearable transistor devices based on publication year and number of self-healing components. Reprinted with permission from ref. 63, 192 and 196 copyright 2016, 2024, & 2025 Springer Nature, and ref. 59 copyright 2019 American Association for the *Advancement of Science*, ref. 207, 208, and 250 copyright 2016, 2022, & 2023 American Chemical Society, and ref. 251 copyright 2023 John Wiley & Sons.

heightened market demand in subsequent years. In conclusion, this sustained academic-industry cooperation highlights how foundational research in materials science, combined with scalable fabrication techniques, is accelerating commercialization pathways and addressing growing market demands for flexible, skin-like electronics.

Recent rapid advancements in fully stretchable and self-healing transistors highlight their significant potential for integration into wearable skin-like electronic devices. Although these devices have demonstrated promising performance at the laboratory scale,[63,192] commercial-scale manufacturing remains challenging and necessitates careful consideration of factors such as scalability of material innovation production, quality control, and cost-effectiveness. The scalable production of innovative materials largely depends on optimizing synthesis parameters such as operational temperature and reaction time to ensure consistent quality and yield. At the same time, advances in scalable device fabrication techniques, such as printing and lithography, have demonstrated the potential for mass-producing stretchable electronic components with better uniformity and throughput.[195,245] However, many fully stretchable and self-healing devices still rely on manual, layer-by-layer assembly techniques, which are labor-intensive and limit scalability, indicating a pressing need for further automation and process optimization before commercial adoption.[192] In addition, maintaining strict quality standards for both material properties and device performance is imperative to ensure product reliability. The use of flexible and self-healing materials introduces additional complexities in fabrication due to their inherently rough or irregular surfaces, necessitating the development of robust standardization and characterization protocols to achieve consistent device quality.[248] Cost considerations also play a critical role, as production expenses must be balanced against device performance to deliver economically viable products.

Despite these challenges, market demand for skin-like electronic devices continues to grow rapidly, driven by the need for applications in healthcare, wearable technology, and long-term human–machine interfaces.[249] Drawing on insights from prior commercial successes in flexible electronics, such as bendable displays and wearable sensors, the transition of fully stretchable and self-healing transistors from laboratory research to scalable commercial technologies is increasingly feasible. Continued innovation in materials engineering, fabrication processes, and quality control strategies will be key to unlocking their full commercial potential and enabling them to compete effectively with conventional rigid electronic devices.

5. Concluding remarks and perspectives

In this review, we summarize the latest advances in rubber-like synthetic polymers for wearable transistor devices. The evolution of these devices spans from designs that primarily maintain structural integrity and performance under simple bending and twisting to those engineered for intrinsic tensile strain levels exceeding 30%. More recently, significant progress has been made toward integrating self-healing capabilities, offering an optimal solution for addressing mechanical damages, fractures and surface degradation, thereby enhancing the durability and longevity of wearable transistors. All types of elastomers discussed in this review are reported to be commercially available. Therefore, their availability and large-scale production are beyond doubt. As presented in Table 3, among rubber-like materials, PDMS and SEBS are the most commonly used in fully wearable transistor devices. This preference is attributed to their skin-like mechanical properties, processability, ease of fabrication, optical transparency (>90% in the visible range), and excellent skin safety that surpass those of PU, SBR, supramolecular polymers, and PI.[178,192] Advances in porous PDMS and SEBS structures improve breathability and skin compatibility by allowing sweat vapour to escape, reducing irritation during

prolonged use. They are also highly compatible with soft lithography techniques, enabling micro-scale patterning and molding for flexible electronic and microfluidic devices.[14] While PU typically has lower optical transparency and higher stiffness that may reduce comfort and conformability, it excels due to its solvent processability and facile incorporation of self-healing bonds that preserve device performance after repeated mechanical damage. PU is widely favored by researchers for chemical incorporation into the backbone or side chains of conjugated polymers, as it strengthens intermolecular interactions and facilitates controlled phase separation to achieve more uniform microstructures, which ultimately improve both mechanical durability and electronic functionality. SBR, while offering excellent flexibility and a low T_g (ranging from −65 °C to −35 °C depending on styrene content and additives such as fillers or plasticizers), remains inherently non-porous and lacks breathability. This limits its ability to transmit air and water vapour under ambient conditions, thereby restricting its direct use in epidermal device applications. Supramolecular polymers present tunable elasticity and dynamic bonding for self-healing but generally lack the well-established processing technologies and environmental robustness necessary for large-scale wearable device fabrication. Nevertheless, several studies have demonstrated successful applications of PU, SBR, and supramolecular polymers as functional components, such as active layers, dielectrics, and substrates, in wearable transistor devices (Table 3). Meanwhile, the modified or copolymerized PI-based materials show considerable promise due to their elasticity and self-healing properties that closely resemble human tissue mechanics. However, PI-based materials have primarily been explored as individual stretchable and self-healing thin film within rigid-dominant device architectures and have not yet been fully integrated into complete wearable transistor systems (Table 3). Therefore, further research is needed to escalate their integration and optimize compatibility with other device components to fully leverage their unique mechanical and biological advantages within complete wearable transistor systems.

Efficient and reliable self-healing mechanisms are crucial for enhancing the durability and lifespan of wearable electronic devices. Hydrogen bond-based self-healing features are widely preferred for self-healing applications due to their reversible and dynamic interactions, which serve as physical cross-links that enhance both mechanical strength and healing efficiency. Moreover, the tunable density and multiplicity of hydrogen bonds enable tailoring of mechanical properties and healing efficiencies, supporting both high performance and durability in self-healing elastomers. This combination of mechanical robustness and reversible interaction makes hydrogen bonding particularly suitable for wearable devices that require both flexibility and reliable recovery from damage. However, the integration of self-healing elastomers within such devices still remains limited and typically confined to a single device component (Fig. 14).[59,196,207,208,250,251] Achieving uniform self-healing functionality throughout all device components represents a promising and essential direction for advancing the development of robust, fully self-healing wearable electronics. Recent efforts in incorporating self-healing elastomers into multiple skin-like transistor layers have predominantly employed simple blending techniques.[63,192] In this context, PDMS has demonstrated the ability to go beyond its conventional applications as a substrate or dielectric by serving as a functional self-healable matrix for active layers. This is achieved by blending modified PDMS with semiconducting polymers or vapor-deposited metal nanoclusters to fabricate all three critical transistor device layers, including conductor, semiconductor, and dielectric. Constructing all layers from a compatible modified PDMS facilitates strong interlayer adhesion and seamless interfaces, thereby enabling the devices to restore both mechanical integrity and electrical functionality following mechanical damage or environmental stress. Nonetheless, reliance on a simple blending approach can result in heterogeneity across device layers, especially in the active layer, since blending with semiconducting polymers or metallic nanoclusters can alter the original performance of the modified PDMS. This can lead to inconsistent mechanical behavior and variable self-healing efficiencies, ultimately impacting the overall device reliability and uniformity. Therefore, further study on uniform self-healing properties across all components present an opportunity for future development of skin-like wearable transistor devices. In recent years, flexible devices have made notable progress toward commercialization, as evidenced by the commercialization success of Samsung's smartphone with foldable display. This achievement underscores the potential for commercializing skin-like electronics that can be achieved with continued innovation in material engineering, fabrication processes, and quality control strategies.

Author contributions

Y.-C. C. supervised the project, acquired funding, administered project resources, and contributed to conceptualization and manuscript review and editing. L. L. developed the manuscript outline. L. L., D. B., and D. M. S. contributed to conceptualization, performed the original draft writing, participated in review and editing, and visualization. A. C. H. was involved in conceptualization, original draft writing, and visualization. H.-K. B. participated in the original draft writing and visualization. Y.-C. L. contributed to review and editing. The manuscript was written through contributions from all the authors. All the authors have given approval to the final version of the manuscript.

Conflicts of interest

There are no conflicts to declare.

Data availability

No primary research results, software or code have been included and no new data were generated or analysed as part of this review.

Acknowledgements

The authors thankfully acknowledge of the National Science and Technology Council in Taiwan (NSTC 114-2223-E-011-002-MY4 and NSTC 114-2811-E-011-008-MY4).

References

1 K. Zhang, S. Kong, Y. Li, M. Lu and D. Kong, Soft elastomeric composite materials with skin-inspired mechanical properties for stretchable electronic circuits, *Lab Chip*, 2019, **19**, 2709–2717.
2 Z. Zhang, W. Cao, M. Wang, L. Tuo, T. Xie, F. Ou, X. Duan, R. Cong, C. Ning, W. Pan, S. Zhao, Z. Li and W. Gao, Elastomers with ultrahigh mechanical properties for flexible sensing and triboelectric nanogenerators, *Chem. Eng. J.*, 2024, **481**, 148442.
3 S. Masihi, M. Panahi, D. Maddipatla, A. J. Hanson, A. K. Bose, S. Hajian, V. Palaniappan, B. B. Narakathu, B. J. Bazuin and M. Z. Atashbar, Highly sensitive porous PDMS-based capacitive pressure sensors fabricated on fabric platform for wearable applications, *ACS Sens.*, 2021, **6**, 938–949.
4 G. B. Pradhan, S. Jeong, S. Sharma, S. Lim, K. Shrestha, Y. Lee and J. Y. Park, A breathable and strain-insensitive multi-layered e-skin patch for digital healthcare wearables, *Adv. Funct. Mater.*, 2024, **34**, 2407978.
5 R. J. Jackman, D. C. Duffy, O. Cherniavskaya and G. M. Whitesides, Using elastomeric membranes as dry resists and for dry lift-off, *Langmuir*, 1999, **15**, 2973–2984.
6 B. K. Hong and W. H. Jo, Effects of molecular weight of SEBS triblock copolymer on the morphology, impact strength, and rheological property of syndiotactic polystyrene/ethylene–propylene rubber blends, *Polymer*, 2000, **41**, 2069–2079.
7 L. V. Kayser and D. J. Lipomi, Stretchable conductive polymers and composites based on PEDOT and PEDOT:PSS, *Adv. Mater.*, 2019, **31**, 1806133.
8 S. Li, P. Tan, J. Cao, Y. Yao, X. Ren and Y.-X. Xu, High performance, self-healing and recyclable polyisoprene rubbers enabled by modulating sulfide bond structures, *Polymer*, 2025, 128570.
9 S. Xu, Y. Zhang, L. Jia, K. E. Mathewson, K.-I. Jang, J. Kim, H. Fu, X. Huang, P. Chava, R. Wang, R. Bhole, L. Wang, Y. J. Na, Y. Guan, M. Flavin, Z. Han, Y. Huang and J. A. Rogers, Soft microfluidic assemblies of sensors, circuits, and radios for the skin, *Science*, 2014, **344**, 70–74.
10 F. Liu, D. Xie, F. Lv, L. Shen, Z. Tian and J. Zhao, Additive manufacturing of stretchable polyurethane/graphene/multiwalled carbon nanotube-based conducting polymers for strain sensing, *ACS Appl. Nano Mater.*, 2023, **6**, 4522–4531.
11 R. Morent, N. De Geyter, F. Axisa, N. De Smet, L. Gengembre, E. De Leersnyder, C. Leys, J. Vanfleteren, M. Rymarczyk-Machal and E. Schacht, Adhesion enhancement by a dielectric barrier discharge of PDMS used for flexible and stretchable electronics, *J. Phys. D: Appl. Phys.*, 2007, **40**, 7392.
12 P. Meredith, C. Bettinger, M. Irimia-Vladu, A. Mostert and P. E. Schwenn, Electronic and optoelectronic materials and devices inspired by nature, *Rep. Prog. Phys.*, 2013, **76**, 034501.
13 M. M. Mburu, K. T. Lu, N. L. Prine, A. N. Au-Duong, W. H. Chiang, X. Gu and Y. C. Chiu, Conjugated polymer-wrapped single-wall carbon nanotubes for high-mobility photonic/electrical fully modulated synaptic transistor, *Adv. Mater. Technol.*, 2022, **7**, 2101506.
14 M. D. Guillemette, E. Roy, F. A. Auger and T. Veres, Rapid isothermal substrate microfabrication of a biocompatible thermoplastic elastomer for cellular contact guidance, *Acta Biomater.*, 2011, **7**, 2492–2498.
15 A. Ryspayeva, T. D. Jones, M. N. Esfahani, M. P. Shuttleworth, R. A. Harris, R. W. Kay, M. P. Desmulliez and J. Marques-Hueso, A rapid technique for the direct metallization of PDMS substrates for flexible and stretchable electronics applications, *Microelectron. Eng.*, 2019, **209**, 35–40.
16 A. Ahmed, Y.-S. Guan, I. Hassan, C. Ling, Z. Li, I. Mosa, G. Phadke, P. R. Selvaganapathy, S. Chang and S. Ren, Multifunctional smart electronic skin fabricated from two-dimensional like polymer film, *Nano Energy*, 2020, **75**, 105044.
17 G. Liu, Y. Chen, M. Gong, X. Liu, Z.-K. Cui, Q. Pei, J. Gu, C. Huang and Q. Zhuang, Enhanced dielectric performance of PDMS-based three-phase percolative nanocomposite films incorporating a high dielectric constant ceramic and conductive multi-walled carbon nanotubes, *J. Mater. Chem. C*, 2018, **6**, 10829–10837.
18 C. Gu and J.-S. Lee, Patterning of amorphous-InGaZnO thin-film transistors by stamping of surface-modified polydimethylsiloxane, *RSC Adv.*, 2016, **6**, 43147–43151.
19 C. C. Hung, Y. C. Chiu, H. C. Wu, C. Lu, C. Bouilhac, I. Otsuka, S. Halila, R. Borsali, S. H. Tung and W. C. Chen, Conception of stretchable resistive memory devices based on nanostructure-controlled carbohydrate-block-polyisoprene block copolymers, *Adv. Funct. Mater.*, 2017, **27**, 1606161.
20 J. Ren, Z. Wang, G. Jiang, Y. Li, Z. Wang, L. Zhao and S. Jia, Multipurpose poly (dimethylsiloxane) dielectric films with superb thermal conductivity by incorporating silver nanoparticle-decorated boron nitride nanosheets, *J. Phys. Chem. C*, 2023, **127**, 13238–13248.
21 Q. Ye, X. Liu, J. Li, Y. Jing, Y. Niu, Q. Li, S. Liang, T. Jiang, Y. Tian and A. Wang, Surfactant-functionalized SEBS for fabrication of flexible electrodes, *Colloids Surf., A*, 2025, **720**, 137132.
22 R. Lin, C. Jiang, S. Achavananthadith, X. Yang, H. P. A. Ali, J. Ping, Y. Liu, X. Zhang, B. C. Tee, Y. L. Kong and J. S. Ho, Soft electronics based on particle engulfment printing, *Nat. Electron.*, 2025, **8**, 127–134.
23 I. You, M. Kong and U. Jeong, Block copolymer elastomers for stretchable electronics, *Acc. Chem. Res.*, 2018, **52**, 63–72.

24 J. Chen, F. Li, Y. Luo, Y. Shi, X. Ma, M. Zhang, D. Boukhvalov and Z. Luo, A self-healing elastomer based on an intrinsic non-covalent cross-linking mechanism, *J. Mater. Chem. A*, 2019, **7**, 15207–15214.

25 D. Qi, K. Zhang, G. Tian, B. Jiang and Y. Huang, Stretchable electronics based on PDMS substrates, *Adv. Mater.*, 2021, **33**, 2003155.

26 D. C. Duffy, J. C. McDonald, O. J. Schueller and G. M. Whitesides, Rapid prototyping of microfluidic systems in poly(dimethylsiloxane), *Anal. Chem.*, 1998, **70**, 4974–4984.

27 N. Sun, X.-N. Zhang, J.-Z. Li, Y.-W. Cai, Z. Wei, L. Ding and G.-G. Wang, Waterproof, breathable, and UV-protective nanofiber-based triboelectric nanogenerator for self-powered sensors, *ACS Sustain. Chem. Eng.*, 2023, **11**, 5608–5616.

28 J. Zhao, L. Sun, Z. Chu, T. Li, F. Zhang, L. Li and W. Zhang, Trade-off of mechanical and electrical properties in stretchable P3HT/PDMS blending films driven by interpenetrating double networks formation, *AIP Adv.*, 2020, **10**, 035020.

29 Y. Lee, J. Y. Oh, W. Xu, O. Kim, T. R. Kim, J. Kang, Y. Kim, D. Son, J. B.-H. Tok, M. J. Park, T.-W. Lee and Z. Bao, Stretchable organic optoelectronic sensorimotor synapse, *Sci. Adv.*, 2018, **4**, eaat7387.

30 Q. Zhang, Y. Wang, X. Zhang, J. Song, Y. Li, X. Wu and K. Yuan, Self-healing, elastic and deformable novel composite phase change polymer based on thermoplastic elastomer SEBS for wearable devices, *J. Mater. Sci.*, 2022, **57**, 7208–7224.

31 Y. Li, M. Zhou, R. Wang, H. Han, Z. Huang and J. Wang, Self-healing polyurethane elastomers: An essential review and prospects for future research, *Eur. Polym. J.*, 2024, **214**, 113159.

32 X. Zhang, D. Xiang, Y. Wu, E. Harkin-Jones, J. Shen, Y. Ye, W. Tan, J. Wang, P. Wang, C. Zhao and Y. Li, High-performance flexible strain sensors based on biaxially stretched conductive polymer composites with carbon nanotubes immobilized on reduced graphene oxide, *Composites, Part A*, 2021, **151**, 106665.

33 Y. Li, H. Wang, X. Zhang, Q. Zhang, X. Wang, D. Cao, Z. Shi, D. Yan and Z. Cui, Organic thin film transistors with novel photosensitive polyurethane as dielectric layer, *RSC Adv.*, 2016, **6**, 5377–5383.

34 H. C. Avila, P. Serrano, A. R. J. Barreto, Z. Ahmed, C. d. P. Gouvêa, C. Vilani, R. B. Capaz, C. F. N. Marchiori and M. Cremona, High hole-mobility of rrP3HT in organic field-effect transistors using low-polarity polyurethane gate dielectric, *Org. Electron.*, 2018, **58**, 33–37.

35 A. R. J. Barreto, G. Candiotto, H. J. C. Avila, R. S. Carvalho, A. M. dos Santos, M. Prosa, E. Benvenuti, S. Moschetto, S. Toffanin, R. B. Capaz, M. Muccini and M. Cremona, Improved performance of organic light-emitting transistors enabled by polyurethane gate dielectric, *ACS Appl. Mater. Interfaces*, 2023, **15**, 33809–33818.

36 M. Y. Lee, S. Dharmapurikar, S. J. Lee, Y. Cho, C. Yang and J. H. Oh, Regular H-Bonding-Containing polymers with stretchability up to 100% external strain for self-healable plastic transistors, *Chem. Mater.*, 2020, **32**, 1914–1924.

37 D. Pei, C. An, B. Zhao, M. Ge, Z. Wang, W. Dong, C. Wang, Y. Deng, D. Song, Z. Ma, Y. Han and Y. Geng, Polyurethane-based stretchable semiconductor nanofilms with high intrinsic recovery similar to conventional elastomers, *ACS Appl. Mater. Interfaces*, 2022, **14**, 33806–33816.

38 Q. Zhang, C.-Y. Shi, D.-H. Qu, Y.-T. Long, B. L. Feringa and H. Tian, Exploring a naturally tailored small molecule for stretchable, self-healing, and adhesive supramolecular polymers, *Sci. Adv.*, 2018, **4**, eaat8192.

39 H.-Q. Peng, W. Zhu, W.-J. Guo, Q. Li, S. Ma, C. Bucher, B. Liu, X. Ji, F. Huang and J. L. Sessler, Supramolecular polymers: Recent advances based on the types of underlying interactions, *Prog. Polym. Sci.*, 2023, **137**, 101635.

40 A. A. M. Ward, A. M. Ghoneim, A. F. Younan and A. M. Bishai, Mechanical and Dielectric Properties of Styrene-butadiene Rubber Polyester Short-fiber Composites Part 1: Composites Loaded with Semirein Forcing Furnace Carbon Black (SRF), *Int. J. Polym. Mater.*, 2001, **48**, 355–370.

41 D. Khatua, R. N. P. Choudhary and P. G. R. Achary, Styrene butadiene rubber and barium hexaferrite based flexible elastomer –inorganic dielectric systems, *Mater. Today: Proc.*, 2021, **41**, 369–375.

42 S. Sohail, Y. Ma, Q. Mahmood, Z. Hu, Y. Wang, T. Liang and W. H. Sun, Achieving isopropenyl-enriched polyisoprene: unraveling the role of bidentate vs. tridentate iron precatalysts through ligand framework design, *Dalton Trans.*, 2024, **53**, 19325–19336.

43 A.-N. Au-Duong, C.-C. Wu, Y.-T. Li, Y.-S. Huang, H.-Y. Cai, I. Jo Hai, Y.-H. Cheng, C.-C. Hu, J.-Y. Lai, C.-C. Kuo and Y.-C. Chiu, Synthetic concept of intrinsically elastic luminescent polyfluorene-based copolymers via RAFT polymerization, *Macromolecules*, 2020, **53**, 4030–4037.

44 L. Laysandra, D. Bazliah, A. Njotoprajitno, K.-L. Chen and Y.-C. Chiu, Radically modified polyisoprene toward a multifunctional rubber moiety with self-healable and recyclable properties, *ACS Appl. Polym. Mater.*, 2025, **7**, 1921–1933.

45 D. Gong, F. Tang, Y. Xu, Z. Hu and W. Luo, Cobalt catalysed controlled copolymerization: an efficient approach to bifunctional polyisoprene with enhanced properties, *Polym. Chem.*, 2021, **12**, 1653–1660.

46 Y. Xu, J. Zhao, Q. Gan, W. Ying, Z. Hu, F. Tang, W. Luo, Y. Luo, Z. Jian and D. Gong, Synthesis and properties investigation of hydroxyl functionalized polyisoprene prepared by cobalt catalyzed co-polymerization of isoprene and hydroxylmyrcene, *Polym. Chem.*, 2020, **11**, 2034–2043.

47 A. Breuillac, F. Caffy, T. Vialon and R. Nicolaÿ, Functionalization of polyisoprene and polystyrene via reactive processing using azidoformate grafting agents, and its application to the synthesis of dioxaborolane-based polyisoprene vitrimers, *Polym. Chem.*, 2020, **11**, 6479–6491.

48 J. Liu, S. Wang, Z. Tang, J. Huang, B. Guo and G. Huang, Bioinspired Engineering of Two Different Types of Sacrificial Bonds into Chemically Cross-Linked cis-1,4-Polyisoprene toward a High-Performance Elastomer, *Macromolecules*, 2016, **49**, 8593–8604.
49 M. Tang, R. Zhang, S. Li, J. Zeng, M. Luo, Y. X. Xu and G. Huang, Towards a supertough thermoplastic polyisoprene elastomer based on a biomimic strategy, *Angew Chem. Int. Ed. Engl.*, 2018, **57**, 15836–15840.
50 J. S. Taylor and E. Erkek, Latex allergy: diagnosis and management, *Dermatol. Ther.*, 2004, **17**, 289–301.
51 G. L. Sussman, D. H. Beezhold and V. P. Kurup, Allergens and natural rubber proteins, *J. Allergy Clin. Immunol.*, 2002, **110**, S33–S39.
52 I. W. Cheong, C. M. Fellows and R. G. Gilbert, Synthesis and cross-linking of polyisoprene latexes, *Polymer*, 2004, **45**, 769–781.
53 D. Bazliah, Q. A. Hong, L. Laysandra and Y. C. Chiu, "Grafting to" rubber composite for elastic dielectric material, *Macromol. Chem. Phys.*, 2025, **226**, 2400364.
54 H.-C. Wu, S. Nikzad, C. Zhu, H. Yan, Y. Li, W. Niu, J. R. Matthews, J. Xu, N. Matsuhisa and P. K. Arunachala, Highly stretchable polymer semiconductor thin films with multi-modal energy dissipation and high relative stretchability, *Nat. Commun.*, 2023, **14**, 8382.
55 D. J. Lipomi, M. Vosgueritchian, B. C. Tee, S. L. Hellstrom, J. A. Lee, C. H. Fox and Z. Bao, Skin-like pressure and strain sensors based on transparent elastic films of carbon nanotubes, *Nat. Nanotechnol.*, 2011, **6**, 788–792.
56 X. Chen, M. A. Dam, K. Ono, A. Mal, H. Shen, S. R. Nutt, K. Sheran and F. Wudl, A thermally re-mendable cross-linked polymeric material, *Science*, 2002, **295**, 1698–1702.
57 P. Cordier, F. Tournilhac, C. Soulié-Ziakovic and L. Leibler, Self-healing and thermoreversible rubber from supramolecular assembly, *Nature*, 2008, **451**, 977–980.
58 S. Burattini, H. M. Colquhoun, J. D. Fox, D. Friedmann, B. W. Greenland, P. J. Harris, W. Hayes, M. E. Mackay and S. J. Rowan, A self-repairing, supramolecular polymer system: healability as a consequence of donor–acceptor π–π stacking interactions, *Chem. Commun.*, 2009, 6717–6719.
59 J. Y. Oh, D. Son, T. Katsumata, Y. Lee, Y. Kim, J. Lopez, H.-C. Wu, J. Kang, J. Park and X. Gu, Stretchable self-healable semiconducting polymer film for active-matrix strain-sensing array, *Sci. Adv.*, 2019, **5**, eaav3097.
60 Z. Li, R. Yu and B. Guo, Shape-memory and self-healing polymers based on dynamic covalent bonds and dynamic noncovalent interactions: synthesis, mechanism, and application, *ACS Appl. Bio Mater.*, 2021, **4**, 5926–5943.
61 W.-N. Wu, T.-H. Tu, C.-H. Pai, K.-H. Cheng, S.-H. Tung, Y.-T. Chan and C.-L. Liu, Metallo-supramolecular rod–coil block copolymer thin films for stretchable organic field effect transistor application, *Macromolecules*, 2022, **55**, 10670–10681.
62 A.-N. Au-Duong, Y.-C. Hsu, K.-L. Chen, Y.-S. Huang, J.-Y. Lai and Y.-C. Chiu, Intrinsically elastic and self-healing luminescent polyisoprene copolymers formed via covalent bonding and hydrogen bonding design, *Polym. J.*, 2022, **54**, 1331–1343.
63 N. T. P. Vo, T. U. Nam, M. W. Jeong, J. S. Kim, K. H. Jung, Y. Lee, G. Ma, X. Gu, J. B.-H. Tok, T. I. Lee, Z. Bao and J. Y. Oh, Autonomous self-healing supramolecular polymer transistors for skin electronics, *Nat. Commun.*, 2024, **15**, 3433.
64 T. Sekitani and T. Someya, Stretchable, large-area organic electronics, *Adv. Mater.*, 2010, **22**, 2228–2246.
65 G. Schwartz, B. C.-K. Tee, J. Mei, A. L. Appleton, D. H. Kim, H. Wang and Z. Bao, Flexible polymer transistors with high pressure sensitivity for application in electronic skin and health monitoring, *Nat. Commun.*, 2013, **4**, 1859.
66 M. Shin, J. Y. Oh, K.-E. Byun, Y.-J. Lee, B. Kim, H.-K. Baik, J.-J. Park and U. Jeong, Polythiophene nanofibril bundles surface-embedded in elastomer: a route to a highly stretchable active channel layer, *Adv. Mater.*, 2015, **27**, 1255–1261.
67 S. Dai, Y. Zhao, Y. Wang, J. Zhang, L. Fang, S. Jin, Y. Shao and J. Huang, Recent advances in transistor-based artificial synapses, *Adv. Funct. Mater.*, 2019, **29**, 1903700.
68 B. Hwang and J. S. Lee, Recent advances in memory devices with hybrid materials, *Adv. Electron. Mater.*, 2019, **5**, 1800519.
69 S. W. Cho, S. M. Kwon, Y.-H. Kim and S. K. Park, Recent progress in transistor-based optoelectronic synapses: from neuromorphic computing to artificial sensory system, *Adv. Intell. Syst.*, 2021, **3**, 2000162.
70 H.-C. Tien, Y.-W. Huang, Y.-C. Chiu, Y.-H. Cheng, C.-C. Chueh and W.-Y. Lee, Intrinsically stretchable polymer semiconductors: molecular design, processing and device applications, *J. Mater. Chem. C*, 2021, **9**, 2660–2684.
71 L. Laysandra, A. Njotoprajitno, S. P. Prakoso and Y.-C. Chiu, From stretchable and healable to self-healing semiconducting polymers: design and their TFT devices, *Mater. Adv.*, 2022, **3**, 7154–7184.
72 E. G. Rochow, *US Pat.*, 2380995A, 1945.
73 M. Butts, J. Cella, C. D. Wood, G. Gillette, R. Kerboua, J. Leman, L. Lewis, S. Rubinsztajn, F. Schattenmann and J. Stein, *Kirk-othmer encyclopedia of chemical techonology*, Wiley-Interscience, Hoboken, NJ, 4th edn, 2000.
74 P. Emmanuel, T. Jeff, L. Patrice, L.-D. Patrick, G. Francois and B. Bernard, Well-architectured poly(dimethylsiloxane)-containing copolymers obtained by radical chemistry, *Chem. Rev.*, 2010, **110**, 1233–1277.
75 W. H. Daudt and L. J. Tyler, *US Pat.*, 2676182A, 1950.
76 S. Boileau, in *Ring-opening polymerization*, ACS Publications, 1985, ch. 2, vol. 286, pp. 23–35.
77 J. Winterfeld and B. C. Abele, *US Pat.*, 6284907B1, 2001.
78 M. K. Lewis and S. J. Ritscher, *WO Pat.*, 2002044186A1, 2002.
79 J. E. McGrath, in *Ring-opening polymerization*, ACS Publications, 1985, ch. 2, vol. 286, pp. 1–22.
80 O. Nuyken and S. D. Pask, Ring-opening polymerization—an introductory review, *Polymers*, 2013, **5**, 361–403.

81 S. S. Dhanabalan, T. Arun, G. Periyasamy, N. Dineshbabu, N. Chidhambaram, S. R. Avaninathan and M. F. Carrasco, Surface engineering of high-temperature PDMS substrate for flexible optoelectronic applications, *Chem. Phys. Lett.*, 2022, **800**, 139692.

82 I. Park, S. H. Ko, H. Pan, C. P. Grigoropoulos, A. P. Pisano, J. M. Fréchet, E. S. Lee and J. H. Jeong, Nanoscale patterning and electronics on flexible substrate by direct nanoimprinting of metallic nanoparticles, *Adv. Mater.*, 2008, **20**, 489–496.

83 G. Cantarella, N. Münzenrieder, L. Petti, C. Vogt, L. Büthe, G. Salvatore, A. Daus and G. Tröster, Flexible In–Ga–Zn–O thin-film transistors on elastomeric substrate bent to 2.3% strain, *IEEE Electron Device Lett.*, 2015, **36**, 781–783.

84 J. Kang, Y.-W. Lim, I. Lee, S. Kim, K. Y. Kim, W. Lee and B.-S. Bae, Photopatternable poly (dimethylsiloxane)(PDMS) for an intrinsically stretchable organic electrochemical transistor, *ACS Appl. Mater. Interfaces*, 2022, **14**, 24840–24849.

85 S.-W. Jung, J.-S. Choi, J. B. Koo, C. W. Park, B. S. Na, J.-Y. Oh, S. C. Lim, S. S. Lee, H. Y. Chu and S.-M. Yoon, Flexible nonvolatile organic ferroelectric memory transistors fabricated on polydimethylsiloxane elastomer, *Org. Electron.*, 2015, **16**, 46–53.

86 H. Shivashankar, A. Kevin, S. Manohar and S. Kulkarni, Investigation on dielectric properties of PDMS based nanocomposites, *Phys. B*, 2021, **602**, 412357.

87 S.-Y. Liu, J.-G. Lu and H.-P. D. Shieh, Influence of permittivity on the sensitivity of porous elastomer-based capacitive pressure sensors, *IEEE Sens. J.*, 2018, **18**, 1870–1876.

88 X. Qin, W. Lu, X. Wang, Z. Qin, H. Chen, G. Lu, G. Lu and L. Bu, Surface-modified polydimethylsiloxane with soft-plasma as dielectric layer for flexible artificial synaptic transistors, *Appl. Surf. Sci.*, 2023, **627**, 157325.

89 Y. Hu and C. Majidi, Dielectric elastomers with liquid metal and polydopamine-coated graphene oxide inclusions, *ACS Appl. Mater. Interfaces*, 2023, **15**, 24769–24776.

90 G. Zhang, M. McBride, N. Persson, S. Lee, T. J. Dunn, M. F. Toney, Z. Yuan, Y.-H. Kwon, P.-H. Chu, B. Risteen and E. Reichman, Versatile interpenetrating polymer network approach to robust stretchable electronic devices, *Chem. Mater.*, 2017, **29**, 7645–7652.

91 E. Song, B. Kang, H. H. Choi, D. H. Sin, H. Lee, W. H. Lee and K. Cho, Stretchable and transparent organic semiconducting thin film with conjugated polymer nanowires embedded in an elastomeric matrix, *Adv. Electron. Mater.*, 2016, **2**, 1500250.

92 D. Choi, H. Kim, N. Persson, P.-H. Chu, M. Chang, J.-H. Kang, S. Graham and E. Reichmanis, Elastomer–polymer semiconductor blends for high-performance stretchable charge transport networks, *Chem. Mater.*, 2016, **28**, 1196–1204.

93 F. M. de Souza, P. K. Kahol and R. K. Gupta, Polyurethane chemistry: renewable polyols and isocyanates, *Am. Chem. Soc.*, 2021, **1380**(ch. 1), 1–24.

94 Z. Cao, Q. Zhou, S. Jie and B.-G. Li, High cis-1,4 hydroxyl-terminated polybutadiene-based polyurethanes with extremely low glass transition temperature and excellent mechanical properties, *Ind. Eng. Chem. Res.*, 2016, **55**, 1582–1589.

95 Z. P. Zhang, M. Z. Rong and M. Q. Zhang, Mechanically robust, self-healable, and highly stretchable "living" crosslinked polyurethane based on a reversible C-C Bond, *Adv. Funct. Mater.*, 2018, **28**, 1706050.

96 S. Kim, J. W. Kim, Y. H. Lee, Y. R. Jeong, K. Keum, D. S. Kim, H. Lee and J. S. Ha, Tough, self-healing polyurethane with novel functionality for fully recoverable layered sensor arrays, *Chem. Eng. J.*, 2023, **464**, 142700.

97 J.-M. Lehn, in *Supramolecular polymer chemistry—scope and perspectives*, CRC Press, 2005, pp. 17–42.

98 Y.-Q. Zheng, Z.-F. Yao, T. Lei, J.-H. Dou, C.-Y. Yang, L. Zou, X. Meng, W. Ma, J.-Y. Wang and J. Pei, Unraveling the solution-state supramolecular structures of donor–acceptor polymers and their influence on solid-state morphology and charge-transport properties, *Adv. Mater.*, 2017, **29**, 1701072.

99 A. Chortos, C. Zhu, J. Y. Oh, X. Yan, I. Pochorovski, J. W. F. To, N. Liu, U. Kraft, B. Murmann and Z. Bao, Investigating limiting factors in stretchable all-carbon transistors for reliable stretchable electronics, *ACS Nano*, 2017, **11**, 7925–7937.

100 J. H. Yoon, S.-M. Kim, Y. Eom, J. M. Koo, H.-W. Cho, T. J. Lee, K. G. Lee, H. J. Park, Y. K. Kim, H.-J. Yoo, S. Y. Hwang, J. Park and B. G. Choi, Extremely fast self-healable bio-based supramolecular polymer for wearable real-time sweat-monitoring sensor, *ACS Appl. Mater. Interfaces*, 2019, **11**, 46165–46175.

101 K. Subramaniam, *Fundamentals of rubber technology*, Kumaran Press (Pvt) Ltd, Colombo, 2002.

102 F. M. Helaly, A. S. Badran and A. M. Ramadan, Effect of different inorganic fillers on the physical properties of styrene-butadiene rubber vulcanizates, *J. Elastomers Plast.*, 1991, **23**, 301–313.

103 Y. Hamuro, S. J. Geib and A. D. Hamilton, Oligoanthranilamides. Non-peptide subunits that show formation of specific secondary structure, *J. Am. Chem. Soc.*, 1996, **118**, 7529.

104 S. Lee, S. Shin, S. Lee, J. Seo, J. Lee, S. Son, H. J. Cho, H. Algadi, S. Al-Sayari, D. E. Kim and T. Lee, Ag nanowire reinforced highly stretchable conductive fibers for wearable electronics, *Adv. Funct. Mater.*, 2015, **25**, 3114–3121.

105 X. Wang, S. Meng, M. Tebyetekerwa, Y. Li, J. Pionteck, B. Sun, Z. Qin and M. Zhu, Highly sensitive and stretchable piezoresistive strain sensor based on conductive poly(styrene-butadiene-styrene)/few layer graphene composite fiber, *Composites, Part A*, 2018, **105**, 291–299.

106 D. Tian, Y. Xu, Y. Wang, Z. Lei, Z. Lin, T. Zhao, Y. Hu, R. Sun and C.-P. Wong, In-situ metallized carbon nanotubes/poly(styrene-butadiene-styrene) (CNTs/SBS) foam for

electromagnetic interference shielding, *Chem. Eng. J.*, 2021, **420**, 130482.
107 G. Li, C. S. Morlor, C. Leung and H. Wang, Mechanical properties and fractal analysis of cement mortar incorporating styrene-butadiene rubber latex and carboxylated MWCNTs, *Constr. Build. Mater.*, 2021, **309**, 125175.
108 M. Lin, Z. Zheng, L. Yang, M. Luo, L. Fu, B. Lin and C. Xu, A high-performance, sensitive, wearable multifunctional sensor based on rubber/CNT for human motion and skin temperature detection, *Adv. Mater.*, 2022, **34**, 2107309.
109 M. N. Alam, V. Kumar, D.-J. Lee and S.-S. Park, Styrene–butadiene rubber-based nanocomposites toughened by carbon nanotubes for wide and linear electromechanical sensing applications, *Polym. Compos.*, 2024, **45**, 2485–2499.
110 H. Zhang, Y. Yang, K. Zhang, L. Ji, Z. Hua, W. Cao, J. Sun and Q. Liu, Effect of hybrid filler comprising cryptocrystalline graphite and multi-wall carbon nanotubes on the mechanical and conductive properties of styrene butadiene rubber, *Polym. Compos.*, 2024, **45**, 14136–14145.
111 S. S. Islam, G. D. R. N. Ransinchung, B. Singh and S. K. Singh, Effect of short-term and long-term ageing on the elastic and creep behaviour of modified binder containing different SBS copolymer, *Mater. Struct.*, 2022, **55**, 144.
112 L. Yang, S. Sun, X. Yu, Z. Xu, Y. Lu, X. Shi, Y. Song, D. Wang, M. Zuo and Q. Zheng, Modified waste rubber powders filled styrene butadiene rubber toward the combination of high elasticity and low mechanical hysteresis, *Compos. Commun.*, 2024, **49**, 101978.
113 Q. Zhang, Y. Shao, C. Wang, L. Wang, H. Zhou and X. Xia, Preparation of fluorine-free anti-acid and breathable composite fabric based on modified SBS/pitch electrospun nanofibers, *Text. Res. J.*, 2021, **91**, 1535–1545.
114 S. P Subramaniyan, M. A. Imam and P. Prabhakar, Fiber packing and morphology driven moisture diffusion mechanics in reinforced composites, *Composites, Part B*, 2021, **226**, 109259.
115 A. L. H. A. Perera and B. G. K. Perera, Development of an economical method to reduce the extractable latex protein levels in finished dipped rubber products, *BioMed Res. Int.*, 2017, **2017**, 9573021.
116 M. M. Wald and M. G. Quam, *US Pat.*, 3595942A, 1971.
117 J.-J. Lin, I.-J. Cheng, C.-N. Chen and C.-C. Kwan, Synthesis, characterization, and interfacial behaviors of poly (oxyethylene)-grafted SEBS copolymers, *Ind. Eng. Chem. Res.*, 2000, **39**, 65–71.
118 M. De Sarkar, P. P. De and A. K. Bhowmick, Influence of styrene content on the hydrogenation of styrene–butadiene copolymer, *J. Appl. Polym. Sci.*, 1999, **71**, 1581–1595.
119 J.-R. Chang and S.-M. Huang, Pd/Al_2O_3 catalysts for selective hydrogenation of polystyrene-block-polybutadiene-block-polystyrene thermoplastic elastomers, *Ind. Eng. Chem. Res.*, 1998, **37**, 1220–1227.
120 V. A. E. Barrios, R. H. Nájera, A. Petit and F. Pla, Selective hydrogenation of butadiene–styrene copolymers using a Ziegler–Natta type catalyst: 1. Kinetic study, *Eur. Polym. J.*, 2000, **36**, 1817–1834.
121 V. Vijay, A. D. Rao and K. Narayan, In situ studies of strain dependent transport properties of conducting polymers on elastomeric substrates, *J. Appl. Phys.*, 2011, **109**, 084525.
122 K. Shrestha, G. B. Pradhan, M. Asaduzzaman, M. S. Reza, T. Bhatta, H. Kim, Y. Lee and J. Y. Park, A Breathable, reliable, and flexible siloxene incorporated porous SEBS-based triboelectric nanogenerator for human–machine interactions, *Adv. Energy Mater.*, 2024, **14**, 2302471.
123 H. Stoyanov, M. Kollosche, S. Risse, R. Waché and G. Kofod, Soft conductive elastomer materials for stretchable electronics and voltage controlled artificial muscles, *Adv. Mater.*, 2013, **25**, 578–583.
124 H. Stoyanov, M. Kollosche, D. N. McCarthy and G. Kofod, Molecular composites with enhanced energy density for electroactive polymers, *J. Mater. Chem.*, 2010, **20**, 7558–7564.
125 R. M. Grigorescu, F. Ciuprina, P. Ghioca, M. Ghiurea, L. Iancu, B. Spurcaciu and D. M. Panaitescu, Mechanical and dielectric properties of SEBS modified by graphite inclusion and composite interface, *J. Phys. Chem. Solids*, 2016, **89**, 97–106.
126 S. Wang, J. Xu, W. Wang, G.-J. N. Wang, R. Rastak, F. Molina-Lopez, J. W. Chung, S. Niu, V. R. Feig and J. Lopez, Skin electronics from scalable fabrication of an intrinsically stretchable transistor array, *Nature*, 2018, **555**, 83–88.
127 D. Zhong, Y. Nishio, C. Wu, Y. Jiang, W. Wang, Y. Yuan, Y. Yao, J. B.-H. Tok and Z. Bao, Design considerations and fabrication protocols of high-performance intrinsically stretchable transistors and integrated circuits, *ACS Nano*, 2024, **18**, 33011–33031.
128 T. Zhang, Y. Liu, L. Zhang, S. Wang, J. Li, J. Zuo, X. Yu, Q. Zhang and Y. Han, Constructing a desired nanofibril network morphology for stretchable polymer films by weakening the intermolecular interaction of a conjugated polymer in an elastomer matrix and extending the film-forming time, *J. Mater. Chem. C*, 2023, **11**, 2302–2315.
129 S. J. Yoon, H. Kim, C. K. Jeong and Y. K. Lee, Highly stretchable and self-healing SEBS-PVDF composite films for enhanced dielectric elastomer generators, *J. Korean Ceram. Soc.*, 2024, **61**, 429–435.
130 G. J. N. Wang, A. Gasperini and Z. Bao, Stretchable polymer semiconductors for plastic electronics, *Adv. Electron. Mater.*, 2018, **4**, 1700429.
131 M. L. Senyek, Isoprene polymers, *Encycl. Polym. Sci. Technol.*, 2008.
132 A. P. Leber, Overview of isoprene monomer and polyisoprene production processes, *Chem.-Biol. Interact.*, 2001, **135–136**, 169–173.
133 I. W. Cheong, C. M. Fellows and R. G. Gilbert, Synthesis and cross-linking of polyisoprene latexes, *Polym*, 2004, **45**, 769–781.

134 M. M. Mburu, A. N. Au-Duong, W. T. Li, C. C. Wu, Y. H. Cheng, K. L. Chen, W. H. Chiang and Y. C. Chiu, The impacts of polyisoprene physical interactions on sorting of single-wall carbon nanotubes, *Macromol. Rapid Commun.*, 2021, **42**, e2100327.

135 M. Selvan T, A. Haridas C P, S. Karmakar, T. K. Patra and T. Mondal, Hysteresis-free temperature sensing with printable electronic skins made of liquid polyisoprene/CNTs, *ACS Appl. Mater. Interfaces*, 2024, **16**, 48176–48186.

136 L. Xu, M. Valasek, F. Hennrich, E. Sedghamiz, M. Penaloza-Amion, D. Haussinger, W. Wenzel, M. M. Kappes and M. Mayor, Enantiomeric separation of semiconducting single-walled carbon nanotubes by acid cleavable chiral polyfluorene, *ACS Nano*, 2021, **15**, 4699–4709.

137 S. K. Samanta, M. Fritsch, U. Scherf, W. Gomulya, S. Z. Bisri and M. A. Loi, Conjugated polymer-assisted dispersion of single-wall carbon nanotubes: the power of polymer wrapping, *Acc. Chem. Res.*, 2014, **47**, 2446–2456.

138 Y. J. Choi, E. J. C. Nacpil, J. Han, C. Zhu, I. S. Kim and I. Jeon, Recent advances in dispersant technology for carbon nanotubes toward energy device applications, *Adv. Energy Sustainability Res.*, 2024, **5**, 2300219.

139 M. M. Mburu, A. N. Au-Duong, W. T. Li, W. Y. Yu, Y. W. Lan, W. H. Chiang and Y. C. Chiu, Highly stable single-walled carbon nanotube sorting by low molecular weight conjugated polymer with hydrogen-bonded polyisoprene, *Adv. Electron. Mater.*, 2022, **8**, 2200698.

140 A. Dzienia, D. Just, T. Wasiak, K. Z. Milowska, A. Mielanczyk, N. Labedzki, S. Kruss and D. Janas, Size matters in conjugated polymer chirality-selective SWCNT extraction, *Adv. Sci.*, 2024, **11**, 2402176.

141 H. Wang, Y. Yang, M. Nishiura, Y. L. Hong, Y. Nishiyama, Y. Higaki and Z. Hou, Making polyisoprene self-healable through microstructure regulation by rare-earth catalysts, *Angew Chem. Int. Ed. Engl.*, 2022, **61**, e202210023.

142 S. Li, P. Tan, J. Cao, Y. Yao, X. Ren and Y.-X. Xu, High performance, self-healing and recyclable polyisoprene rubbers enabled by modulating sulfide bond structures, *Polymer*, 2025, **332**, 128570.

143 C. Jiang, C. Wang, S. Zhang, H. Bi, Y. Wu, J. Wang, Y. Zhu, J. Qin, Y. Zhao, X. Shi and G. Zhang, Reprocessable and self-healable boronic-ester based poly(styrene-b-isoprene-b-styrene) vitrimeric elastomer with improved thermo-mechanical property and adhesive performance, *React. Funct. Polym.*, 2024, **198**, 105893.

144 R. Takahashi, T. Udagawa, K. Hashimoto, S. Kutsumizu and Y. Miwa, Effect of the Mg^{2+} ratio on the mechanical and self-healing properties of polyisoprene ionomers co-neutralized with Na^{+} and Mg^{2+}, *Polym. J.*, 2024, **56**, 699–704.

145 Y. Huang, Y. Liu, G. Si and C. Tan, Self-healing and recyclable vulcanized polyisoprene based on a sulfur-rich copolymer cross-linking agent derived from inverse vulcanization, *ACS Sustain. Chem. Eng.*, 2024, **12**, 2212–2224.

146 M.-K. Chen, Y.-H. Zhao, R. Zhang, Y. Yang, J. Cao, M.-Z. Tang, G. Huang and Y.-X. Xu, Carbonate nanophase guided by terminally functionalized polyisoprene leading to a super tough, recyclable and transparent rubber, *Chem. Eng. J.*, 2023, **452**, 139130.

147 Y.-C. Hsu, Y.-H. You, A.-N. Au-Duong, Y.-S. Huang, Y.-C. Chiu and L.-Y. Chen, Fabrication of intrinsic, elastic, self-healing, and luminescent CsPbBr3 quantum dot-polymer composites via thiol–ene cross-linking, *ACS Appl. Polym. Mater.*, 2022, **4**, 8987–8995.

148 Q. Wang, Y. Ma, J. Meng, X. Liu and L. Xia, Thermal-triggered Trans-1, 4-polyisoprene/polyethylene wax shape memory and self-healing composites, *Polym. Test.*, 2022, **111**, 107601.

149 J.-B. Hou, Z.-H. Chen, S.-X. Zhang, Z.-J. Nie, S.-T. Fan, H.-R. Shu, S. Zhang, B.-J. Li and Y. Cao, A tough self-healing elastomer with a slip-ring structure, *Ind. Eng. Chem. Res.*, 2020, **60**, 251–262.

150 Y. Miwa, M. Yamada, Y. Shinke and S. Kutsumizu, Autonomous self-healing polyisoprene elastomers with high modulus and good toughness based on the synergy of dynamic ionic crosslinks and highly disordered crystals, *Polym. Chem.*, 2020, **11**, 6549–6558.

151 Y. Miwa, J. Kurachi, Y. Sugino, T. Udagawa and S. Kutsumizu, Toward strong self-healing polyisoprene elastomers with dynamic ionic crosslinks, *Soft Matter*, 2020, **16**, 3384–3394.

152 J. Liu, J. Liu, S. Wang, J. Huang, S. Wu, Z. Tang, B. Guo and L. Zhang, An advanced elastomer with an unprecedented combination of excellent mechanical properties and high self-healing capability, *J. Mater. Chem. A*, 2017, **5**, 25660–25671.

153 P. Thangaraju and S. B. Varthya, in *Medical device guidelines and regulations handbook*, Springer, 2022, pp. 163–187.

154 A. Victor, J. Ribeiro and F. F. Araújo, Study of PDMS characterization and its applications in biomedicine: A review, *J. Biomech. Sci. Eng.*, 2019, **4**, 1–9.

155 C. Jensen, L. Gurevich, A. Patriciu, J. Struijk, V. Zachar and C. P. Pennisi, Increased connective tissue attachment to silicone implants by a water vapor plasma treatment, *J. Biomed. Mater. Res., Part A*, 2012, **100**, 3400–3407.

156 E. Simoni, E. Gentilin, M. Candito, A. Martini and L. Astolfi, Polydimethylsiloxanes biocompatibility in PC12 neuronal cell line, *Colloids Surf., B*, 2019, **173**, 400–406.

157 I. R. Minev, P. Musienko, A. Hirsch, Q. Barraud, N. Wenger, E. M. Moraud, J. Gandar, M. Capogrosso, T. Milekovic and L. Asboth, Electronic dura mater for long-term multimodal neural interfaces, *Science*, 2015, **347**, 159–163.

158 C. G. M. Gennari, G. M. G. Quaroni, C. Creton, P. Minghetti and F. Cilurzo, SEBS block copolymers as novel materials to design transdermal patches, *Int. J. Pharm.*, 2020, **575**, 118975.

159 S. S. Hosseini Salekdeh, H. Daemi, M. Zare-Gachi, S. Rajabi, F. Bazgir, N. Aghdami, M. S. Nourbakhsh and H. Baharvand, Assessment of the efficacy of tributylammonium alginate surface-modified polyurethane as an antibacterial elastomeric wound dressing for both noninfected and infected full-thickness wounds, *ACS Appl. Mater. Interfaces*, 2019, **12**, 3393–3406.

160 K. Park, H. Yuk, M. Yang, J. Cho, H. Lee and J. Kim, A biomimetic elastomeric robot skin using electrical impedance and acoustic tomography for tactile sensing, *Sci. Robot.*, 2022, **7**, eabm7187.

161 C. M. Boutry, M. Negre, M. Jorda, O. Vardoulis, A. Chortos, O. Khatib and Z. Bao, A hierarchically patterned, bioinspired e-skin able to detect the direction of applied pressure for robotics, *Sci. Robot.*, 2018, **3**, eaau6914.

162 A. P. Gerratt, H. O. Michaud and S. P. Lacour, Elastomeric electronic skin for prosthetic tactile sensation, *Adv. Funct. Mater.*, 2015, **25**, 2287–2295.

163 Y. Wu, Y. Liu, Y. Zhou, Q. Man, C. Hu, W. Asghar, F. Li, Z. Yu, J. Shang and G. Liu, A skin-inspired tactile sensor for smart prosthetics, *Sci. Robot.*, 2018, **3**, eaat0429.

164 H. Derakhshandeh, F. Aghabaglou, A. McCarthy, A. Mostafavi, C. Wiseman, Z. Bonick, I. Ghanavati, S. Harris, C. Kreikemeier-Bower, S. M. Moosavi Basri, J. Rosenbohm, R. Yang, P. Mostafalu, D. Orgill and A. Tamayo, A wirelessly controlled smart bandage with 3D-printed miniaturized needle arrays, *Adv. Funct. Mater.*, 2020, **30**, 1905544.

165 H. C. Ates, A. K. Yetisen, F. Güder and C. Dincer, Wearable devices for the detection of COVID-19, *Nat. Electron.*, 2021, **4**, 13–14.

166 N. Luo, W. Dai, C. Li, Z. Zhou, L. Lu, C. C. Poon, S. C. Chen, Y. Zhang and N. Zhao, Flexible piezoresistive sensor patch enabling ultralow power cuffless blood pressure measurement, *Adv. Funct. Mater.*, 2016, **26**, 1178–1187.

167 A. Chortos, G. I. Koleilat, R. Pfattner, D. Kong, P. Lin, R. Nur, T. Lei, H. Wang, N. Liu, Y.-C. Lai, M.-G. Kim, J. W. Chung, S. Lee and Z. Bao, Mechanically durable and highly stretchable transistors employing carbon nanotube semiconductor and electrodes, *Adv. Mater.*, 2016, **28**, 4441–4448.

168 Y. Wan, X. C. Li, H. Yuan, D. Liu and W. Y. Lai, Self-healing elastic electronics: materials design, mechanisms, and applications, *Adv. Funct. Mater.*, 2024, **34**, 2316550.

169 F. Xu, M.-Y. Wu, N. S. Safron, S. S. Roy, R. M. Jacobberger, D. J. Bindl, J.-H. Seo, T.-H. Chang, Z. Ma and M. S. Arnold, Highly stretchable carbon nanotube transistors with ion gel gate dielectrics, *Nano Lett.*, 2014, **14**, 682–686.

170 S. H. Chae, W. J. Yu, J. J. Bae, D. L. Duong, D. Perello, H. Y. Jeong, Q. H. Ta, T. H. Ly, Q. A. Vu, M. Yun, X. Duan and Y. H. Lee, Transferred wrinkled Al_2O_3 for highly stretchable and transparent graphene–carbon nanotube transistors, *Nat. Mater.*, 2013, **12**, 403–409.

171 L. Cai, S. Zhang, J. Miao, Z. Yu and C. Wang, Fully printed stretchable thin-film transistors and integrated logic circuits, *ACS Nano*, 2016, **10**, 11459–11468.

172 Q. Zhou, Z. Wang, Y. Yan, L. Yang, K. Chi, Y. Wu, W. Li, Z. Yi, Y. Liu and Y. Zhao, Strain-enhanced electrical performance in stretchable semiconducting polymers, *npj Flexible Electron.*, 2023, **7**, 35.

173 J. Xu, S. Wang, G.-J. N. Wang, C. Zhu, S. Luo, L. Jin, X. Gu, S. Chen, V. R. Feig and J. W. To, Highly stretchable polymer semiconductor films through the nanoconfinement effect, *Science*, 2017, **355**, 59–64.

174 C. B. Nielsen, M. Turbiez and I. McCulloch, Recent advances in the development of semiconducting DPP-containing polymers for transistor applications, *Adv. Mater.*, 2013, **25**, 1859–1880.

175 Z. Chen, M. J. Lee, R. Shahid Ashraf, Y. Gu, S. Albert-Seifried, M. Meedom Nielsen, B. Schroeder, T. D. Anthopoulos, M. Heeney and I. McCulloch, High-performance ambipolar diketopyrrolopyrrole-thieno [3, 2-b] thiophene copolymer field-effect transistors with balanced hole and electron mobilities, *Adv. Mater.*, 2012, **24**, 647–652.

176 Y. Zheng, Z. Yu, S. Zhang, X. Kong, W. Michaels, W. Wang, G. Chen, D. Liu, J.-C. Lai, N. Prine, W. Zhang, S. Nikzad, C. B. Cooper, D. Zhong, J. Mun, Z. Zhang, J. Kang, J. B.-H. Tok, I. McCulloch, J. Qin, X. Gu and Z. Bao, A molecular design approach towards elastic and multifunctional polymer electronics, *Nat. Commun.*, 2021, **12**, 5701.

177 M. H. Kim, M. W. Jeong, J. S. Kim, T. U. Nam, N. T. P. Vo, L. Jin, T. I. Lee and J. Y. Oh, Mechanically robust stretchable semiconductor metallization for skin-inspired organic transistors, *Sci. Adv.*, 2022, **8**, eade2988.

178 W. Wang, S. Wang, R. Rastak, Y. Ochiai, S. Niu, Y. Jiang, P. K. Arunachala, Y. Zheng, J. Xu and N. Matsuhisa, Strain-insensitive intrinsically stretchable transistors and circuits, *Nat. Electron.*, 2021, **4**, 143–150.

179 S.-H. Kang, J.-W. Jo, J. M. Lee, S. Moon, S. B. Shin, S. B. Choi, D. Byeon, J. Kim, M.-G. Kim, Y.-H. Kim, J.-W. Kim and S. K. Park, Full integration of highly stretchable inorganic transistors and circuits within molecular-tailored elastic substrates on a large scale, *Nat. Commun.*, 2024, **15**, 2814.

180 J. Xu, H.-C. Wu, C. Zhu, A. Ehrlich, L. Shaw, M. Nikolka, S. Wang, F. Molina-Lopez, X. Gu, S. Luo, D. Zhou, Y.-H. Kim, G.-J. N. Wang, K. Gu, V. R. Feig, S. Chen, Y. Kim, T. Katsumata, Y.-Q. Zheng, H. Yan, J. W. Chung, J. Lopez, B. Murmann and Z. Bao, Multi-scale ordering in highly stretchable polymer semiconducting films, *Nat. Mater.*, 2019, **18**, 594–601.

181 P. Fan, Y. Liu, Y. Pan, Y. Ying and J. Ping, Three-dimensional micro-and nanomanufacturing techniques for high-fidelity wearable bioelectronics, *Nat. Rev. Electr. Eng.*, 2025, 1–17.

182 J. H. Han, D.-h. Kim, E. G. Jeong, T.-W. Lee, M. K. Lee, J. W. Park, H. Lee and K. C. Choi, Highly conductive transparent and flexible electrodes including double-stacked thin metal films for transparent flexible electronics, *ACS Appl. Mater. Interfaces*, 2017, **9**, 16343–16350.

183 H. Kang, S. Jung, S. Jeong, G. Kim and K. Lee, Polymer-metal hybrid transparent electrodes for flexible electronics, *Nat. Commun.*, 2015, **6**, 6503.

184 K. Sim, Z. Rao, H.-J. Kim, A. Thukral, H. Shim and C. Yu, Fully rubbery integrated electronics from high effective mobility intrinsically stretchable semiconductors, *Sci. Adv.*, 2019, **5**, eaav5749.

185 J. Liang, L. Li, D. Chen, T. Hajagos, Z. Ren, S.-Y. Chou, W. Hu and Q. Pei, Intrinsically stretchable and transparent thin-film transistors based on printable silver nanowires, carbon nanotubes and an elastomeric dielectric, *Nat. Commun.*, 2015, **6**, 7647.

186 Q. Hua, J. Sun, H. Liu, R. Bao, R. Yu, J. Zhai, C. Pan and Z. L. Wang, Skin-inspired highly stretchable and conformable matrix networks for multifunctional sensing, *Nat. Commun.*, 2018, **9**, 244.

187 Y. C. Lai, B. W. Ye, C. F. Lu, C. T. Chen, M. H. Jao, W. F. Su, W. Y. Hung, T. Y. Lin and Y. F. Chen, Extraordinarily sensitive and low-voltage operational cloth-based electronic skin for wearable sensing and multifunctional integration uses: a tactile-induced insulating-to-conducting transition, *Adv. Funct. Mater.*, 2016, **26**, 1286–1295.

188 F. Li, H. Xue, X. Lin, H. Zhao and T. Zhang, Wearable temperature sensor with high resolution for skin temperature monitoring, *ACS Appl. Mater. Interfaces*, 2022, **14**, 43844–43852.

189 L. Yin, M. Cao, K. N. Kim, M. Lin, J.-M. Moon, J. R. Sempionatto, J. Yu, R. Liu, C. Wicker, A. Trifonov, F. Zhang, H. Hu, J. R. Moreto, J. Go, S. Xu and J. Wang, A stretchable epidermal sweat sensing platform with an integrated printed battery and electrochromic display, *Nat. Electron.*, 2022, **5**, 694–705.

190 C. Zhu, A. Chortos, Y. Wang, R. Pfattner, T. Lei, A. C. Hinckley, I. Pochorovski, X. Yan, J. W.-F. To, J. Y. Oh, J. B.-H. Tok, Z. Bao and B. Murmann, Stretchable temperature-sensing circuits with strain suppression based on carbon nanotube transistors, *Nat. Electron.*, 2018, **1**, 183–190.

191 Y. Liu, P. Fan, Y. Pan and J. Ping, Flexible microinterventional sensors for advanced biosignal monitoring, *Chem. Rev.*, 2025, **125**(17), 8246–8318.

192 J. Jang, H. Choo, S. Lee, J. Song, K. Park, J. Yoon, D. Seong, S. An, H. Jung, J. Ju, J. Kang, J. Kang, I. S. Kim, M. Shin, J.-H. Park and D. Son, Reconfigurable assembly of self-healing stretchable transistors and circuits for integrated systems, *Nat. Electron.*, 2025, **8**, 474–484.

193 D. Chen, D. Wang, Y. Yang, Q. Huang, S. Zhu and Z. Zheng, Self-healing materials for next-generation energy harvesting and storage devices, *Adv. Energy Mater.*, 2017, **7**, 1700890.

194 J. Kang, J. B.-H. Tok and Z. Bao, Self-healing soft electronics, *Nat. Electron.*, 2019, **2**, 144–150.

195 J. Kang, D. Son, G. J. N. Wang, Y. Liu, J. Lopez, Y. Kim, J. Y. Oh, T. Katsumata, J. Mun, Y. Lee, L. Jin, J. B.-H. Tok and Z. Bao, Tough and water-insensitive self-healing elastomer for robust electronic skin, *Adv. Mater.*, 2018, **30**, 1706846.

196 J. Y. Oh, S. Rondeau-Gagné, Y.-C. Chiu, A. Chortos, F. Lissel, G.-J. N. Wang, B. C. Schroeder, T. Kurosawa, J. Lopez and T. Katsumata, Intrinsically stretchable and healable semiconducting polymer for organic transistors, *Nature*, 2016, **539**, 411–415.

197 G. Pedretti, V. Milo, S. Ambrogio, R. Carboni, S. Bianchi, A. Calderoni, N. Ramaswamy, A. Spinelli and D. Ielmini, Memristive neural network for on-line learning and tracking with brain-inspired spike timing dependent plasticity, *Sci. Rep.*, 2017, **7**, 5288.

198 P. C. Harikesh, C.-Y. Yang, D. Tu, J. Y. Gerasimov, A. M. Dar, A. Armada-Moreira, M. Massetti, R. Kroon, D. Bliman, R. Olsson, E. Stavrinidou, M. Berggren and S. Fabiano, Organic electrochemical neurons and synapses with ion mediated spiking, *Nat. Commun.*, 2022, **13**, 901.

199 D. Debanne and Y. Inglebert, Spike timing-dependent plasticity and memory, *Curr. Opin. Neurobiol.*, 2023, **80**, 102707.

200 H. Ling, D. A. Koutsouras, S. Kazemzadeh, Y. Van De Burgt, F. Yan and P. Gkoupidenis, Electrolyte-gated transistors for synaptic electronics, neuromorphic computing, and adaptable biointerfacing, *Appl. Phys. Rev.*, 2020, **7**, 011307.

201 T. Shibata, Implementing intelligence in silicon integrated circuits using neuron-like high-functionality transistors, *J. Robot. Mechatron.*, 1996, **8**, 508–515.

202 F. Alibart, S. Pleutin, D. Guérin, C. Novembre, S. Lenfant, K. Lmimouni, C. Gamrat and D. Vuillaume, An organic nanoparticle transistor behaving as a biological spiking synapse, *Adv. Funct. Mater.*, 2010, **20**, 330–337.

203 Q. Lai, L. Zhang, Z. Li, W. F. Stickle, R. S. Williams and Y. Chen, Ionic/electronic hybrid materials integrated in a synaptic transistor with signal processing and learning functions, *Adv. Mater.*, 2010, **22**, 2448–2453.

204 T. Chang, S.-H. Jo, K.-H. Kim, P. Sheridan, S. Gaba and W. Lu, Synaptic behaviors and modeling of a metal oxide memristive device, *Appl. Phys. A*, 2011, **102**, 857–863.

205 Y. Fu, L.-a. Kong, Y. Chen, J. Wang, C. Qian, Y. Yuan, J. Sun, Y. Gao and Q. Wan, Flexible neuromorphic architectures based on self-supported multiterminal organic transistors, *ACS Appl. Mater. Interfaces*, 2018, **10**, 26443–26450.

206 X. Wang, Y. Yan, E. Li, Y. Liu, D. Lai, Z. Lin, Y. Liu, H. Chen and T. Guo, Stretchable synaptic transistors with tunable synaptic behavior, *Nano Energy*, 2020, **75**, 104952.

207 Y. Wang, D. Liu, Y. Zhang, L. Fan, Q. Ren, S. Ma and M. Zhang, Stretchable temperature-responsive multimodal neuromorphic electronic skin with spontaneous synaptic plasticity recovery, *ACS Nano*, 2022, **16**, 8283–8293.

208 R. Qiu, J. Wang, Q. Ren, W. Huang, J. Zhu, D. Liu, X. Gao, W. Wang, Q. Liu and M. Zhang, Bilingual Bidirectional Stretchable Self-Healing Neuristors with Proprioception, *ACS Nano*, 2023, **17**, 12652–12662.

209 J. Zhou, C. Wan, L. Zhu, Y. Shi and Q. Wan, Synaptic behaviors mimicked in flexible oxide-based transistors on plastic substrates, *IEEE Electron Device Lett.*, 2013, **34**, 1433–1435.

210 F. Yu, L. Q. Zhu, W. T. Gao, Y. M. Fu, H. Xiao, J. Tao and J. M. Zhou, Chitosan-Based Polysaccharide-Gated Flexible Indium Tin Oxide Synaptic Transistor with Learning Abilities, *ACS Appl. Mater. Interfaces*, 2018, **10**, 16881–16886.

211 A. A. Bessonov, M. N. Kirikova, D. I. Petukhov, M. Allen, T. Ryhänen and M. J. A. Bailey, Layered memristive and memcapacitive switches for printable electronics, *Nat. Mater.*, 2014, **14**, 199–204.
212 R. Anderson, J. Goff, A. Imamura, E. Kimble, G. Lockwood, J. Matisons, Y. Pan and M. Reinert, *Silicon compounds: silanes and silicones*, Gelest, Inc., Morrisville, PA, 3 edn, 2013.
213 D. Son, J. Kang, O. Vardoulis, Y. Kim, N. Matsuhisa, J. Y. Oh, J. W. F. To, J. Mun, T. Katsumata, Y. Liu, A. F. McGuire, M. Krason, F. Molina-Lopez, J. Ham, U. Kraft, Y. Lee, Y. Yun, J. B. H. Tok and Z. Bao, An integrated self-healable electronic skin system fabricated via dynamic reconstruction of a nanostructured conducting network, *Nat. Nanotechnol.*, 2018, **13**, 1057–1065.
214 J. Park, D. Seong, Y. J. Park, S. H. Park, H. Jung, Y. Kim, H. W. Baac, M. Shin, S. Lee, M. Lee and D. Son, Reversible electrical percolation in a stretchable and self-healable silver-gradient nanocomposite bilayer, *Nat. Commun.*, 2022, **13**, 5233.
215 W. A. Lopes and H. M. Jaeger, Hierarchical self-assembly of metal nanostructures on diblock copolymer scaffolds, *Nature*, 2001, **414**, 735–738.
216 S. Miller and P. McWhorter, Physics of the ferroelectric nonvolatile memory field effect transistor, *J. Appl. Phys.*, 1992, **72**, 5999–6010.
217 S.-J. Kim and J.-S. Lee, Flexible organic transistor memory devices, *Nano Lett.*, 2010, **10**, 2884–2890.
218 Y. Ni, Y. Wang and W. Xu, Recent process of flexible transistor-structured memory, *Small*, 2021, **17**, 1905332.
219 D. Kahng and S. M. Sze, A floating gate and its application to memory devices, *Bell Syst. Tech. J.*, 1967, **46**, 1288–1295.
220 B. Cho, S. Song, Y. Ji, T. W. Kim and T. Lee, Organic resistive memory devices: performance enhancement, integration, and advanced architectures, *Adv. Funct. Mater.*, 2011, **21**, 2806–2829.
221 J. Choi, J. S. Han, K. Hong, S. Y. Kim and H. W. Jang, Organic–inorganic hybrid halide perovskites for memories, transistors, and artificial synapses, *Adv. Mater.*, 2018, **30**, 1704002.
222 G. Dearnaley, A. Stoneham and D. Morgan, Electrical phenomena in amorphous oxide films, *Rep. Prog. Phys.*, 1970, **33**, 1129.
223 R. Waser and M. Aono, Nanoionics-based resistive switching memories, *Nat. Mater.*, 2007, **6**, 833–840.
224 S.-Y. WANG and T.-Y. TSENG, Interface engineering in resistive switching memories, *J. Adv. Dielectr.*, 2011, **1**, 141–162.
225 T. W. Kim, Y. Yang, F. Li and W. L. Kwan, Electrical memory devices based on inorganic/organic nanocomposites, *NPG Asia Mater.*, 2012, **4**, e18.
226 Y. Shan, Z. Lyu, X. Guan, A. Younis, G. Yuan, J. Wang, S. Li and T. Wu, Solution-processed resistive switching memory devices based on hybrid organic–inorganic materials and composites, *Phys. Chem. Chem. Phys.*, 2018, **20**, 23837–23846.
227 D. Gust, T. A. Moore and A. L. Moore, Molecular switches controlled by light, *Chem. Commun.*, 2006, 1169–1178.
228 F. Xu and B. L. Feringa, Photoresponsive supramolecular polymers: from light-controlled small molecules to smart materials, *Adv. Mater.*, 2023, **35**, 2204413.
229 M. Kim, H. Park, E. Kim, M. Chung and J. H. Oh, Photo-crosslinkable organic materials for flexible and stretchable electronics, *Mater. Horiz.*, 2025, **13**, 4573–4607.
230 S. T. Han, Y. Zhou and V. Roy, Towards the development of flexible non-volatile memories, *Adv. Mater.*, 2013, **25**, 5425–5449.
231 M. T. Ghoneim and M. M. Hussain, Review on physically flexible nonvolatile memory for internet of everything electronics, *Electronics*, 2015, **4**, 424–479.
232 K. Rajan, E. Garofalo and A. Chiolerio, Wearable intrinsically soft, stretchable, flexible devices for memories and computing, *Sensors*, 2018, **18**, 367.
233 P. Maji and K. Naskar, Styrenic block copolymer-based thermoplastic elastomers in smart applications: Advances in synthesis, microstructure, and structure–property relationships—A review, *J. Appl. Polym. Sci.*, 2022, **139**, e52942.
234 T. U. Nam, N. T. P. Vo, M. W. Jeong, K. H. Jung, S. H. Lee, T. I. Lee and J. Y. Oh, Intrinsically stretchable floating gate memory transistors for data storage of electronic skin devices, *ACS Nano*, 2024, **18**, 14558–14568.
235 Y. Dai, H. Hu, M. Wang, J. Xu and S. Wang, Stretchable transistors and functional circuits for human-integrated electronics, *Nat. Electron.*, 2021, **4**, 17–29.
236 X. Wang, Y. Liu, Q. Chen, Y. Yan, Z. Rao, Z. Lin, H. Chen and T. Guo, Recent advances in stretchable field-effect transistors, *J. Mater. Chem. C*, 2021, **9**, 7796–7828.
237 X. Xu, Y. Zhao and Y. Liu, Wearable electronics based on stretchable organic semiconductors, *Small*, 2023, **19**, 2206309.
238 E. K. Lee, M. Y. Lee, C. H. Park, H. R. Lee and J. H. Oh, Toward environmentally robust organic electronics: approaches and applications, *Adv. Mater.*, 2017, **29**, 1703638.
239 D. W. Kim, M. Kong and U. Jeong, Interface design for stretchable electronic devices, *Adv. Sci.*, 2021, **8**, 2004170.
240 J. H. Hong, J. M. Shin, G. M. Kim, H. Joo, G. S. Park, I. B. Hwang, M. W. Kim, W. S. Park, H. Y. Chu and S. Kim, 9.1-inch stretchable AMOLED display based on LTPS technology, *J. Soc. Inf. Disp.*, 2017, **25**, 194–199.
241 J. Mun, J. Kang, Y. Zheng, S. Luo, H. C. Wu, N. Matsuhisa, J. Xu, G. J. N. Wang, Y. Yun, G. Xue, J. B.-H. Tok and Z. Bao, Conjugated carbon cyclic nanorings as additives for intrinsically stretchable semiconducting polymers, *Adv. Mater.*, 2019, **31**, 1903912.
242 J. Liu, J. Wang, Z. Zhang, F. Molina-Lopez, G.-J. N. Wang, B. C. Schroeder, X. Yan, Y. Zeng, O. Zhao, H. Tran, T. Lei, Y. Lu, Y.-X. Wang, J. B.-H. Tok, R. Dauskardt, J. W. Chung, Y. Yun and Z. Bao, Fully stretchable active-matrix organic light-emitting electrochemical cell array, *Nat. Commun.*, 2020, **11**, 3362.

243 J. Mun, Y. Ochiai, W. Wang, Y. Zheng, Y.-Q. Zheng, H.-C. Wu, N. Matsuhisa, T. Higashihara, J. B.-H. Tok, Y. Yun and Z. Bao, A design strategy for high mobility stretchable polymer semiconductors, *Nat. Commun.*, 2021, **12**, 3572.

244 J. Kang, J. Mun, Y. Zheng, M. Koizumi, N. Matsuhisa, H.-C. Wu, S. Chen, J. B.-H. Tok, G. H. Lee, L. Jin and Z. Bao, Tough-interface-enabled stretchable electronics using non-stretchable polymer semiconductors and conductors, *Nat. Nanotechnol.*, 2022, **17**, 1265–1271.

245 D. Zhong, C. Wu, Y. Jiang, Y. Yuan, M.-g. Kim, Y. Nishio, C.-C. Shih, W. Wang, J.-C. Lai, X. Ji, T. Z. Gao, Y.-X. Wang, C. Xu, Y. Zheng, Y. Ochiai, S. Liu, S. Wei, J. B.-H. Tok and Z. Bao, High-speed and large-scale intrinsically stretchable integrated circuits, *Nature*, 2024, **627**, 313–320.

246 S. Liu, A. L. Briseno, S. C. Mannsfeld, W. You, J. Locklin, H. W. Lee, Y. Xia and Z. Bao, Selective crystallization of organic semiconductors on patterned templates of carbon nanotubes, *Adv. Funct. Mater.*, 2007, **17**, 2891–2896.

247 M. C. LeMieux, M. Roberts, S. Barman, Y. W. Jin, J. M. Kim and Z. Bao, Self-sorted, aligned nanotube networks for thin-film transistors, *Science*, 2008, **321**, 101–104.

248 Y. Luo, M. Wang, C. Wan, P. Cai, X. J. Loh and X. Chen, Devising materials manufacturing toward lab-to-fab translation of flexible electronics, *Adv. Mater.*, 2020, **32**, 2001903.

249 A. Fatimi, Biomimetic-hydrogel-based electronic skin: An overview based on patenting activities and the market, *Mater. Proc.*, 2025, **20**, 2.

250 Y.-L. Rao, A. Chortos, R. Pfattner, F. Lissel, Y.-C. Chiu, V. Feig, J. Xu, T. Kurosawa, X. Gu and C. Wang, Stretchable self-healing polymeric dielectrics cross-linked through metal–ligand coordination, *J. Am. Chem. Soc.*, 2016, **138**, 6020–6027.

251 Y. Wang, K. L. Chen, N. Prine, S. Rondeau-Gagné, Y. C. Chiu and X. Gu, Stretchable and self-healable semiconductive composites based on hydrogen bonding cross-linked elastomeric matrix, *Adv. Funct. Mater.*, 2023, **33**, 2303031.